1973

High strength steel composite beams with formed metal deck and low partial shear connections

John Angus Grant Jr.
Lehigh University

HIGH STRENGTH STEEL COMPOSITE BEAMS WITH FORMED METAL DECK AND LOW PARTIAL SHEAR CONNECTIONS

by

John Angus Grant, Jr.

A THESIS

Presented to the Graduate Committee

of Lehigh University

in Candidacy for the Degree of

Master of Science

in

Department of Civil Engineering

Lehigh University

October 1973

CERTIFICATE OF APPROVAL

This thesis is accepted and approved in partial fulfillment of the requirements for the degree of Master of Science.

Sept. 10, 1973
(date)

John W. Fisher
John W. Fisher
Professor In Charge

David A. VanHorn
David A. VanHorn
Chairman of Department

ACKNOWLEDGMENTS

The work described in this thesis was conducted at Fritz Engineering Laboratory, Department of Civil Engineering, Lehigh University, Bethlehem, Pennsylvania. Dr. Lynn S. Beedle is Director of the Laboratory and Dr. David A. VanHorn is Chairman of the Department.

The project was sponsored by the American Iron and Steel Institute. Technical guidance was provided by an advisory committee of AISI consisting of Mr. W. C. Hansell, Chairman, and Messrs. J. F. Culver, R. E. Lee, E. W. Gradt, T. J. Jones, D. H. Landis, R. G. Linden, M. Malter, J. H. Ryan, R. Simon, R. C. Singleton, T. E. Thompson.

Dr. John W. Fisher was Director of the project and supervised the work of this thesis. The author wishes to thank him for his encouragement, advice and critical review. Dr. Roger G. Slutter was an associate investigator and his assistance and suggestions are also appreciated.

Thanks are also due to Mr. K. Harpel, Laboratory Superintendent, and his staff for their help during testing. The photographs were prepared by Mr. R. N. Sopko and the drawings by Mr. J. M. Gera and Mr. D. E. VanCott. The manuscript was typed with care by Mrs. D. Fielding and Mrs. R. Grimes. Their cooperation is appreciated.

TABLE OF CONTENTS

		Page
	ABSTRACT	1
1.	INTRODUCTION	2
2.	DESCRIPTION OF TEST	5
	2.1 Test Program	5
	2.2 Test Specimens	6
	2.3 Control Tests	8
	2.3.1 Steel Beams	8
	2.3.2 Concrete Slabs	9
	2.3.3 Stud Shear Connectors	11
	2.3.4 Slab Reinforcement	12
	2.4 Test Procedure	12
	2.5 Instrumentation	13
3.	THEORETICAL ANALYSIS	15
	3.1 Connectors	15
	3.2 Beams	16
	3.2.1 Working Load	16
	3.2.2 Ultimate Strength	17
4.	TEST RESULTS AND ANALYSIS	18
	4.1 Load Deflection Behavior	
	4.2 Load-Strain Behavior	23
	4.3 Load-Slip Behavior	26

		Page
4.4	Failure	28
4.5	Connector Force Load Behavior	33
4.6	Connector Force - Slip Behavior	36
4.7	Ultimate Connector Strength	39
5.	SUMMARY AND CONCLUSIONS	42
6.	TABLES	46
7.	FIGURES	53
8.	REFERENCES	101
9.	Appendices	
	A - Computation of Shear Connector Strength for Specimen 1C2a	103
	B - Computation for Elastic Analysis for Specimen 1C2a	104
	C - Computation of Ultimate Strength for Specimen 1C2a	108
10.	Vita	110

LIST OF TABLES

Table		Page
1	Experiment Design	46
2	Summary of Results	47
3	Steel Properties	48
4	Concrete Mix	50
5	Concrete Properties	51
6	Stud Properties	52

LIST OF FIGURES

Figure		Page
1	Details of Specimen 1C1	53
2	Details of Specimen 1C2a	54
3	Details of Specimen 1C2b	55
4	Details of Specimen 1C3	56
5	Details of Specimen 1C4	57
6	Specimen 1C3--Before Testing	58
7	Deck Profiles	59
8	Typical Stress - Strain Curves (Steel)	60
9	Typical Load - Strain Curve (Concrete)	61
10	Test Set-Up	62
11	Instrumentation - Slip Measurements	63
12	Instrumentation - Strain Gages	64
13	Load versus Midspan Deflection - Specimen 1C1	65
14	Load versus Midspan Deflection - Specimen 1C2a	66
15	Load versus Midspan Deflection - Specimen 1C2b	67
16	Load versus Midspan Deflection - Specimen 1C3	68
17	Load versus Midspan Deflection - Specimen 1C4	69
18	Load versus Midspan Deflection - Specimens 1C1 through 1C4	70
19	Stiffness versus Degree of Shear Connection	71
20	Stiffness versus "Effective" Stiffness	72

Figure		Page
21	Safety Factor versus Rib Width Over Height Ratio	73
22	Safety Factor versus Degree of Shear Connection	74
23	Load versus Strain in Bottom Fiber - Spec. 1C2a	75
24	Load versus Strain in Bottom Fiber - Spec. 1C4	76
25	Strain Distribution Across Slab	77
26	Load versus Slip - Spec. 1C2a	78
27	Load versus Slip - Spec. 1C4	79
28	Slip distribution - Spec. 1C3	80
29	Typical Rib Failure Mode	81
30	Atypical Rib Failure Mode	82
31	Typical Plastic Hinge	83
32	Typical Local Buckling of Top Flange	84
33	Typical Slab Uplift	85
34	Typical Flexural Crack	86
35	Typical Longitudinal Cracking	87
36	Typical Transverse Bending	88
37	Typical Bond Failure	89
38	Typical Negative Moment Cracks	90
39	Model of Force and Strain Distribution	91
40	Connector Force versus Load - Spec. 1C2a	92
41	Connector Force versus Load - Spec. 1C3	93
42	Idealized Connector Force versus Load Curve	94
43	Connector Force versus Slip - Spec. 1C1	95

Figure		Page
44	Connector Force versus Slip - Spec. 1C2a	96
45	Connector Force versus Slip - Spec. 1C2b	97
46	Connector Force versus Slip - Spec. 1C3	98
47	Connector Force versus Slip - Spec. 1C4	99
48	Connector Strength versus Rib Width Over Height Ratio	100

ABSTRACT

This report summarizes a study to determine the strength and behavior of high strength steel composite beams with formed metal deck and low partial shear connection and the strength and behavior of the stud shear connectors embedded within, as well. Prior investigations in this area are few and uncoordinated making conclusions and design recommendations difficult to evaluate. This investigation provides material to help in such an evaluation.

This study is based on tests of five composite beams. The steel used was A572, Grade 50. The concrete was lightweight with a unit weight of 113 pcf and a design strength of 4000 psi. The metal deck was plain 18 gauge with rib heights of 1-1/2, 2, and 3 inches. The shear connectors were 3/4 inch diameter studs embedded in ribs, 1-1/2 inches above the height of the ribs. The rib width over height ratios were set at 1.5 and 2.0. The degree of partial shear connection varied between 20 and 50 percent.

The characteristics of load applied to the beam as a function of midspan deflection, bottom fiber strain at midspan, and slips of the slab relative to the steel beam are reported as well as the load slip-behavior of the stud connectors embedded in the beams. Also failure modes are presented. These results are compared with the work of other investigators and existing design criteria.

The results indicate that the load-deformation behavior of a stud shear connector in a composite beam with formed metal deck is similar to that of a connector in a solid slab composite beam. Also it was found that the ultimate strength of such a connector can be related to the ultimate strength of a similar connector in a solid slab by a function of the rib geometry. The results also indicate that composite beams with formed metal deck and low degrees of partial shear connection are less stiff than similar beams with full shear connection. For situations which require it, the loss in stiffness may be accounted for by an empirically derived correction. It was also found that the flexural capacity of the composite beams with formed metal deck can be accurately predicted provided the capacity of the shear connection is adjusted.

1. INTRODUCTION

During the past forty years, formed metal deck has become the most common floor system used in high rise steel frame structures. A natural off shoot of this popular floor system was the development of composite beam design wherein composite action is achieved by means of shear connectors welded through the deck to the steel beam flange. This development occurred for two entirely different circumstances. When the corrugations of the deck run parallel to the beam, it seems reasonable to assume that the condition of a haunched slab is simulated. There is not much experimental work available on this condition since the few tests made indicated that the shear connection was not significantly affected by the ribs. It is probable that for certain uncommon rib geometries, that is, very high, narrow ribs, the shear capacity of the connector may be reduced somewhat. This case does not appear to be common in current design practice and is not investigated in this report. The second case, and the one more pertinent to the study presented in this paper, is when the corrugations are placed perpendicular to the beam and the shear connectors are placed in the ribs of the corrugations. The behavior of the composite beams for this case has been observed to differ substantially from that expected of a similar composite beam without the metal decking[1].

Most initial studies of this latter case were made on a proprietary basis for specific products in building applications[1]; however, since these studies were not coordinated, considerable variance among controlled parameters existed and therefore it was difficult to come to any conclusions.

In 1967 a detailed study was reported by Robinson[2] who observed that for high, narrow ribs the horizontal shear capacity was a function of the rib geometry and was substantially less than the capacity of the studs in a solid slab. This study as well as others indicated that decking with small corrugations had no effect and the behavior was that of solid slab composite beams.

In 1970, Fisher[1] summarized the investigations that had been done to date and suggested design recommendations. The pertinent conclusions that were drawn are as follows:

(1) Within the working load range, beam performance is not greatly affected by rib geometry.

(2) The limiting rib width to height ratio for a shear capacity equivalent to that of a stud in a solid slab is approximately 2.

(3) Once the shear connection strength is known, the beam performance can be predicted using the same criteria as for solid slab composite beams.

(4) Connector strength is dependent on slab width as well as the geometry of the ribs.

Currently, the American Iron and Steel Institute and a number of deck and stud manufacturers are sponsoring a research project to study

the effect or rib geometry, stud spacing, number of studs per cell, stud geometry, type of steel, type of concrete, slab reinforcement, deck embossments, degree of partial shear connection, and loading. The result of that project will be the development of design criteria for composite beams with formed metal deck. The study reported herein is a part of that on-going comprehensive study.

The purpose of the study reported herein was twofold: (1) to evaluate the capacity and behavior of both composite beams with formed metal deck as a whole as well as the shear connectors within the beams, and (2) to compare the results obtained from this evaluation with existing design criteria. This study involved the fabrication and testing of five composite specimens utilizing high strength steel beams in conjunction with lightweight concrete slabs cast on formed metal deck. The specimens were designed with relatively low degrees of partial shear connection and varying rib geometries.

2. DESCRIPTION OF TEST

2.1 Test Program

The experimental program of the study reported herein consisted of tests on 5 simple span composite beams. The experiment design of this study maintained grade of steel, strength of concrete, type of decking, diameter of studs, slab reinforcement, rib slope, and loading as one level factors. This permitted the direct evaluation of varying width over height values and their influence on the connector shear strength and behavior for a low range of partial shear connection. Table 1 shows the breakdown of the experiment design in terms of steel section, clear span, and number of studs per shear span.

Steel and concrete properties were maintained as constants within fabrication tolerances. Minimal wire mesh reinforcement used for shrinkage control was held constant for all specimens and was ignored in strength considerations. The steel beam sections selected were all the same except for one case which varied slightly. Slab widths were taken as 16 times the thickness plus the flange width. In several beams this resulted in span lengths which slightly violated the L/4 limitation on effective width. However, it was decided to maintain the wider width since the connection strength is apparently dependent upon slab width as well as the geometry of the ribs[1,7]. The thickness of the slab above the rib was held constant. The span length and number

of connectors per cell varied in order to maintain the degree of partial shear connection desired. The stud spacing was adjusted to accommodate the varying rib geometry. All shear connectors used were 3/4 inch diameter studs. Their embedment height above the rib was kept constant by varying their total height in accordance with the rib geometry.

The shear connection for all of the specimens reported in this study provide a partial shear connection of less than 50 percent. Specimens 1C2a, 1C2b, and 1C3 were proportioned such that the steel beam would control the ultimate strength of the member if full composite action were considered. Hence the magnitude of the horizontal shear force would be governed by either the connectors or the steel beam. For specimens 1C1 and 1C4 the concrete slab controls; thus either the connectors or the slab govern the horizontal shear. The degree of partial shear connection can be expressed as the ratio of the horizontal shear force governed by the connectors to that governed by the steel beam or slab, as applicable, and is shown for each of the specimens in Table 2.

Four-point loading was used to provide shear and moment conditions comparable to uniform loading conditions. The locations of the loading points were varied slightly so that each of the concentrated loads were applied through a rib and not over a void.

2.2 Test Specimens

All test specimens were composite beams of high strength steel and lightweight concrete with formed metal decking. Details of these beams

are shown in Figs. 1 through 5. A photograph of beam 1C3 before testing is shown in Fig. 6.

The steel section chosen for all the specimens except one was a W16 X 40. For specimen 1C4 the steel section chosen was a W16 X 45. The concrete slabs for specimens 1C2a, 1C2b and 1C4 were 5-1/2 inches by 96 inches in cross section. For specimens 1C1 and 1C3 the slabs were 4 inches by 72 inches and 4-1/2 inches by 80 inches, respectively. Reinforcement of the slabs was the same for all specimens and consisted of 6 inch x 6 inch, 10/10 welded wire mesh. It was placed at the mid-depth of the solid part of the slab which was also held constant for all of the specimens at 2-1/2 inches above the top of the rib. The concrete slabs were cast without shoring.

The metal decking for all of the specimens was 18 gauge with no embossments. Specimens 1C1, 1C2a and 1C2b had a width to height ratio of 1.5. Specimen 1C1 had a rib height of 1.5 inches and a rib spacing of 6 inches. Both specimen 1C2a and 1C2b had ribs 3 inches high, with rib spacing of 12 inches. For specimens 1C3 and 1C4, the width to height ratio of the metal deck was 2.0. The rib height and rib spacing for specimen 1C3 was 2 inches and 6 inches, respectively and for specimen 1C4, 3 inches and 12 inches, respectively. The deck profiles are shown in Fig. 7. It should be noted that a 6 inch module was used for the 1-1/2 inch and 2 inch deck profiles while a 12 inch module is used for the 3 inch profile. The change in module size was dictated by the desire to limit the number of variables in the parent study mentioned in Chapter 1. Decking with the 1-1/2 inch and 2 inch profiles

were fabricated in 24 inch widths and that with the 3 inch profile in 36 inch widths.

The shear connectors were all embedded in the concrete slab 1-1/2 inches above the top of the rib. This resulted in a connector length of 4-1/2 inches for specimens 1C2a, 1C2b, and 1C4; 3 inches for specimen 1C1; and 3-1/2 inches for specimen 1C3. The connector spacing, as shown in Figs. 1 through 5, was set at every other rib valley for all five specimens, that is, 12 inches for specimens 1C1 and 1C3 with a 6 inch rib module and 24 inches for specimens 1C2a, 1C2b, and 1C4 with a 12 inch rib module. Note that the spacing never exceeded the maximum recommended for solid slab construction. All single studs were welded to the outstanding legs of the flanges in a staggered pattern.

2.3 Control Tests

In order to determine the characteristics of the elements which made up the composite beams, control tests of the elements were conducted. For each of the elements, a description of these tests and their results follow.

2.3.1 Steel Beams

The properties of the W16 X 40 and W16 X 45 sections of A572, Grade 50 steel used for fabrication of the beams were determined from standard tensile test specimens. Since the steel beams came from different heats of steel, the coupons were machined from a 24 inch section of each beam, flame cut a few feet from the support. A total of 4 coupons were taken per beam: 2 from the web and 2 from the bottom flange.

Results from the steel tensile coupon tests are summarized in Table 3. The variances between the web and flange properties for each beam were not great; however, the properties of the web tended to be higher for all specimens. The average properties of the steel coupons which correspond to each specimen are listed in Table 2. These include the static yield strength for both the flange and web.

The static yield stress was used in the analysis of the specimens because it most closely approximates the steel strength expected from the specimen, considering the rate of loading. The measured yield stress for all of the specimens was much higher than that anticipated for Grade 50 steel; in fact it more closely approximated that of a Grade 65 steel. Since the steel strength profoundly effects the overall strength of the composite member, the strength predictions for each member using the theory described in Chapter 3, were based on the actual strength of the steel. The modulus of elasticity of the steel was taken as 29×10^3 ksi.

A typical stress-strain curve for a flange coupon from specimen 1C2a is given in Fig. 8.

2.3.2 Concrete Slabs

The structural lightweight concrete used for the slabs was made with Nytralite expanded shale aggregate following the mix design given in Table 4. All of the concrete mixes satisfied the requirements of ASTM C330 (Specification for Lightweight Aggregates for Structural Concrete). The cement was Type 1 Portland Cement; the fine aggregate was sand.

The plastic consistency (slump) was measured for each mix. Air content was periodically checked on a few mixes. Normally the slump was 3 - 4 inches and the air content was 5 - 7% as determined by a volumetric meter.

At the same time the beam specimens were cast, six standard 6 inch by 12 inch control cylinders were also cast to determine the compressive strength, tensile strength, modulus of elasticity and density of the concrete. In conjunction with the beam specimens the cylinders were moist cured for 14 days, then stripped and air cured until the day of testing.

The cylinders used to determine the concrete compressive strength were capped with a sulfur capping compound and tested according to ASTM Standard 39 (Standard Method of Test for Compressive Strength of Molded Concrete Cylinders).

The concrete tensile strength was obtained from split cylinder tests as described in ASTM C496 (Methods of Test for Splitting Tensile Strength of Molded Concrete Cylinders).

The modulus of elasticity was obtained from the compression test of the cylinders. In order to measure the strain, an averaging compressometer with a 6-inch gage length was mounted on the cylinder. During testing the dial gage was read at each 5 kip load increment which corresponded to a stress increment of 0.177 ksi. The modulus of elasticity was calculated from the difference in readings at 5 and 40 kips on the second cycle of loading to 50 percent of ultimate. Often the modulus of elasticity is taken as the tangent modulus at zero load.

Obviously this might result in a slightly higher value than the secant modulus determined from the deformations at 5 and 40 kips.

The density of the concrete was determined from the weight and volume of the cylinders. The volume was computed from the average dimensions of the cylinders.

The results of the concrete cylinder tests are listed in Table 5. The variance was not significant within each batch of concrete. The average properties of the cylinders that correspond to the beam specimen are listed in Table 2. These include the concrete compressive strength f'_c and the modulus of elasticity, E_c. A typical load-strain curve for the elastic range is given in Fig. 9.

2.3.3. Stud Shear Connectors

The stud shear connectors conformed to ASTM A108 specification and were welded directly through the metal decking to the upper beam flange using a stud welding gun. The soundness of the weld was tested by hitting the stud with a heavy hammer. Those studs with questionable welds were bent 45 degrees from vertical. Those sustaining the deformation were bent back to vertical; those not were replaced.

The ultimate tensile strength of the stud shear connectors, as provided in a mill report accompanying the studs, are summarized in Table 6. Greater detail was not taken in determining the tensile properties of the studs, since the degree of partial shear connection and strength of the concrete were sufficiently low so as to insure that tensile or shear failure of the stud would not occur.

2.3.4. Slab Reinforcement

The 6 x 6, 10/10 welded wire fabric used as shrinkage and temperature reinforcement in the slab conformed to ASTM A/85-64 specifications. No control tests were performed on the reinforcement.

2.4 Test Procedure

Load was applied hydraulically to the beam specimens utilizing the 5,000 kip testing machine in Fritz Engineering Laboratory. The load was distributed to four transverse spreader beams, approximately equally spaced, by means of a series of three simply supported loading beams. Sheets of 0.5 inch Homosite were placed under the transverse spreader beams in order to obtain a uniform load distribution on the bearing surface of the slabs. Both specimens 1C1 and 1C3 were simply supported on a clear span of 24'-0". Specimens 1C2a, 1C2b and 1C4 were supported on a span of 32'-0". The test setup for the specimens is shown in Fig. 10.

Each beam specimen was loaded in small increments of 5 or 10 kips from zero load to approximately its working load. Each beam was then cycles ten times between 5 kips and its working load. After cycling, the beams were again loaded in increments to near the ultimate load. At load levels near ultimate, load relaxation was observed, accompanied by unstable deflections and slips. Readings were taken when the displacement stabilized. The load recorded was the maximum load obtained. Once on the plateau of the load-deflection curve, load was applied to produce fixed increments of deflection. Loading was terminated when

deflections became excessive. For the specimens reported herein, the final midspan deflection measurements ranged between 13 and 21 inches.

2.5 Instrumentation

The instrumentation used for each test consisted of dail gages to measure end slip and centerline deflections, electrical slip gages to measure other slips at specified locations, and electric resistance strain gages for strain measurements.

A 0.001 inch dial gage was used to measure the deflection at midspan and the slip between the top flange of the steel beam and the midheight of the solid part of the concrete slab at each end of the beam.

To relate connector displacements with connector forces, slip measurements of the concrete slab between ribs were taken relative to the steel beam flange. Slip measurements of the slab directly at a rib containing connectors were found to contain a contribution due to rotation. Therefore threaded steel rods, 3/8 of an inch in diameter, were embedded in the solid part of the slab in the void on either side of a rib containing a connector group. The rods were embedded 2 inches in the slab at a distance of 1-1/2 inches from the edge of the steel beam flange. Placement of the rods is shown in Fig. 11. The movement of these rods was then averaged fro the relative displacement of the connector.

To determine the force on an isolated connector group, six Type 60 electrical resistance strain gages were placed on the steel beam,

either side of the connector group in a plane coincident with slip rods described above. This placement is shown in Fig. 12.

For all of the specimens except one, a total of four connector groups were isolated as described above. These four groups were all located on one half of the beam. For specimen 1C2a, a total of ten connector groups were so isolated, five per half-beam symmetrically located about midspan. Strain gages on the web were eliminated at two of the five locations nearest the supports. The connector groups isolated on each of the specimens are circled in Figs. 1 through 5.

The top of the slab on specimen 1C2a was also gaged to determine the transverse stress distribution and to confirm that the shear lag conditions were comparable to solid slab construction. The gages were Type A9 electrical resistance strain gages. The gages were placed symmetrically about the centerline of the slab with a 16 inch spacing at two locations. The locations were 54 inches and 126 inches from the end support.

3. THEORETICAL ANALYSIS

3.1 Connectors

The design criteria for the connector force was based on the following formula advanced by Fisher[1].

$$Q_{u\text{-}rib} = 0.5 \frac{w}{h} Q_{u\text{-}sol}$$

where

$Q_{u\text{-}rib}$ = ultimate shear connector strength in a cellular rib

$Q_{u\text{-}sol}$ = ultimate shear connector strength in a solid slab

w = average rib width

h = rib height

Ollgaard[3] has determined the strength of stud shear connectors in lightweight and normal weight concrete solid slabs as

$$Q_{u\text{-}sol} = 1.106\, A_s\, f_c'^{0.3}\, E_c^{0.44}$$

where f_c' and E_c are in ksi and A_s in the normal stud area. The current AISC design values for normal weight concrete were found to be about half that connector strength[3].

The allowable shear connector strength in a cellular rib used to determine the working load was taken as one-half Q_u-rib.

Computations of the shear connector strength for specimen IC2a are given in Appendix A as an example.

3.2 Beams

3.2.1 Working Load

The working load strength of the specimens was computed in accordance with AISC Specification for composite beams with the modifications recommended by Fisher[1] to account for the effect of the metal decking.

The elastic properties for the composite section were determined on the basis of the moment of inertia of the transformed composite section assuming only the concrete above the metal deck to be effective. However, the full slab depth including the ribs was used to determine the effective width of the slab.

The section modulus for the beams was determined by the linear interpolation formula in the AISC Specification shown below to account for the partial shear connection.

$$S_{eff} = S_s + \frac{V_h'}{V_h} (S_b - S_s)$$

where

S_s = section modulus of steel section

S_b = section modulus of the bottom flange of the composite section

V_h' = the total horizontal shear for a partial shear connection (ΣQ_u-rib)

V_h = the total horizontal shear for a full shear connection.

For the deflection computations the beams were assumed to be as stiff as they would be if they had a full shear connection.

An example of the computations of the working load strength are given in Appendix B for Specimen IC2a.

3.2.2 Ultimate Strength

The method for computing the flexural capacity of the beams is essentially that suggested by Slutter and Driscoll[4] for composite beams. The slab force was assumed to be equal to the number of connectors in the shear span multiplied by their ultimate load as determined in Sec. 3.1. It was further assumed that the slab force acts at the centroid of the solid portion of the concrete slab above the top of the ribs. The same composite section considered for allowable stress computations is assumed for ultimate strength analysis.

The ultimate strength computations for Specimen IC2a are given in Appendix C as an example.

4. TEST RESULTS AND ANALYSIS

4.1 Load Deflection Behavior

Figures 13 through 17 show the complete load-deflection curves for the five specimens reported herein. The predicted working load, yield load, and the idealized elastic-plastic load deflection curves are indicated in these plots. Figure 18 shows the load-deflection curves within the working load range for all the specimens, plotted on a non-dimensionalized scale. The dead load due to the wet concrete and the self weight of the beam has been accounted for.

All of the specimens were found to be 30 to 40 percent more flexible at the working load than similar specimens assuming full shear connection. In addition the loss of flexibility seemed to vary in proportion to the degree of partial shear connection, with the exception of Specimen 1C4. Baldwin[5] has shown that similar losses in stiffness can be expected for solid slab composite beams with the same degrees of partial shear connection. In fact, even for a 100 percent shear connection, Baldwin found that losses on the order of 15 percent can be expected. The question to consider here is how significant is this loss of stiffness. The practice described in the AISC specification for solid slab construction is to ignore the loss in stiffness but limit the degree of partial shear connection to 50 percent. This seems reasonable since losses of 15 percent are not significant.

When the partial shear connection was less than 50 percent the losses in stiffness increased by another 20 percent. The question then becomes--is this additional loss acceptable and if so can it be ignored?

To address the first part of this question consider not the loss in stiffness from an ideal composite system, but rather the gain in stiffness over a non-composite system. A comparison of such a gain in stiffness is shown in Fig. 19 for the specimens reported herein. Beam stiffness is non-dimensionalized on the ordinate by dividing it by the idealized stiffness of a non-composite system. The degree of partial shear connection is shown on the abscissa. The specimens reported herein are shown on the plot along with the idealized stiffness if fully composite. From this plot, it is obvious that the gain in stiffness for specimens with a very low degree of shear connection is quite high when compared to a non-composite system. In fact, it is almost equal to a fully composite system, if a 15 percent loss from the idealized case is taken into consideration. From such a comparison the loss in stiffness associated with decreasing degrees of shear connection seems insignificant. But can it be ignored?

For cases where deflections are not of major concern it would seem as justifiable to ignore them at very low degrees of partial shear connection as it does to ignore them at shear connections of 50 percent. However, for cases where deflections are of concern, they could be accounted for. Baldwin[5] demonstrates for solid slab construction that a linear interpolation of the beam stiffness with respect to the degree of shear connection (similar to the AISC Specification

for effective section modulus) is conservative at shear connections of 80 percent and less. Defining such a linear interpolation as an "effective" stiffness, a comparison can be made between the actual and the "effictive" stiffnesses for the specimens reported herein. Such a comparison is made in Fig. 20. In this figure the measured stiffness of each specimen is non-dimensionalized by its corresponding "effective" stiffness on the ordinate. The degree of partial shear connection is shown on the abscissa. For all the specimens the "effective" stiffness is shown to be very conservative; extremely so for the lower degrees of shear connection.

A better "effective" stiffness could be defined by a parabola of the form:

$$EI_{eff} = EI_s + \sqrt{\frac{V'_h}{V_h}} (EI_c - EI_s)$$

where EI_c and EI_s are the stiffnesses of the composite and non-composite systems, respectively, and V'_h/V_h is the degree of partial shear connection. This second definition of "effective" stiffness is also compared to the measured stiffnesses in Fig. 20. It is apparent from this plot that this "effective" stiffness is a much better approximation of the actual stiffness and at worst is no less accurate than the accepted expression for stiffness at a 100 percent shear connection in a solid slab composite beam. Thus, in cases where deflections can not be ignored they could be accounted for to the degree desired in members with low degrees of partial shear connection.

Comparable permanent sets in the specimens after unloading from the working load were not directly obtainable since the working load predicted before testing was based on assumed steel properties and deviated from the actual working load in most cases. However, a permanent set of about 20 percent of the predicted working load deflection seems to be a reasonable evaluation.

For all of the specimens except 1C4 yielding of the bottom flange was observed at or above the predicted yield load level, as indicated on Figs. 13 through 17. The observed yielding typically defined the beginning of the "knee" portion of the load deflection curve. Also characteristic of all the load-deflection curves was an observed plastic hinge near midspan at the end of the knee portion where the plateau begins. This observation is also noted in Figs. 13 through 17.

All of the specimens fell within ± 6 percent of their predicted ultimate load, thus demonstrating considerable reliability in the recommended design criteria[1]. The actual and predicted flexural capacity for each specimen is shown in Table 2. Also the specimens all demonstrated considerable ductility which is indicated by midspan deflections between 13 and 22 inches. These values represent deflections in excess of 15 times the predicted working load deflection for all of the specimens.

There were three major differences between the two specimens which slightly exceeded their predicted ultimate and the three which fell just short. These differences are: (1) span length; (2) connector

spacing; and (3) number of connectors per rib. The first difference, span length, should have little effect on beam strength since the shear and moment gradients were the same for all specimens. Studies on connector spacing have indicated that spacing may have an effect on the performance and strength of composite beams[6]. However, the range over which the specimens deviate from their predicted ultimates is too small and the number of specimens presented herein is too few to conclude anything specific concerning connector spacing. It seems reasonable to assume that the effect of connector spacing in composite beams with solid slabs is about the same for composite beams with formed metal deck and that the closer the connector spacing the better.

Lastly, it was found for the specimens reported herein that the ratio of maximum test moments to predicted flexural capacity tended to decrease as the ratio of ribs with two connectors per rib to the total number of ribs with connectors increased. Robinson[7] has noted that ribs with double connectors do not provide twice the strength of ribs with single connectors. However, the model developed in Ref. (1) for connector strength in a rib was based on pushout specimens with two connectors in a rib and beam tests with single and double connectors. Therefore, it should provide a lower limit on the average connector strength. Thus, as with connector spacing, the deviation from predicted beam strength is too small and the number of specimens reported herein are too few to conclude anything other than that the more single connectors per rib the better.

Another way to evaluate the recommended design criteria[1] is to consider the safety factor for each specimen. The factor of safety may

be considered as the ratio of the maximum flexural capacity observed to the calculated working load moment. Such ratios have been computed and are listed in Table 2 for each of the specimens. All of the specimens have a factor of safety between 2.20 and 1.90 with Specimen 1C4 representing the lower end of this range. The factors of safety support the recommended design criteria. A comparison of working load moment based on the recommended criteria with the flexural capacity of available beam tests[8] as a function of the rib width over height ratio and the degree of partial shear connection is shown in Figs. 21 and 22 respectively. Superimposed on these plots are data from the specimens reported herein. The data for these specimens agree with the results of earlier studies.

4.2 Load-Strain Behavior

For Specimens 1C2a and 1C4, the strain in the bottom fiber at midspan is plotted as the abscissa with the applied load as an ordinate in Figs. 23 and 24, respectively. Specimen 1C2a demonstrated load-strain behavior typical of all of the specimens except Specimen 1C4. The yield load and the yield strain is indicated on each graph for reference. Both the loads and the strains have the dead load effect subtracted. Also shown in the figures are the idealized linear slopes of the load-strain curves for both a rigid connection and the actual partial shear connection of the member using the AISC effective section modulus.

All of the specimens exhibited a linear load-strain relationship in the working load range. Above the working load, the load-strain

curves become increasingly non-linear until at the yield strain they begin a plateau. The slope of the load-strain curve is a function of the elastic modulus, the section modulus, and the length only. The length is constant and the section modulus is a function of the degree of shear connection and the cross section geometry. Therefore, the deviation from linearity before reaching the yield strain can only be attributed to the material properties of the high strength steel and/or a breakdown in the shear connection. For all of the specimens except 1C4, it was observed that the load-strain curves deviate from linearity at about the same strain that non-linearity begins on the stress-strain curves of the control specimens. Also, for these specimens the deviation from linearity at the yield strain for the load strain curves is comparable to that for the stress-strain curves. Compare, for example, the stress-strain curve for Specimen 1C2a shown in Fig. 8 with Fig. 23. Therefore, for the specimens reported herein, it is believed that the non-linearity of the load-strain curve below the yield level is due to the non-linearity of the stress-strain relationship of the high strength steel and not a breakdown in the shear connection.

For specimen 1C4, however, the pattern described above was not observed. Deviation from linearity on the load-strain curve occurs at a much lower strain than that observed for the steel stress-strain curve. Also the deviation at the yield strain is much greater on the load-strain curve than on the stress-strain curve. Therefore, it is reasoned that a change in shear connection must occur during the loading to affect the section modulus.

It is interesting to note the linearity of the load-strain curves in the working load range for all specimens when considering the section modulus of the members. Since the linearity implies constant variables, the load-strain plots show that the effective section modulus calculated from the AISC formula is a conservative approximation of the actual section modulus. This difference between the actual and predicted section modulus is in line with the previous discussion on beam stiffness presented in Section 4.1 above. Also Baldwin[5] has noted similar discrepencies between actual and predicted section modulus for solid slab composite beams.

For Specimen 1C2a additional strain measurements were taken on the top surface of the concrete slab. The measurements were taken at the locations described in Section 2.5 and the distribution of strain for various load levels across the slab at the innermost location is shown in Fig. 25. The sections instrumented showed an increase in the strain distribution for each load level up to the onset of longitudinal cracking. At this point both sections showed a drop in strain across the slab. The section nearest the end then showed an increase in strain for successive load increments while at the section further in from the support a continued decrease was observed. These strain distributions indicate the effectiveness of the full width of the slab in accounting for the non-uniform distribution of stress across the slab due to shear lag. These distributions were found to be in agreement with both theoretical predictions[9] and a previous test on a composite beam with formed metal deck and a full shear connection[10]. For comparison purposes the equivalent uniform strain distribution required

in the slab for an applied load of 45 kips, approximately the working load, is shown as a dotted line in Fig. 25. This distribution assumes an adequate shear connection. It is seen to lay just above the actual strain distribution for this load as would be expected.

4.3 Load-Slip Behavior

For Specimens 1C2a and 1C4 the slip between the slab and the beam at the ends was plotted as the abscissa in Figs. 26 and 27, respectively with the applied load as the ordinate. The working, yield, ultimate load levels minus the dead load are indicated on each graph. The plot for Specimen 1C2a is typical of all the specimens except Specimen 1C4.

All of the specimens except 1C4 had similar slips on either end of the member until within 4 percent of their ultimate load. For these four specimens the ratios of the maximum end-slips ranged between 1.1 and 1.6. For specimen 1C4, the end slips begin to deviate about halfway between the working and the yield load levels or at about 60 percent of the ultimate load. The ratio of the maximum end slips for specimen 1C4 was found to be 2.5. All of the specimens behaved symmetrically about midspan except 1C4.

The amount of slip at the working load after 10 cycles of loading was observed to be between 0.04 and 0.11 inches for all specimens. The amount of slip was generally found to be inversely proportional to the degree of partial shear connection with the exception of Specimen 1C4.

All of the load-slip curves become non-linear after the first few increments of load during the first cycle. Thereafter, they all

demonstrate linearity up to their unloading point on the tenth cycle of load. The loss of slip between the first and tenth cycle at the unloading point ranged from 0.005 to 0.015 inches, or about 10 percent of the total slip after ten cycles.

As the load approached ultimate the load-slip curves become nearly horizontal. The corresponding slips at the beginning of this plateau range from 0.5 to 0.8 inches for all the specimens. The maximum slip recorded before termination of testing in all cases was observed to range from 1 to 2.4 inches or about 20 times the slip at working load, thus demonstrating considerable ductility of the shear connection.

The method for determining the slip of the connector group relative to the steel beam flange was described in Section 2.5. Slip was measured on either side of the connector as opposed to right at the rib because it had been observed in previous tests that the deformation of the rib contained a contribution due to rotation as well as translation. This rotation resulted from the cracking of the corner of the concrete rib and the simultaneous bending deformation of the stud embedded in the cracked rib. The slip on either side of the connection group was then averaged to obtain the relative slip of the connector. The single exception to this procedure was for the outermost gaged section nearest the support on both ends of specimen 1C2a. This section corresponded to the last connector group in the shear span and experienced rotation. Hence only the reading of the gage on the other side of the connector group was taken.

The slip distributions for each specimen are typified by the distribution shown in Fig. 38 for Specimen 1C3. The distributions shown are for a load near the working load, a load near the yield load and a load near failure. A study of such plots reveals that the slips seem to occur on two plateaus which is consistent with the amount of shear present at these locations. Also one would expect the magnitude of the slip to increase from the center of the span towards the support. However, a slight deviation in this expected behavior was noted in the specimens with a 32 foot span at those sections nearest the support for load levels approaching the ultimate load. These deviations can be attributed to the decrease in sensitivity of the electronic slip gage to these large slips. Also these deviations could reflect some rotation in the slab. If this latter possibility was correct, it would matter little in relating the force on the connector to these slips since the connector force has already reached its maximum value for all practical purposes.

4.4 Failure

As the load approached the ultimate strength the stud shear connectors attempted to punch out through the ribs. There were only a few isolated incidences of horizontal shear cracking at the top of the concrete ribs: one in Specimen 1C2a and three in Specimen 1C2b. The photograph in Fig. 29 shows a typical rib failure. Figure 30 shows one of the few incidences of horizontal shear cracking.

Coincident with the onset of rib failure was the formation of a plastic hinge. It generally formed under one of the two interior load points and in three of the five specimens preceded the local buckling of the flange of the steel beam in the same region. Photographs of a typical plastic hinge and a buckled compression flange are provided in Figs. 11 and 12, respectively. Also, the first observation that a plastic hinge had formed is indicated on the load-deflection curves in Figs. 13 through 17.

It was also observed that a certain amount of slab uplift between ribs with connectors was present in all specimens at ultimate load. It has been shown that the presence of uplift tends to decrease the ultimate strength of connectors embedded in a solid slab[3]. This decrease in strength would also seem reasonable for slabs with metal deck since the slab is acting as an eccentrically loaded compression member, spanning between connectors, with no vertical restraint between connectors. The uplift forces caused by bowing of the slab away from the steel beam must then be counteracted by tensile forces in the connectors which act in combination with shearing stresses. The maximum uplift was found to be as little as 1/8 inch for Specimen 1C1, approximately 1/2 inch for Specimens 1C2a, 1C2b and 1C3, and as much as 1 inch for Specimen 1C3. The first observed occurrence of slab uplift is indicated on the load deflection curves in Figs. 13 through 17. This uplift occurred first and most prominently in the outer shear span, between the support and the outermost load point, on each end. Figure 33 is a photograph showing typical slab uplift.

Contributing to the general deterioration of the concrete slab, and therefore possibly to the shear connection in the beam, were several localized failures common to all of the specimens. One of these was flexural cracks which originated at the bottom of the solid part of the slab near a rib corner and progressed upwards in the manner of diagonal tensile cracks. These cracks occurred only in the region of the load points and always at the outer load points first. The fact that the load points are points of sudden changes in shear is probably related to the formation of these type cracks. Also these flexural cracks could in part be due to the restraint of rib rotation by the transverse spreader beams. The flexural cracks were also noted to occur at about the same time that yielding was observed in the bottom flange as indicated on the load deflection curves, Figs. 13 through 17. Figure 34 is a photograph of a typical flexural crack.

Another localized failure commonly observed for all the specimens was the longitudinal cracking of the concrete slab along its centerline at approximately the working load. These cracks first appeared on the upper surface of the slab as hairline cracks in the outer shear spans extending from the outer load points to the end of the beam then propagated along the entire major axis of the slab as loading progressed. In some instances, particularly near midspan the main cracks dispersed into two or three parallel cracks, 4 to 6 inches apart or approximately the width of the steel beam flange. The cracks gradually opened up and appeared to penetrate the entire thickness of the solid part of the slab above the ribs, but in no case was the cracking severe until very near the ultimate load. This longitudinal cracking was caused by the

transverse warping of the slab developed by the loading condition and was resisted by the nominal wire mesh reinforcement as well as the metal decking. For service load conditions this amount of resistance appeared adequate. The first incidence of longitudinal cracking observed for each specimen is indicated in Figs. 13 through 17 and Figs. 35 and 36 show typical longitudinal cracking and transverse warping, respectively.

Generally accompanying the longitudinal cracking of the slabs was bond failure between the metal deck and the slab. The first observance of bond failure is indicated in Figs. 13 through 17. The amount of separation between the deck and the slab was very slight at first but became quite pronounced as the ultimate load was approached. The loss of stiffness of the slab due to bond failure probably contributed to the amount of uplift mentioned previously. Also, considering that bond failure occurred at the service loads for these specimens, it is pertinent to recall that the metal decking used in these specimens had no embossments. Embossments are commonly found on commercially produced deck and are generally considered to contribute to the bond strength. Though difficult to evaluate, a comparison with tests on solid slab composite beams revealed that bond failure did not influence the behavior on strength of the specimens. Typical bond failure at ultimate load is shown in Fig. 37.

Commonly preceding longitudinal cracking and bond failure in all of the specimens was the occurrence of transverse, negative moment type cracking in the top of the slab just inside the first and second connector groups from each end of the beam. These cracks occurred

because in the region near the support the local negative moment produced rotation of the rib due to the transfer of the horizontal shear force. The occurrence of these cracks is noted on the load-deflection curves, Figs 13 through 17 and Fig. 38 shows some typical cracks.

Another factor which contributed to the failure of Specimen 1C4 was the lack of symmetry in behavior about the midspan. This lack of symmetrical behavior was most evident in the load-slip behavior of the beam as discussed in Section 4.3 and illustrated in Fig. 27. There are two possible explanations for this lack of symmetry: (1) a shear connector failure, or (2) a misalignment in the test setup. As discussed in Section 4.3, the effective section modulus seems to have been affected at the working load level for this specimen. However, it should be noted that no sudden localized failure, such as a connector shearing off, was observed during testing that would indicate premature failure. Rather, by comparison of the load deflection behavior with the other specimens, the performance of Specimen 1C4 is similar. See, for example, the load-deflection curves with observations noted in Figs. 13 through 17. Thus the possibility of a premature connector failure is doubtful.

The only other plausible explanation for the unsymmetrical but otherwise similar behavior and the lower than predicted strength is misalignment of the load beams. It can be shown that a small misalignment in the load points could produce a 5 percent reduction in the load carrying capacity of the members, which is consistent with the 6

percent lower than predicted strength experience by Specimen 1C4. Although carefully aligned prior to testing, the specimen as well as the load beams were supported on rollers. Some change in loading could have occurred, but was not apparent during the test.

For whatever reason this non-symmetrical behavior occurred, its effect on beam strength, though detrimental, was small. The deviation between actual and predicted flexural capacities for Specimen 1C4 was on the same order as that of the other specimens reported herein.

4.5 Connector Force - Load Behavior

The forces on a connector group were obtained by measuring the strain profiles on either side of a connector group as described in Section 2.5. These profiles were then converted to stress distributions, which were integrated to determine the net force and moment in the steel beam. The force in the slab was then found from equilibrium. Assuming that all the shear is transmitted by the shear connectors, the force in the shear connector group must then be equal to the difference in slab force on either side of the connector group.

The value of the slab force was checked by comparing the internal moment to the external moment using the model shown schematically in Fig. 39. It assumes that the slab and beam have equal curvatures. The horizontal force, F, transmitted between the slab and beam by connectors is assumed to act at the centroids of the solid part of the slab and the beam cross sections. The total internal moment is then equal to the sum of the individual moments in the slab and beam, M_s

and M_b, respectively, plus the additional couple due to the horizontal forces, F. Thus

$$M = M_b + M_s + Fz$$

where z equals the distance between the centroids of the beam and slab cross sections.

The only unknown in the above expression is the moment in the slab, M_s. There was no way to gage the slab to accurately determine the strain distribution and thereby the resulting slab force and moment because of the metal decking on the bottom side of the slab. However, in regions of high moment, near the middle of the span, the maximum contribution that this slab moment could make is negligible in comparison to the combined moment produced by the steel beam moment, M_b, and the couple resulting from the horizontal forces, Fz. Therefore, the slab moment was assumed to equal zero.

The effect of assuming the slab moment equal to zero for the above model is that any difference between the external and internal moments reflects the slab moment. For a check on the slab force to be reliable using this model, the difference would have to be negligible near the middle of the span. Good correlation between internal and external moments was observed for all isolated connector groups except those near a support. The average difference between the two was less than 5 percent of the external bending moment for those connectors greater than 5 feet from the end. For the other connector groups the difference was as great as 25 percent. Therefore, it was concluded that the strain distributions away from the support accurately reflect

the slab force and, thus, the force on the connector group. Since the strain distributions at sections near a support were found to be in agreement with those near midspan it is believed that they reflect the actual slab force also and that the difference between external and internal moments in these regions gives a good indication of the actual moment in the slab.

For Specimens 1C2a and 1C3 the connector force, Q, found by the above procedure, is plotted as a function of the load in Figs. 40 and 41 respectively. These plots are representative of similar plots for the other specimens. For comparison purposes both the connection force and the load are plotted on a non-dimensional scale as Q/Q_u versus P/P_u where Q_u is the ultimate rib strength and P_u is the ultimate load, both of which are predicted by the theory discussed in Section 3. The working load and yield load were found to be approximately 45 and 72 percent of the ultimate load, respectively for all of the specimens and are so indicated on the plots.

A study of the plots reveals a pattern which is idealized in Fig. 42. First, these plots indicate that those connector groups in the outer shear span redistribute shear forces to those in the inner shear span as the load is increased. The outer connector groups seem to reach a peak in their connector force value at about the working load then fall off slightly. As these outer connector groups begin to experience a decrease in resistance the inner connector groups begin to resist more force. Nearly all of the connector groups for all of the specimens exhibit this characteristic. One of the outer connector

groups in Specimen 1C4 did not peak near the working load level, but continued to increase in value until near ultimate. For Specimens 1C2a and 1C2b this trend varied slightly in that the peaks for the inner and outer connector groups occurred near the yield load level. The connector force values seems to average between 1/2 to 3/4 of Q_u throughout the loading range until the ultimate load is approached. Connector force values of this magnitude are consistent with the theoretical predictions for beam strength which assume a connector force equal to 1/2 Q_u at both working and yield loads. Both Specimens 1C2a and 1C2b deviated from this second generalization. The average value of the connector force for these specimens seems to be steadily increasing with values slightly below Q_u at the working load level and slightly higher than Q_u at the yield load level. As the ultimate load is approached and the plateau is begun on the load deflection curve, the connector force values are seen to increase and often exceed their predicted capacity. This behavior is also in line with the theoretical model used to predict strength and behavior. As the plastic hinge starts to form, the neutral axis will shift and the connectors are subjected to increasing load and finally equal or exceed their expected capacity. Thus with a reasonable amount of tolerance for the scatter typical of test data, it can be seen from the connector force versus load plots that the specimens generally behaved in the manner predicted.

4.6 Connector Force - Slip Behavior

The connector forces were related to the localized slips at the connector. A non-dimensional plot of the connector force over its

predicted ultimate value as a function of its slip is shown in Figs. 43 through 47 for each of the specimens. For ribs with two connectors, the predicted ultimate strength is twice that of one connection.

A general trend or pattern is not as readily obvious for these plots as was the case for the connector force-load and load-slip plots. The Q/Q_u curves generally rise in a non-linear fashion and then level off or peak and drop to some slightly lower value for a considerable amount of deformation. The curves do behave linearly upon reloading as can readily be seen in Fig. 55 for Specimen 1C2a. The dotted non-linear lines indicates the first cycle of loading and the solid lines show behavior on the last cycle.

The load-slip relationship for continuous loading of stud shear connectors in composite beams with solid slabs has been determined[3] as:

$$Q/Q_u = (1 - e^{-18\gamma})0.4$$

where:

Q = connector force

Q_u = ultimate connector strength

γ = connector slip relative to steel beam flange

This relationship is shown on the connector force - slip plots for each specimen, see Figs. 43 through 47.

The connector force - slip curves shown in the figures bear a remarkable resemblance to the load-slip relationship for solid slabs. This observation is further substantiated by the connector load-slip curves presented in Ref. (5). In fact only the magnitude of the

ordinate in these figures is different. Therefore, if each connector group were plotted on a non-dimensional scale of the connector force divided by the ultimate connector force obtained for that group, the resulting curves would within experimental tolerances, be the same curve as for solid slabs.

Because of the load level to which the composite beam was loaded prior to cycling, the difference in behavior of the connector for continuous loading and reloading is not distinguishable except for Specimen 1C2a. The initial load level prior to cycling was quite high for this specimen and the resulting initial connector load-slip curves are easily identified in Fig. 45. The initial loading curves for Specimen 1C2a are also compatible with the load-displacement expression found for solid slabs. The stiffness of the reloading curve is observed to be considerably less than obtained for connectors in solid slabs. Ollgaard[3] found the initial slope of the reloading curve of solid slabs to be about 80.

The initial slope of the reloading curves for connectors between the end support and the first load point was found to be between 10 and 20. For connectors between the first and second load points the slope was between 25 and 35. Specimen 1C3 provided steeper slopes which were between 35 and 50. This decrease in stiffness for connectors embedded in slabs with metal decking seems reasonable since there is less concrete around the connector and hence it is more susceptible to permanent deformation during loading. Ollgaard's expression for reloading is dependent on the level of preload and slip. A similar

dependency is noted for connectors in slabs with metal deck and explains the difference in slopes of the reloading curves for connectors near the support and those closer to midspan.

4.7 Ultimate Connector Strength

The maximum load obtained for each of the specimens was used to find the average ultimate connector force acting in the member at failure. The value of this average force divided by the predicted ultimate connector force is indicated on the non-dimensional connector force-slip plots in Figs. 43 through 47. This average ultimate value compares favorably with the average maximum connector force shown on the Q/Q_u - γ plot in all cases but one. For Specimen 1C3 the average maximum value of the connector forces plotted is well below the average ultimate calculated. A plausible explanation for this occurrence is that the four connector groups isolated for instrumentation did not develop their full capacity and their shortage was carried by some of the other connectors or the friction developed by the ribs under a load point. This explanation can best be seen by considering the Q/Q_u - γ plot for Specimen 1C1 in Fig. 43. For this specimen three of the connector groups are lower than the average ultimate per connector group. However, the one remaining connector group peaks at a load in excess of the average ultimate value, then levels off at this value confirming the ability to redistribute force to other connectors as mentioned above. Also it must be remembered that the slip gages were disconnected as the load approached ultimate for the beam. Therefore, the strength of the connectors in this range

is not shown. However, the connector force - load curve for Specimen 1C3 showed an increase in the connector force for the two inner connector groups as the ultimate load of the beam was approached.

The relationship suggested by Fisher[1] was used to predict the ultimate strength of a connector in a rib. This relationship for connector strength as a function of the rib width over height ratio is given in Fig. 48. The average ultimate load per connector found from the maximum test load for each specimen is compared with this relationship. Also the measured ultimate values of the isolated connector groups is also shown. The comparison shows a substantial amount of scatter of the data. The original relationship was developed from push-off and beam tests. Comparable scatter was observed between the test data and the line fitted to it. The results are also reasonably compatible with the scatter in test data for solid slabs[3]. The comparison suggests that the relationship for ultimate connector strength in a beam is reasonable. It is also apparent that connectors can maintain enough strength and ductility to establish a predictable average.

The value of the average ultimate connector force is extremely sensitive to small changes in the applied moment near ultimate. It was found for the specimens discussed herein that a one percent change in the value of the ultimate moment caused approximately a four percent change in the value of the average ultimate connector force. A similar relationship can be shown to exist for solid slab composite beams. This relationship explains the amount of scatter of the test data found in Fig. 48. Also, considering the demonstrated ductility and

variability in strength of isolated connectors, this relationship indicates that the factor of safety for the connectors need not be emphasized as strongly as that for the flexural capacity of the composite member as a whole.

5. SUMMARY AND CONCLUSIONS

This study summarizes the results of tests on five high strength steel composite beams with formed metal deck and low partial shear connection. The purpose of the investigation was twofold: (1) to evaluate the capacity and behavior of both the composite beam as a whole as well as the stud shear connectors within the beams; and (2) to compare test results with existing design criteria.

The steel used was high strength A572, Grade 50. The sections selected were W16 X 40 for all test specimens except one which had a W16 X 45 section. The concrete was lightweight with a unit weight of 113 pcf and a design strength of 4000 psi. The slab thickness was kept constant at 2-1/2 inches above the metal deck rib. Slab width was set at 16 times the total slab thickness, including the height of the rib, plus the width of the steel beam flange. Minimal reinforcement of 6 inch x 6 inch, 10/10 welded wire mesh was used. The metal deck was plain 18 gauge. The rib heights of the deck were set at 1-1/2, 2, and 3 inches to establish variable rib width over height ratios of 1.5 and 2.0. The shear connectors were 3/4 inch diameter studs. Their embedment length was kept at a constant 1-1/2 inches above the top of the metal deck rib. Spacing of the connectors was at 12 and 24 inches. Single connectors were staggered on the flange to avoid placement directly over the web. The degree of partial shear connection varied between 20 and 50 percent.

The analytical model used to determine the connector strength was that recommended by Fisher[1]. Beam behavior was predicted from criteria outlined in the AISC Steel Construction Manual with adjustment for connector strength. The model used to compute the flexural capacity was that suggested by Slutter and Driscoll[4] with similar modifications of connector strength.

The characteristics of load as a function of midspan deflection, bottom fiber strain at midspan, and slips of the slab relative to the steel beam were obtained. Also the maximum load and failure modes were recorded. In order to evaluate the behavior of the studs, strain profiles were converted to stress distributions which were integrated to obtain net forces and moments. Assuming that shear is transmitted to the slab only by the shear connectors, the force on the connectors was found from equilibrium. These forces were correlated with slip measurements at the connector to obtain the load-slip behavior of the studs. The average ultimate strength of the connectors was obtained from the measured flexural capacity of the beams. Results were compared with the work of other investigators and with existing design criteria.

The conclusions drawn from this study are the following:

1. The load-deformation behavior of a stud shear connector in a composite beam with formed metal deck is similar to a connector in a solid slab composite beam. Furthermore the expression for the load-slip relationship of a stud connector embedded in a solid slab developed by Ollgaard[3] can be used with equal certainty to determine the load-slip relationship of connectors embedded in a slab with formed metal deck.

2. The average ultimate strength of a connector embedded in a rib may be accurately predicted from the expression $Q_{u\text{-}rib} = 1/2\ w/h\ Q_{u\text{-}sol}$. The variance of isolated connectors from this average strength is the same as that found for studs embedded in solid slab composite beams.

3. Composite beams with formed metal deck and low degrees of partial shear connection are less stiff than similar beams with adequate shear connection. However, this loss in stiffness is no more severe than that found in solid slab composite beams with the same degree of shear connection. Also this loss in stiffness is far less significant than the gain in stiffness to be found when compared to a similar beam slab system with no shear connector. For design purposes the loss in stiffness may be taken as an interpolation between the stiffness of the steel beam alone and that of the composite beam with adequate shear connection based on the degree of partial shear connection.

4. The flexural capacity of high strength steel composite beams with formed metal deck and low degrees of partial shear connection may be reliably predicted using the method developed by Slutter and Driscoll[4] for solid slab composite beams providing the ultimate connector strength is adjusted as recommended by Fisher[1].

5. Shear lag is no more severe in a slab with formed metal deck than in a solid slab. Therefore the effective slab width in composite beams with formed metal deck need not be limited anymore than for solid slab composite beams. In fact the effective slab width should be taken as wide as possible to provide maximum connector strength. Also

the effective slab width should take into account the total slab thickness including rib height when governed by the thickness.

6. Connector spacing in composite beams with formed metal deck need not be limited anymore than that for solid slab composite beams.

7. Ribs with a single connector provide a slightly better shear connection than those with double connectors with respect to beam strength although both are adequate.

TABLE 1 - EXPERIMENT DESIGN

Rib Ht. h		$w_1 = 1.5h$ Rib Width						$w_2 = 2.0h$ Rib Width	
	Spec	Section	Span	Studs/ Shear Span	Spec	Section	Span	Studs/ Shear Span
1½"	1C1	16 X 40	24'	11				
2 "								
3 "					1C3	16 X 40	24'	8
	1C2 a	16 X 40	32'	9				
	1C2 b	16 X 40	32'	12	1C4	16 X 45	32'	14

TABLE 2 - SUMMARY OF RESULTS

BEAM	f'_c (psi)	f_y* (ksi)	E_c (ksi)	Q_u (kips)	$\frac{V'h}{V_h}$	M_u (kip-ft)	M_{max} (kip-ft)	$\frac{M_{max}}{M_u}$	M_w (kip-ft)	$\frac{M_{max}}{M_w}$
1C1	4350	57.7f 62.4w	2490	17.8	0.294	479.6	507.9	1.060	230.7	2.200
1C2a	4130	66.0f 67.2w	2480	17.7	0.205	534.9	521.4	0.975	263.9	1.975
1C2b	3990	66.2f 69.1w	2540	17.4	0.267	568.9	534.4	0.938	274.4	1.945
1C3	4840	69.2f 74.7w	2500	24.5	0.240	564.3	576.1	1.022	274.8	2.095
1C4	3250	64.9f 68.2w	2090	20.1	0.425	660.1	617.8	0.937	324.9	1.900

*f denotes flange specimen
w denotes web specimen

TABLE 3 - STEEL PROPERTIES

BEAM	NUMBER OF SPECIMEN	STATIC YIELD STRESS (KSI)	ULTIMATE STRENGTH (KSI)	PERCENT ELONGATION	MODULUS OF ELASTICITY IN TENSION (KSI)
1C1	1 w	63.3	85.9	22.1	30.6
	2 w	61.5	84.8	22.9	30.2
	Average w	62.4	85.4	22.5	30.4
	3 f	57.1	84.6	22.9	28.5
	4 f	58.3	61.0	24.8	28.3
	Average f	57.7	72.8	23.9	28.4
	Average	60.1	79.1	23.2	29.4
1C2a	1 w	67.9	87.4	20.7	30.3
	2 w	66.5	86.7	20.7	29.8
	Average w	67.2	87.1	20.7	30.0
	3 f	66.4	91.1	20.9	29.5
	4 f	65.5	91.6	21.5	30.6
	Average f	66.0	91.4	21.2	30.1
	Average	66.6	89.3	21.0	30.1
1C2b	1 w	69.6	89.8	20.4	29.8
	2 w	68.5	89.4	20.2	29.7
	Average w	69.1	89.6	20.3	28.8
	3 f	65.6	91.8	21.1	28.8
	4 f	66.7	94.6	20.2	29.1
	Average f	66.2	93.2	20.7	29.0
	Average	67.7	91.4	20.5	28.9
1C3	1 w	74.5	98.6	20.5	29.9
	2 w	74.9	99.4	20.2	29.7
	Average w	74.7	99.0	20.4	29.8
	3 f	69.6	97.3	20.0	28.9
	4 f	68.8	98.4	19.8	29.1
	Average f	69.2	97.9	19.9	29.0
	Average	72.0	98.4	20.1	29.4

TABLE 3 - STEEL PROPERTIES (continued)

BEAM	NUMBER OF SPECIMEN	STATIC YIELD STRESS (KSI)	ULTIMATE STRENGTH (KSI)	PERCENT ELONGATION	MODULES OF ELASTICITY IN TENSION (KSI)
IC4	1 w	69.0	90.6	19.7	29.5
	2 w	67.3	89.3	20.4	29.7
	Average w	68.2	90.0	20.1	29.6
	3 f	64.8	93.2	21.5	27.9
	4 f	64.9	92.2	22.4	28.3
	Average f	64.9	92.7	22.0	28.2
	Average	66.6	91.3	21.0	28.9

Footnotes:

w indicates web
f indicates flange

TABLE 4 - CONCRETE MIX

Materials	Quantity per Cubic Yard
Coarse Aggregate (Nytralite	955 lbs.
Sand	1350
Cement (Type 1 Portland)	480
Water	285
Darex (AEA)	5½ ozs.
Slump	3-4"
Air Percentage	5-7%
Dry Unit Weight	113.5 pcf
Compressive Strength	4000 psi

TABLE 5 - CONCRETE PROPERTIES

SPEC.	AGE	CYLINDER NO.	Ec (ksi)	f'_c (psi)	fsp (psi)	w (pcf)
1C1	58 days	E I	2520			116.3
		E II	2450			116.8
		C I		4370		116.3
		C II		4320		116.8
		T I			456	116.3
		T II			449	116.8
		AVERAGE	2485	4345	453	116.6
1C2a	58 days	E I	*			113.3
		E II	*			113.3
		C I		4280		113.3
		C II		3980		112.8
		T I			367	113.3
		T II			394	113.8
		AVERAGE	2480+	4130	381	113.3
1C2b	38 days	E I	*			113.3
		E II	*			113.3
		C I		4030		113.8
		C II		3940		113.8
		T I			429	113.3
		T II			398	113.3
		AVERAGE	2540+	3985	414	113.5
1C3	64 days	E I	2500			117.3
		E II	2500			118.3
		C I		4950		117.3
		C II		4730		118.4
		T I			423	117.9
		T II			*	118.4
		AVERAGE	2500	4840	423	117.9
1C4	34 days	E I	2050			118.9
		E II	2120			118.4
		C I		3360		118.9
		C II		3140		118.4
		T I			394	118.9
		T II			416	118.9
		AVERAGE	2085	3250	405	118.7

* denotes observation missed due to incorrect testing procedures

+ Ec calculated from ACI formula $33w^{1.5}\sqrt{f'_c}$ (ACI Standard 318-71, Section 8.3.1)

TABLE 6. - STUD PROPERTIES

STUD DIMENSIONS	ULTIMATE STRENGTH (KSI)
3/4" X 3½"	73.4
3/4" X 4"	75.6
3/4" X 4½"	78.8

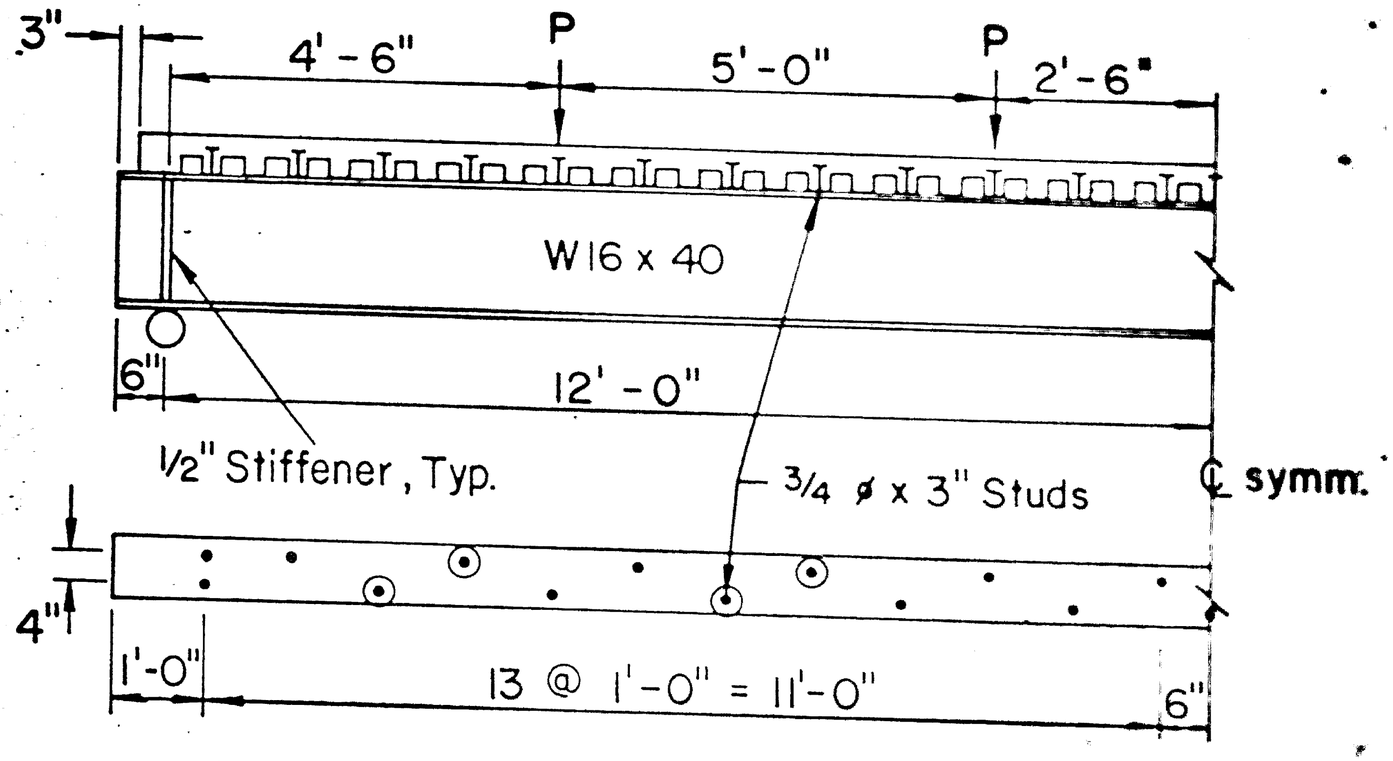

Fig. 1 Details of Specimen 1C1

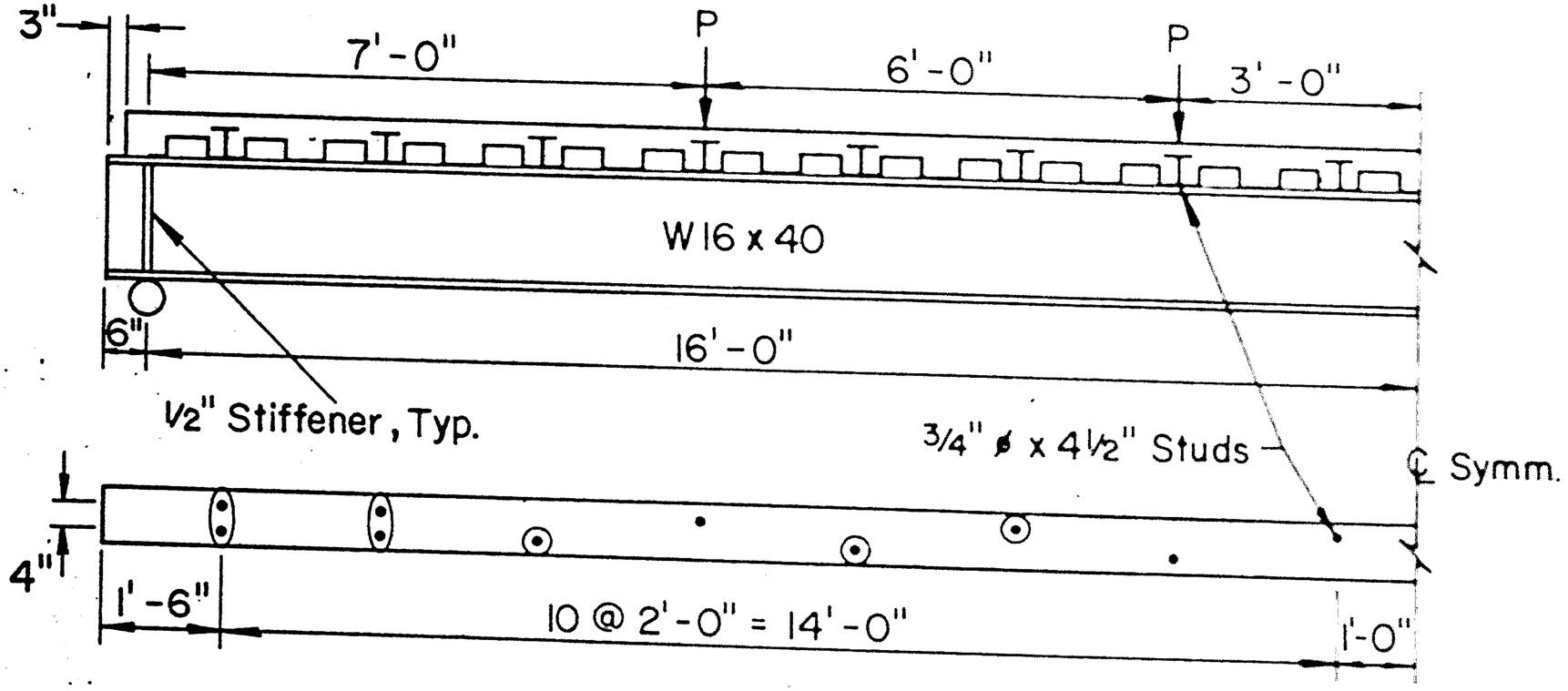

Fig. 2 Details of Specimen 1C2a

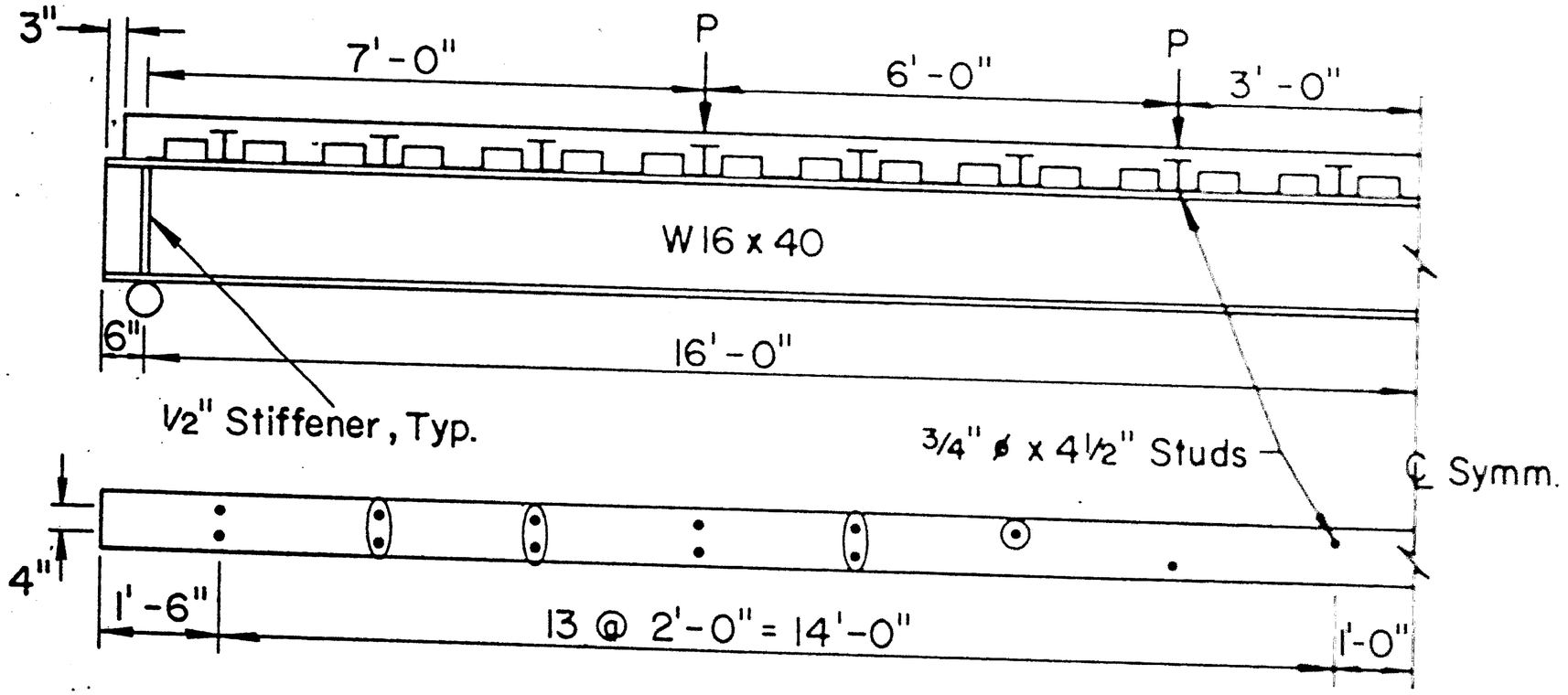

Fig. 3 Details of Specimen 1C2b

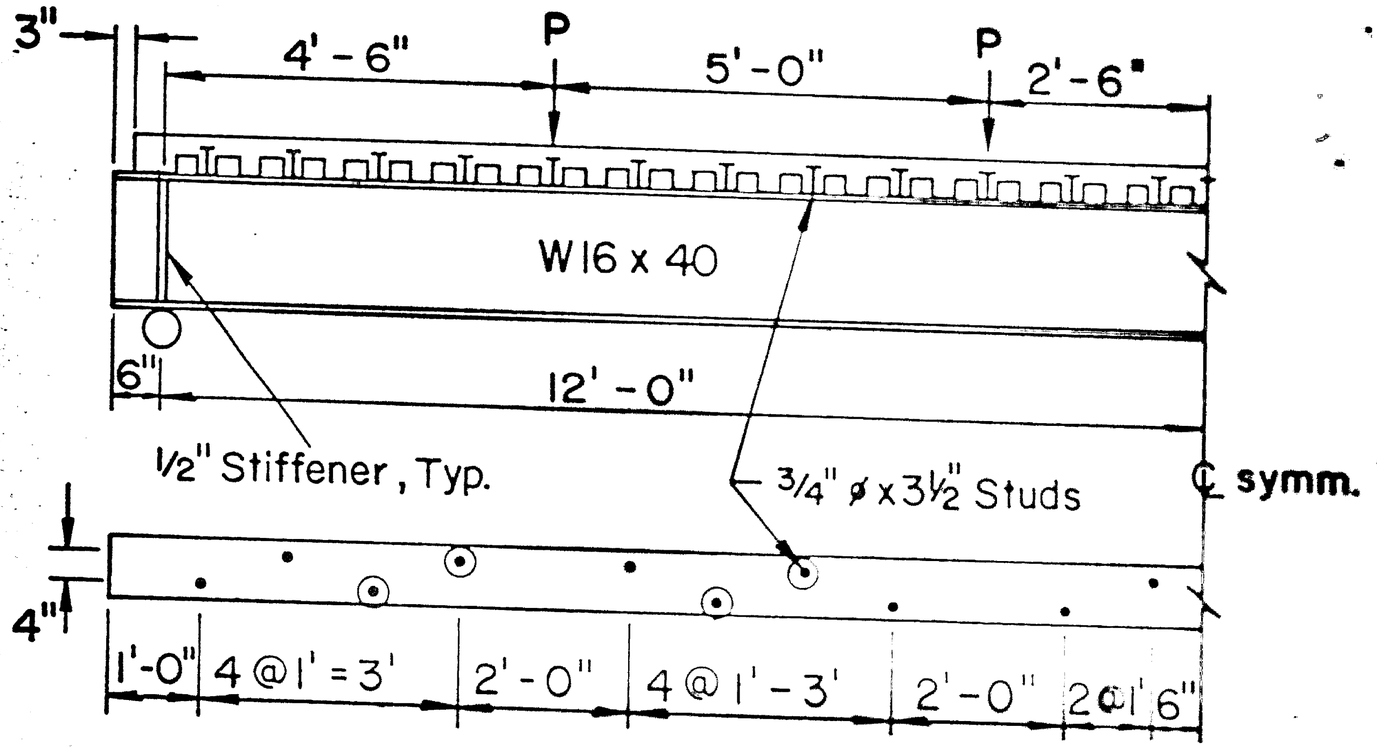

Fig. 4 Details of Specimen 1C3

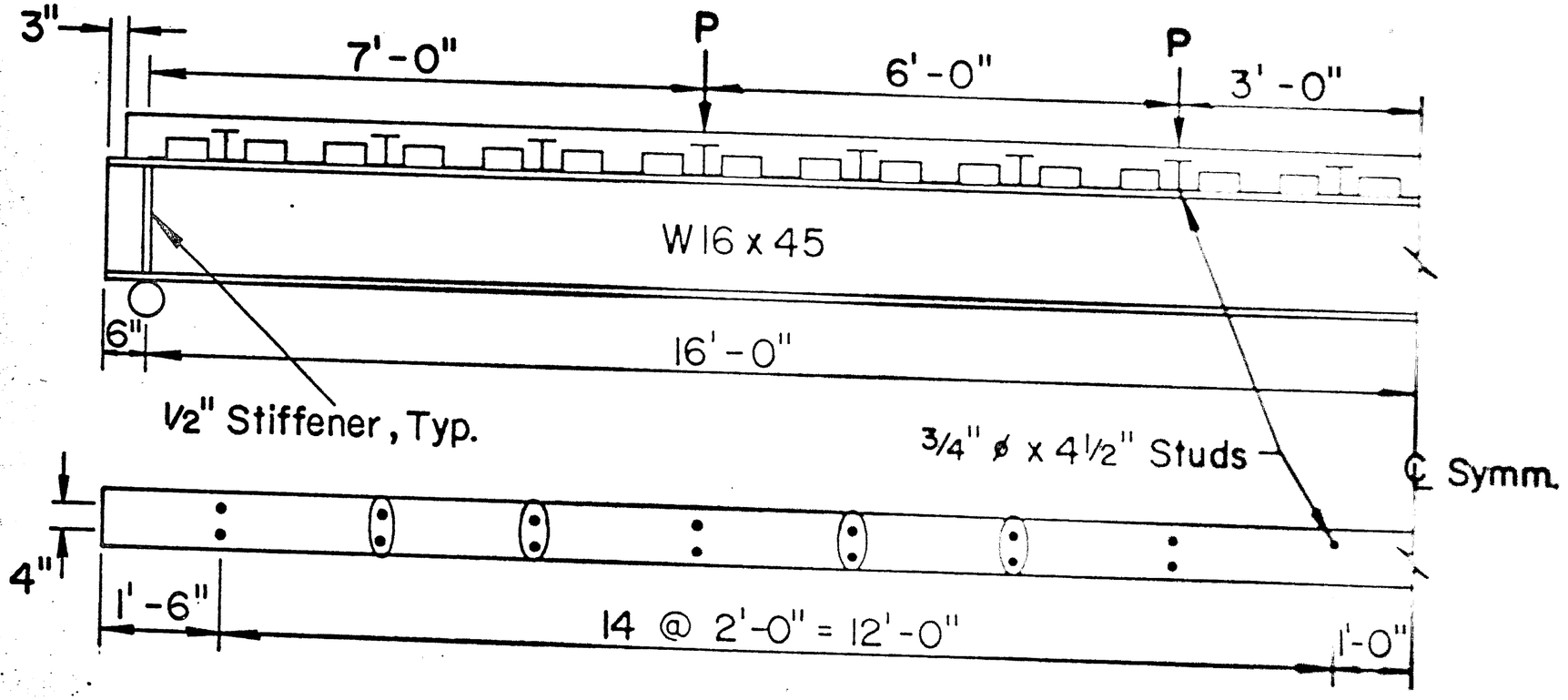

Fig. 5 Details of Specimen 1C4

Fig. 6 Specimen 1C3--Before Testing

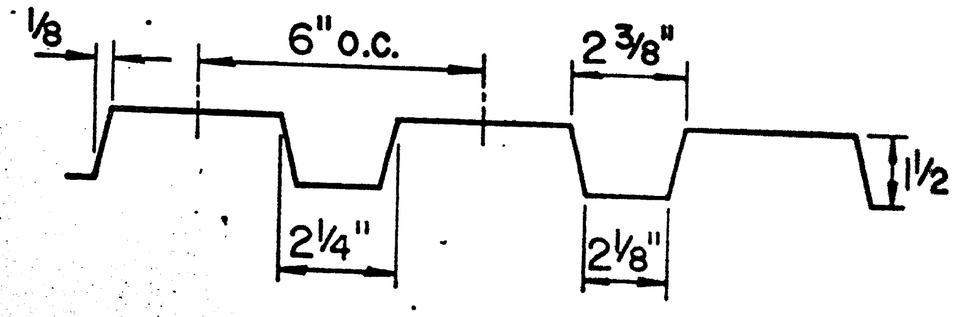

Spec. IC1

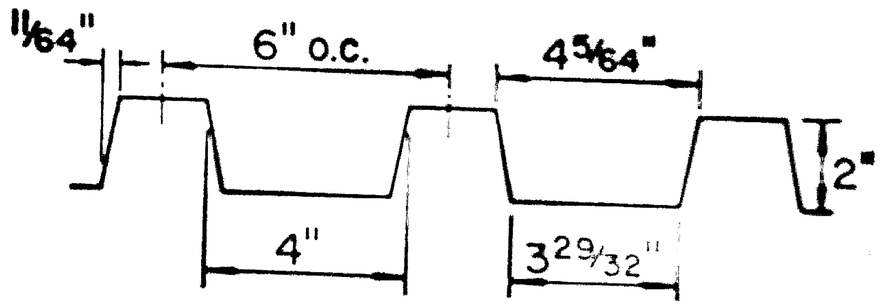

Spec. IC3

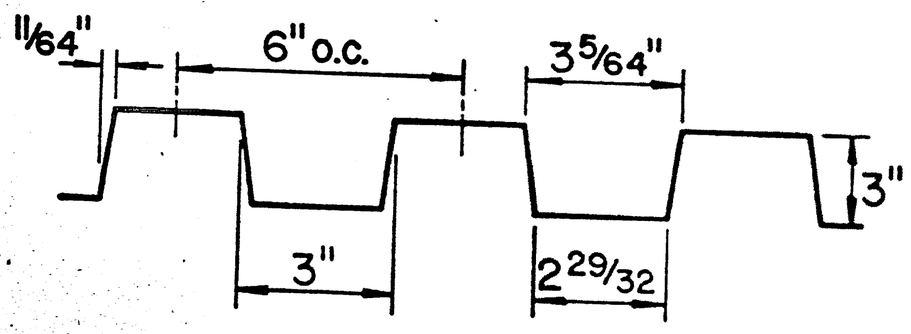

Spec. IC2A + B

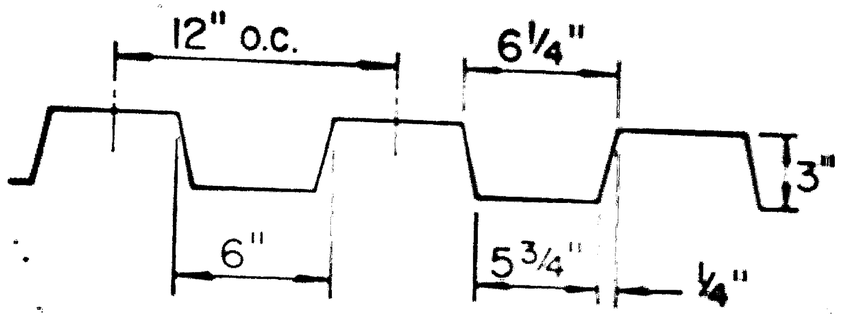

Spec. IC4

Fig. 7 Deck Profiles

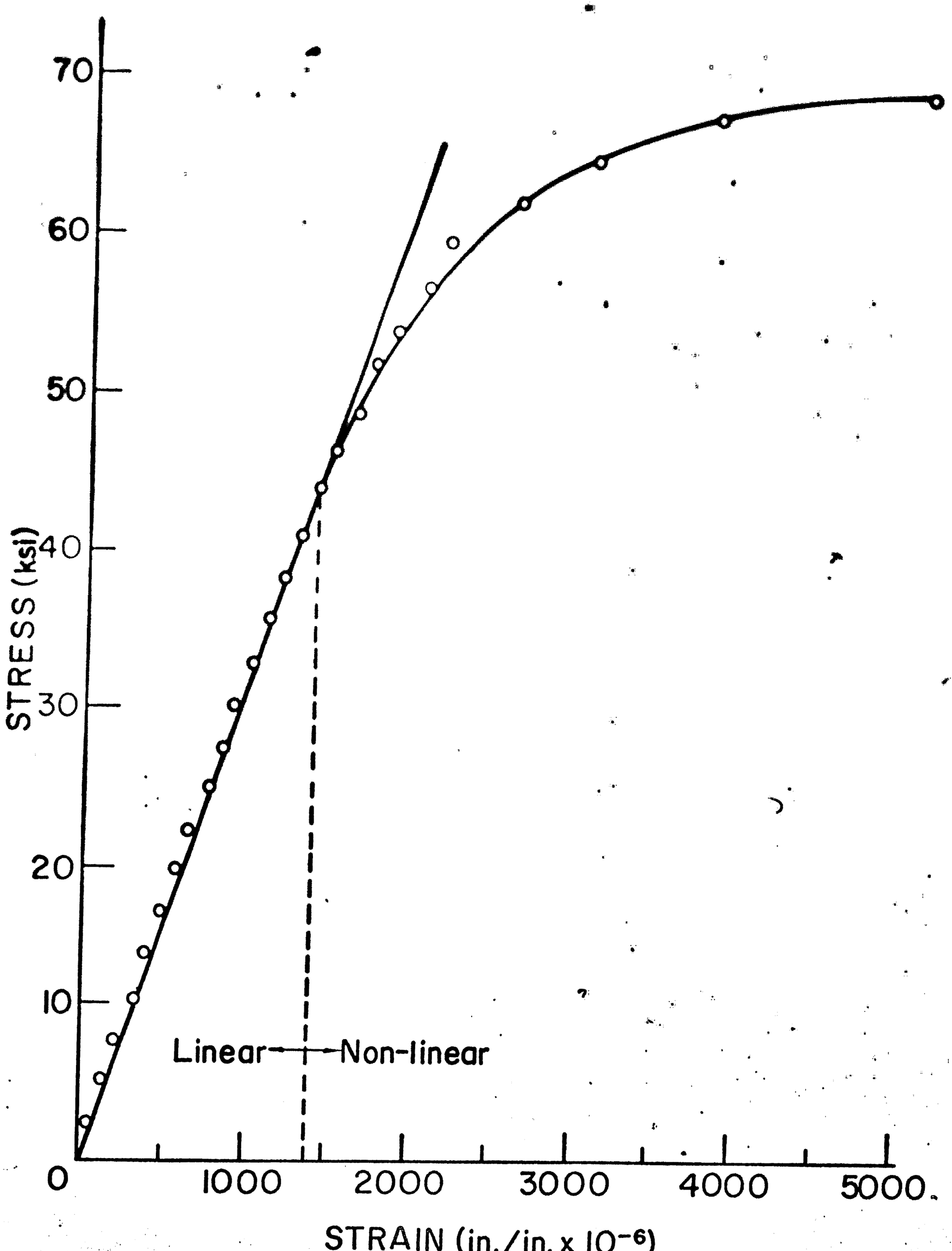

Fig. 8 Typical Stress - Strain Curves (Steel)

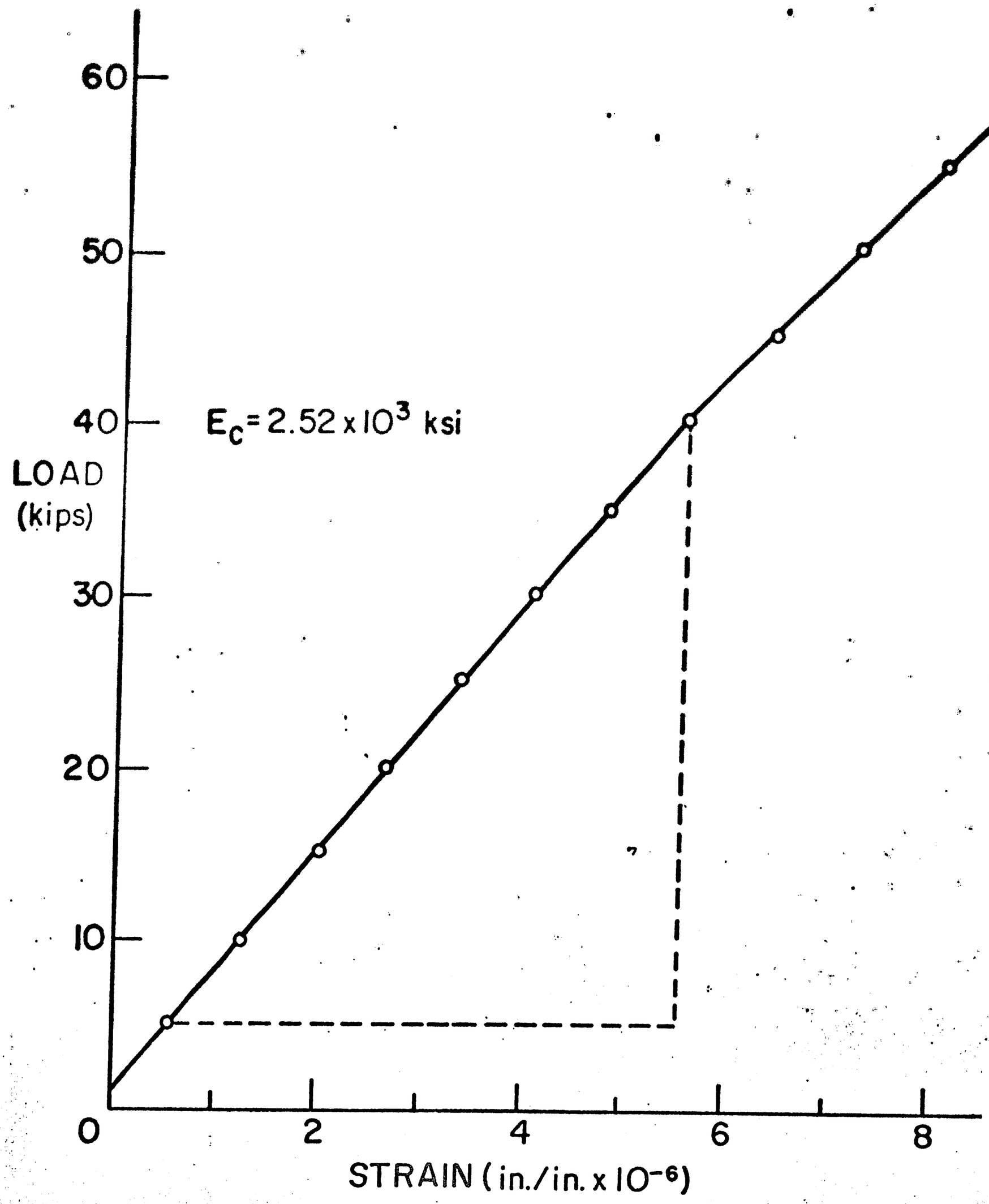

Fig. 9 Typcial Load - Strain Curve (Concrete)

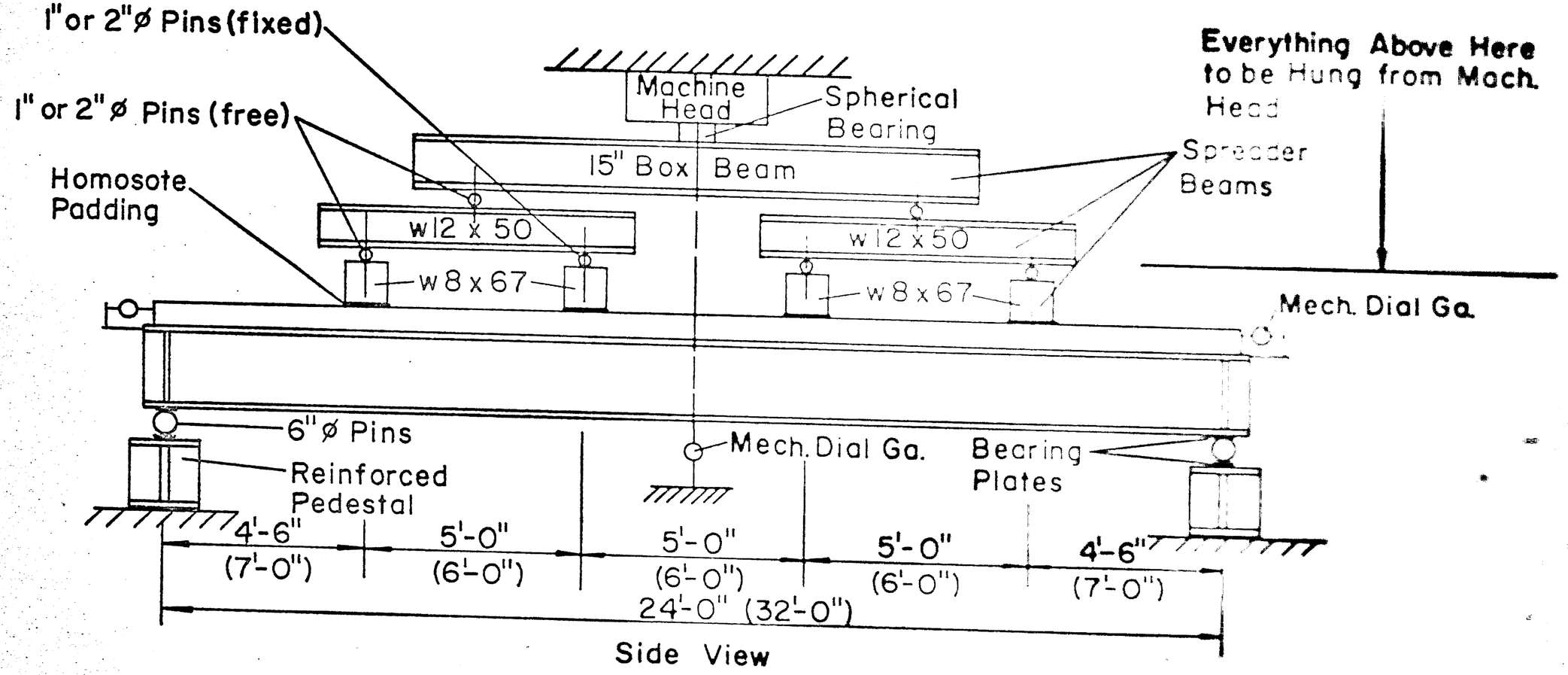

Fig. 10 Test Set-Up

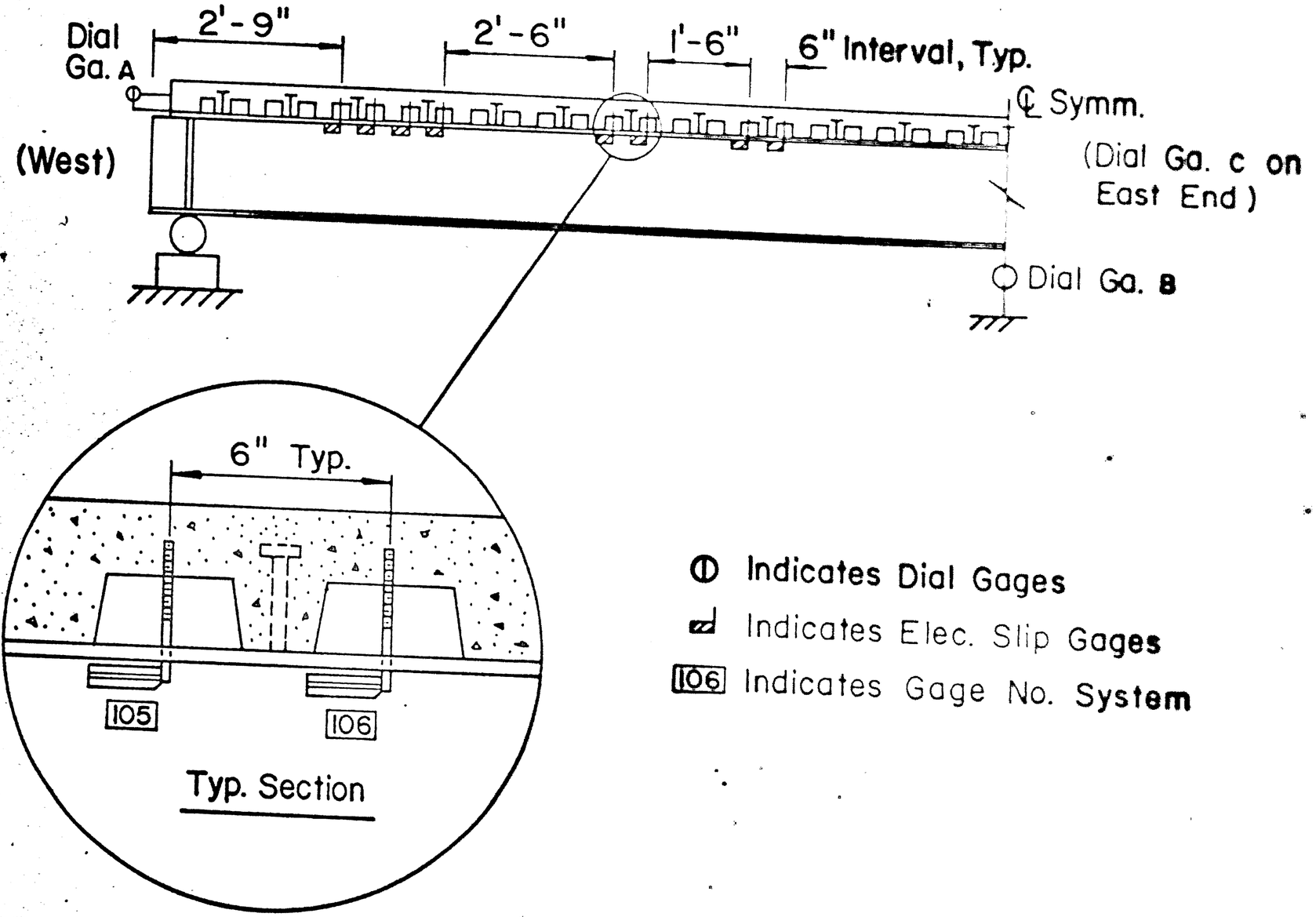

Fig. 11 Instrumentation - Slip Measurements

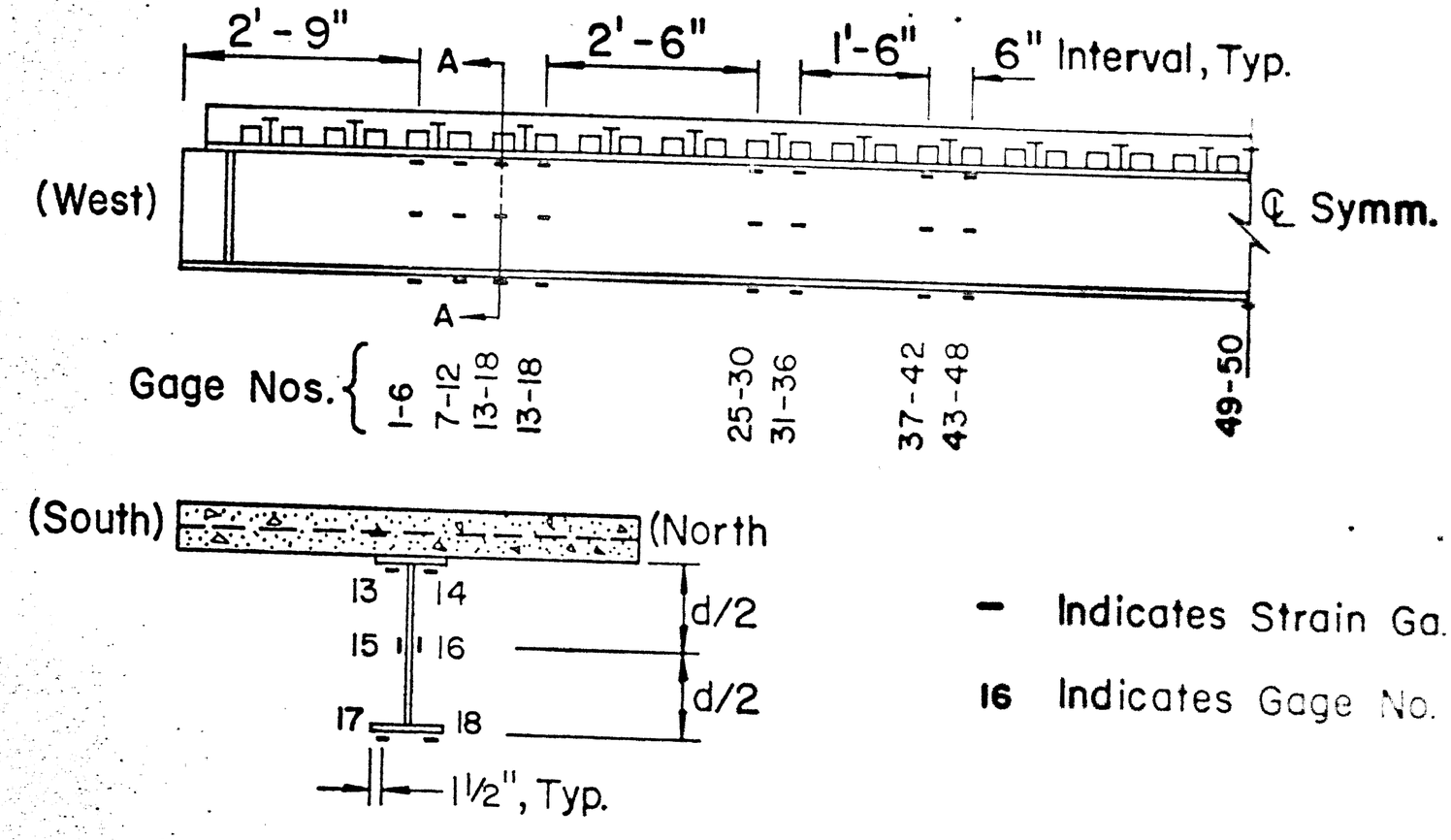

Fig. 12 Instrumentation - Strain Gages

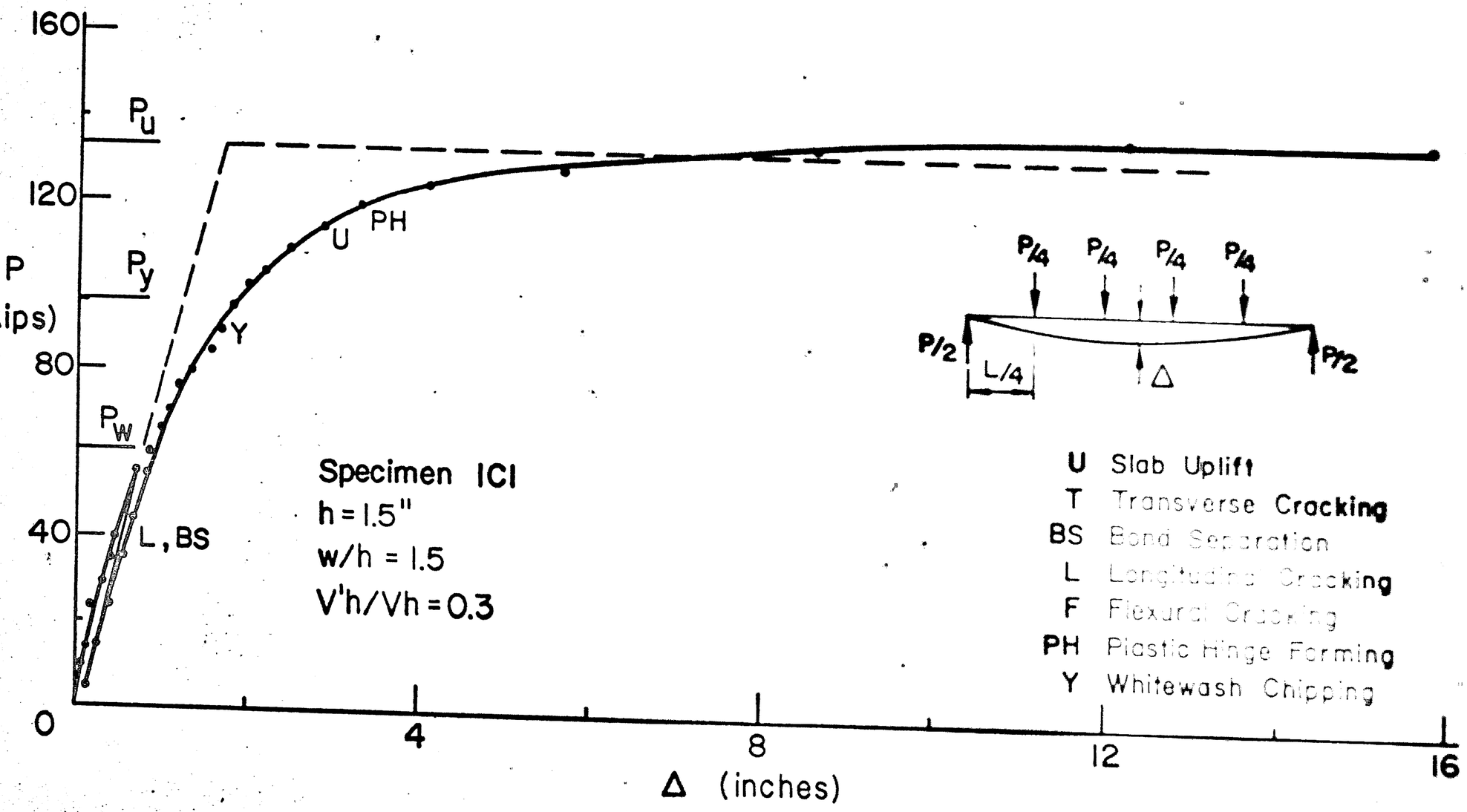

Fig. 13 Load versus Midspan Deflection - Specimen 1C1

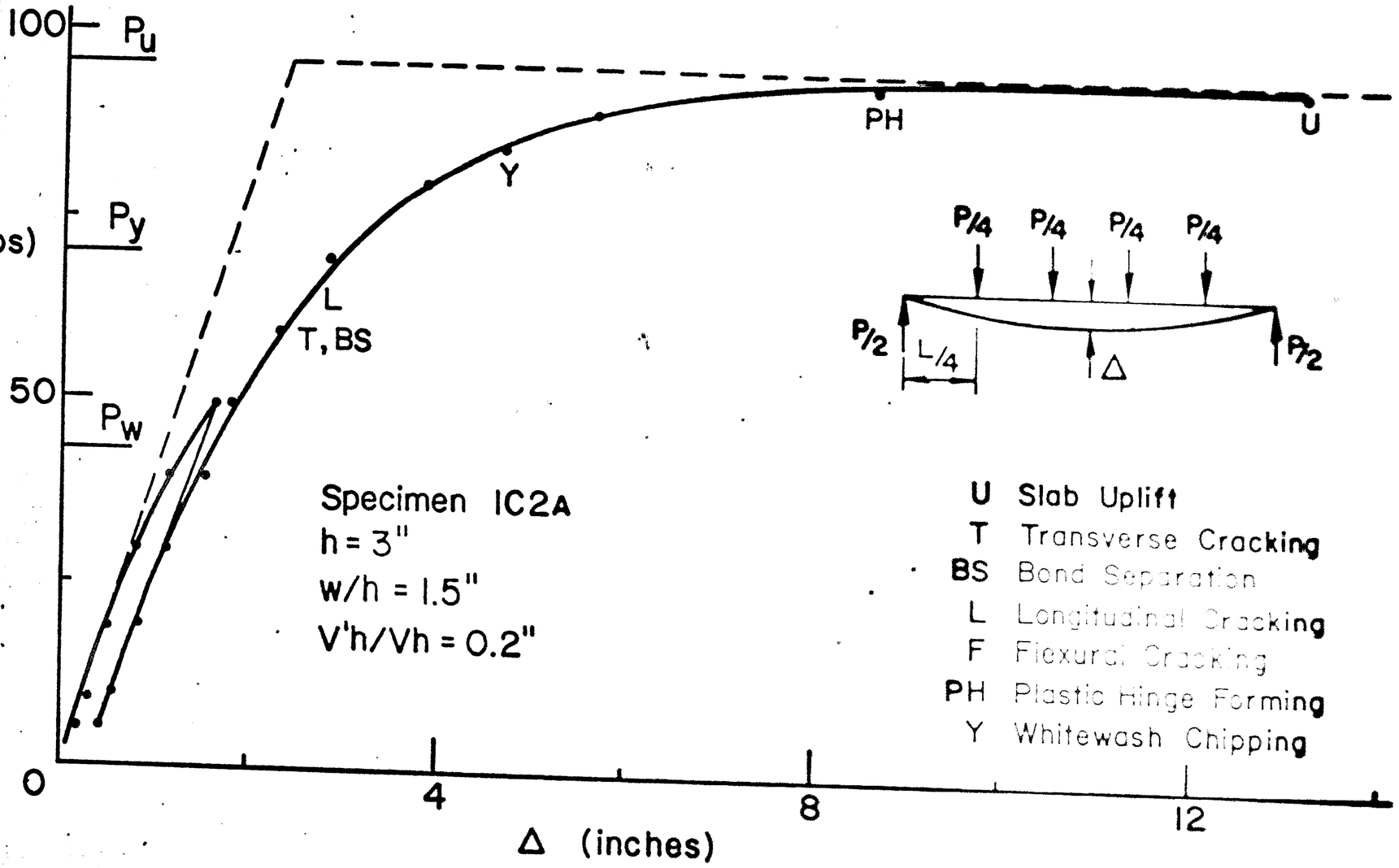

Fig. 14 Load versus Midspan Deflection - **Specimen 1C2a**

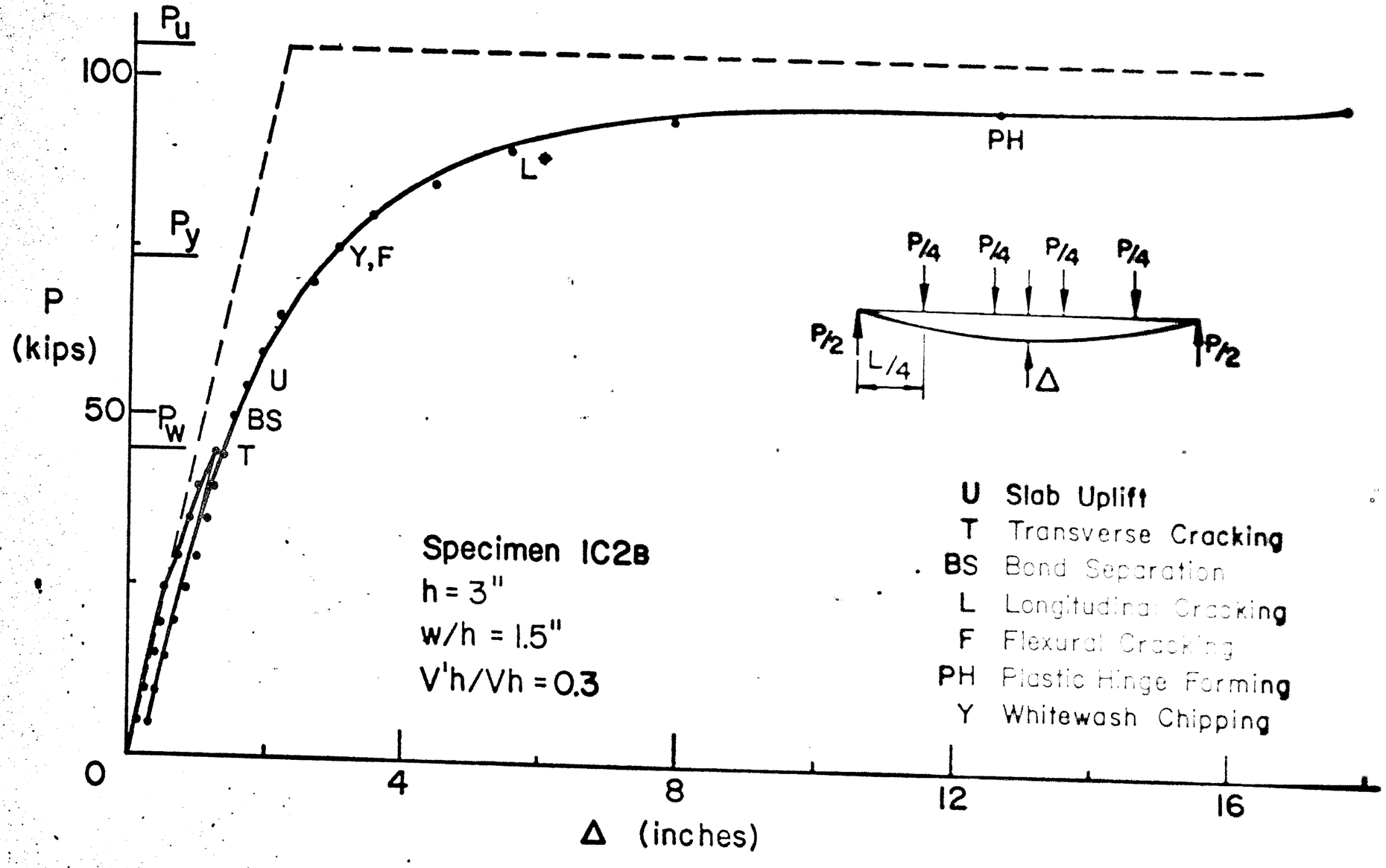

Fig. 15 Load versus Midspan Deflection - Specimen 1C2b

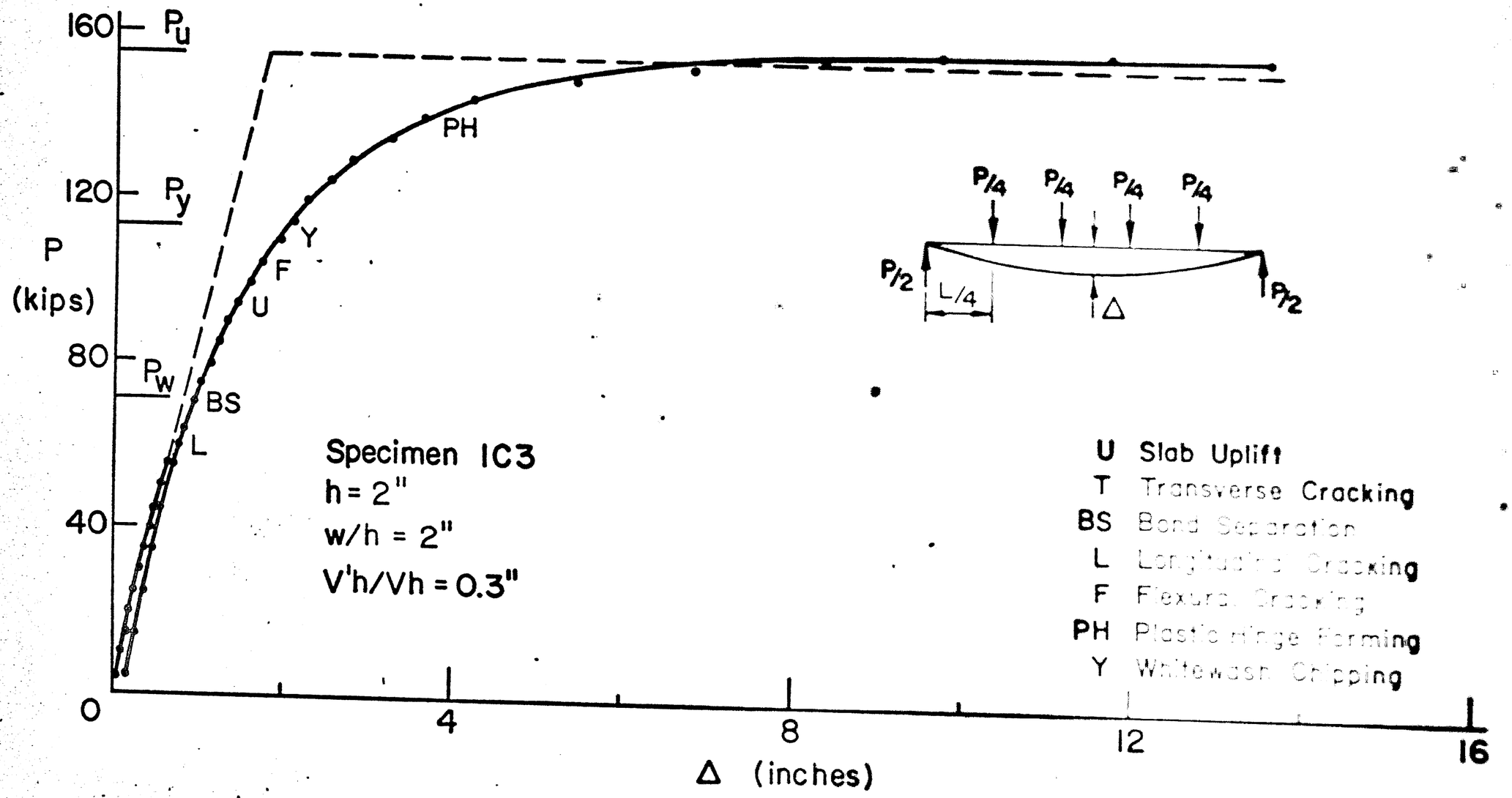

Fig. 16 Load versus Midspan Deflection - Specimen 1C3

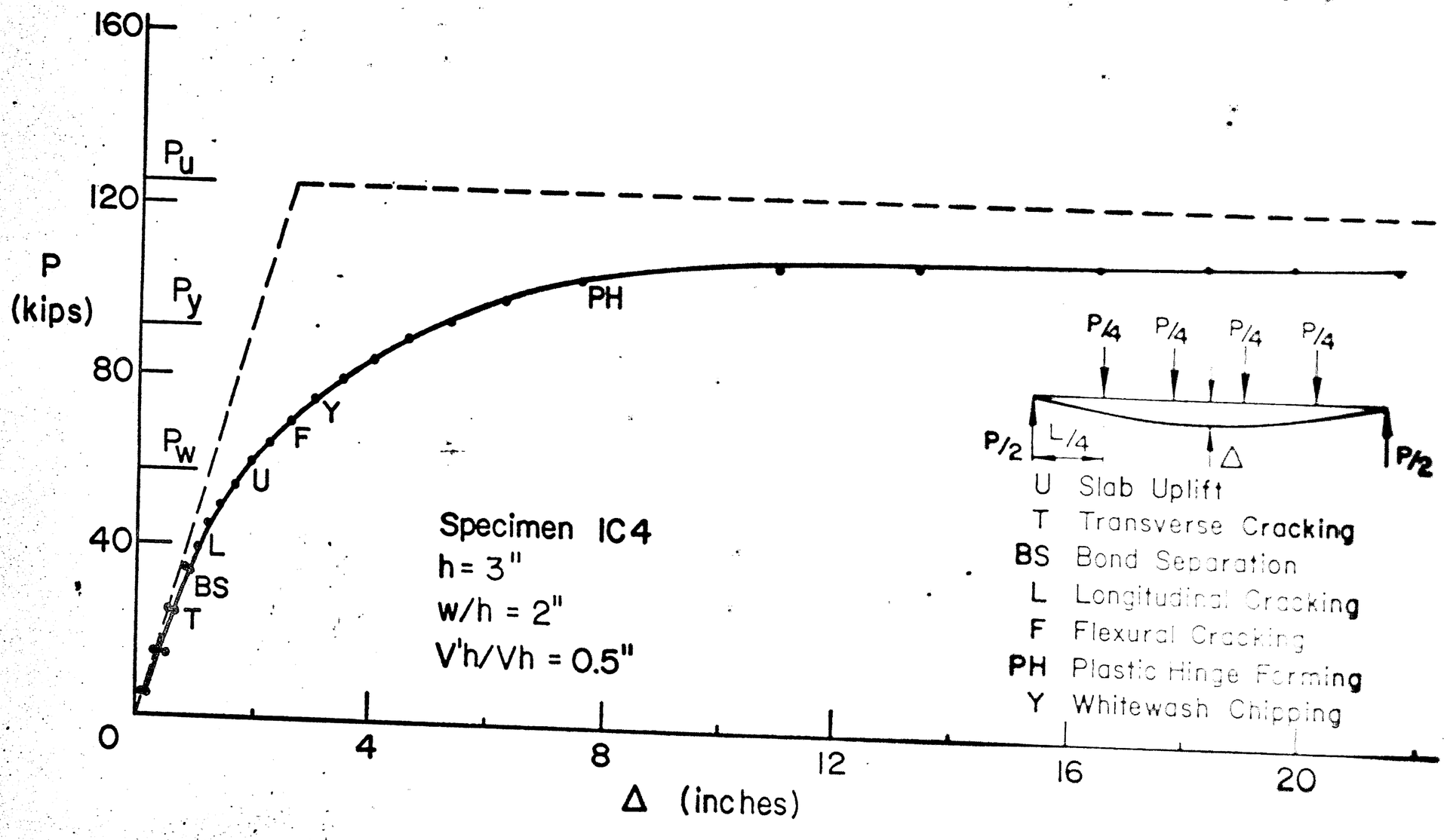

Fig. 17 Load versus Midspan Deflection - Specimen 1C4

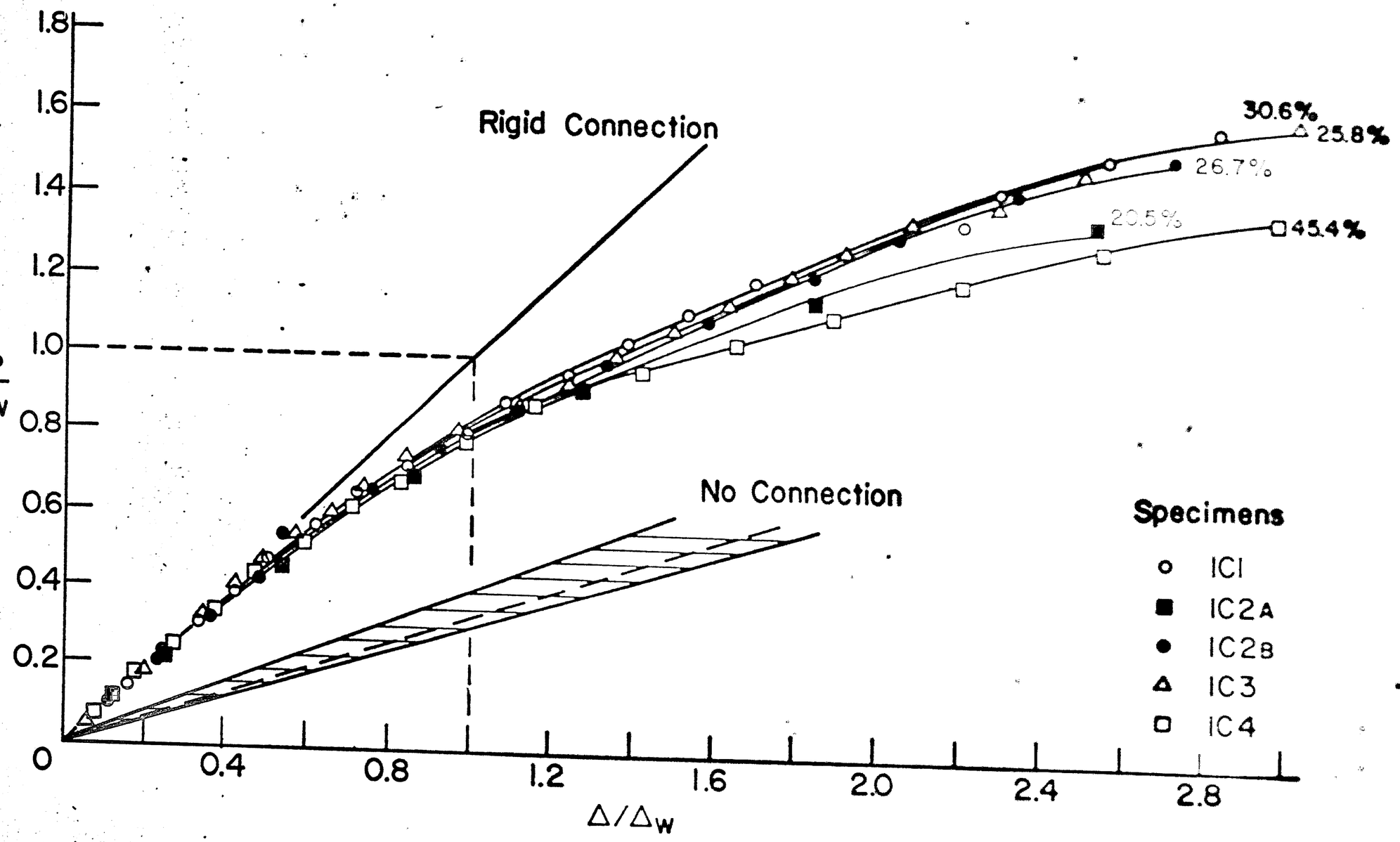

Fig. 18 Load versus Midspan Deflection - Specimens 1C1 through 1C4

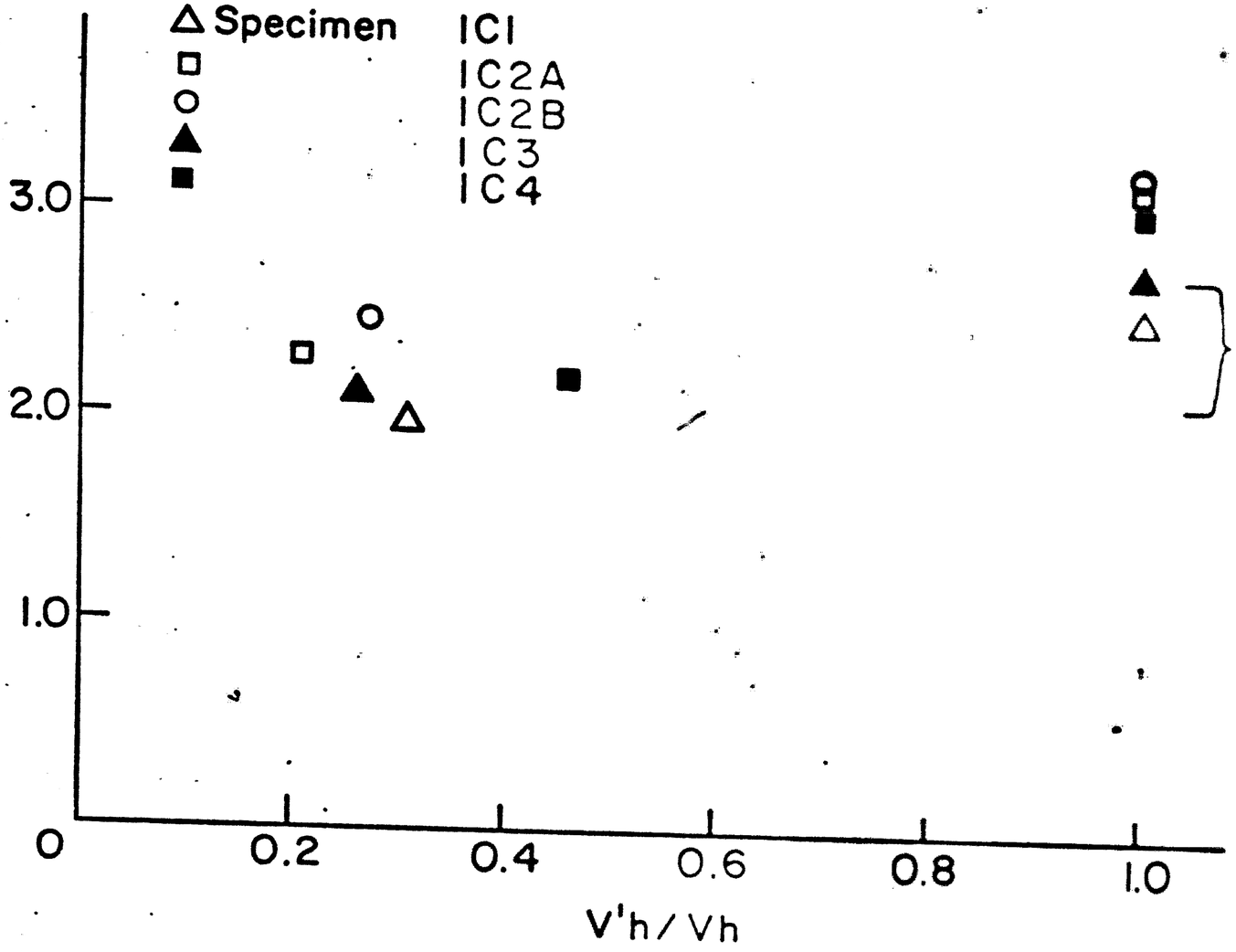

Fig. 19 Stiffness versus Degree of Shear Connection

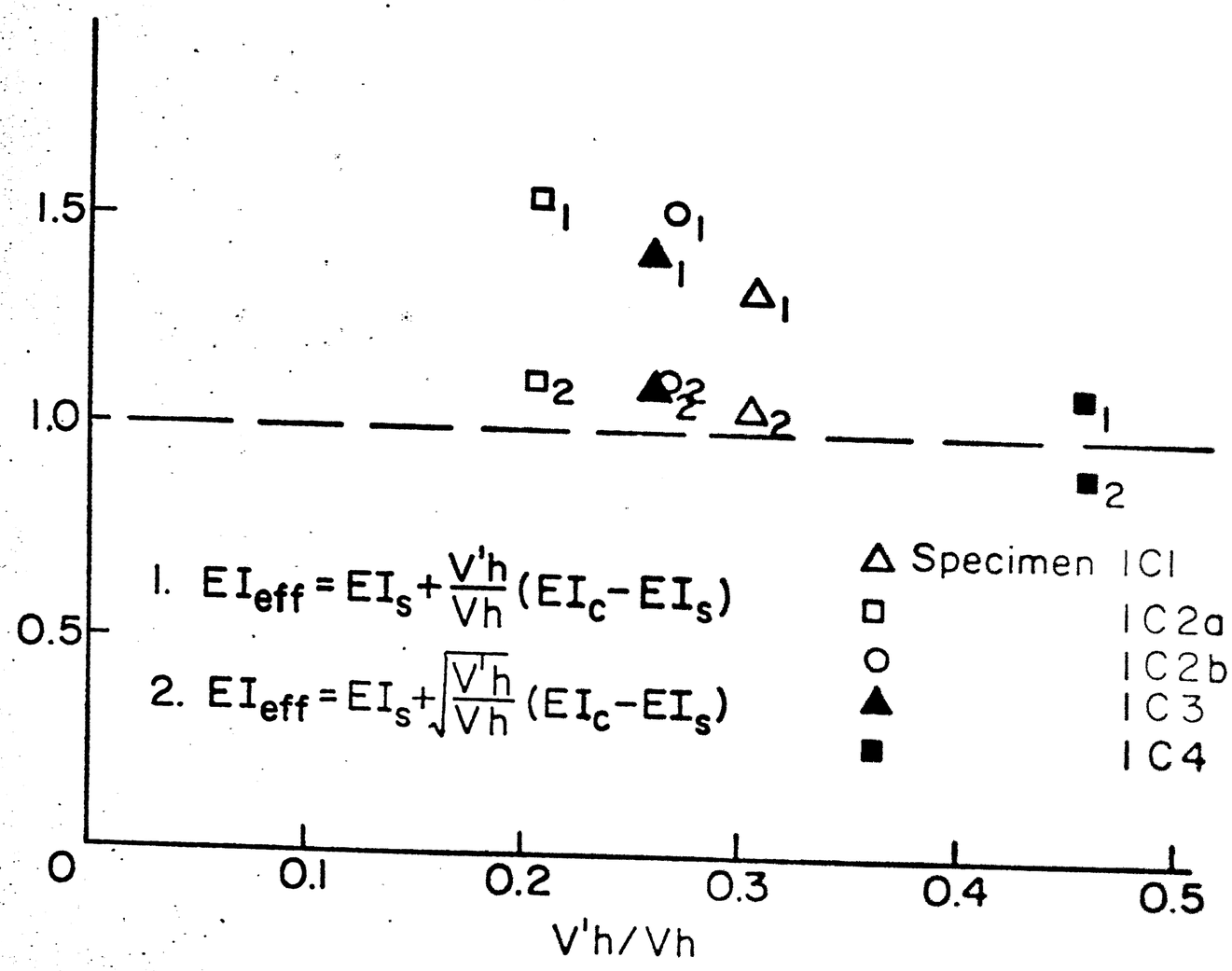

Fig. 20 Stiffness versus "Effective" Stiffness

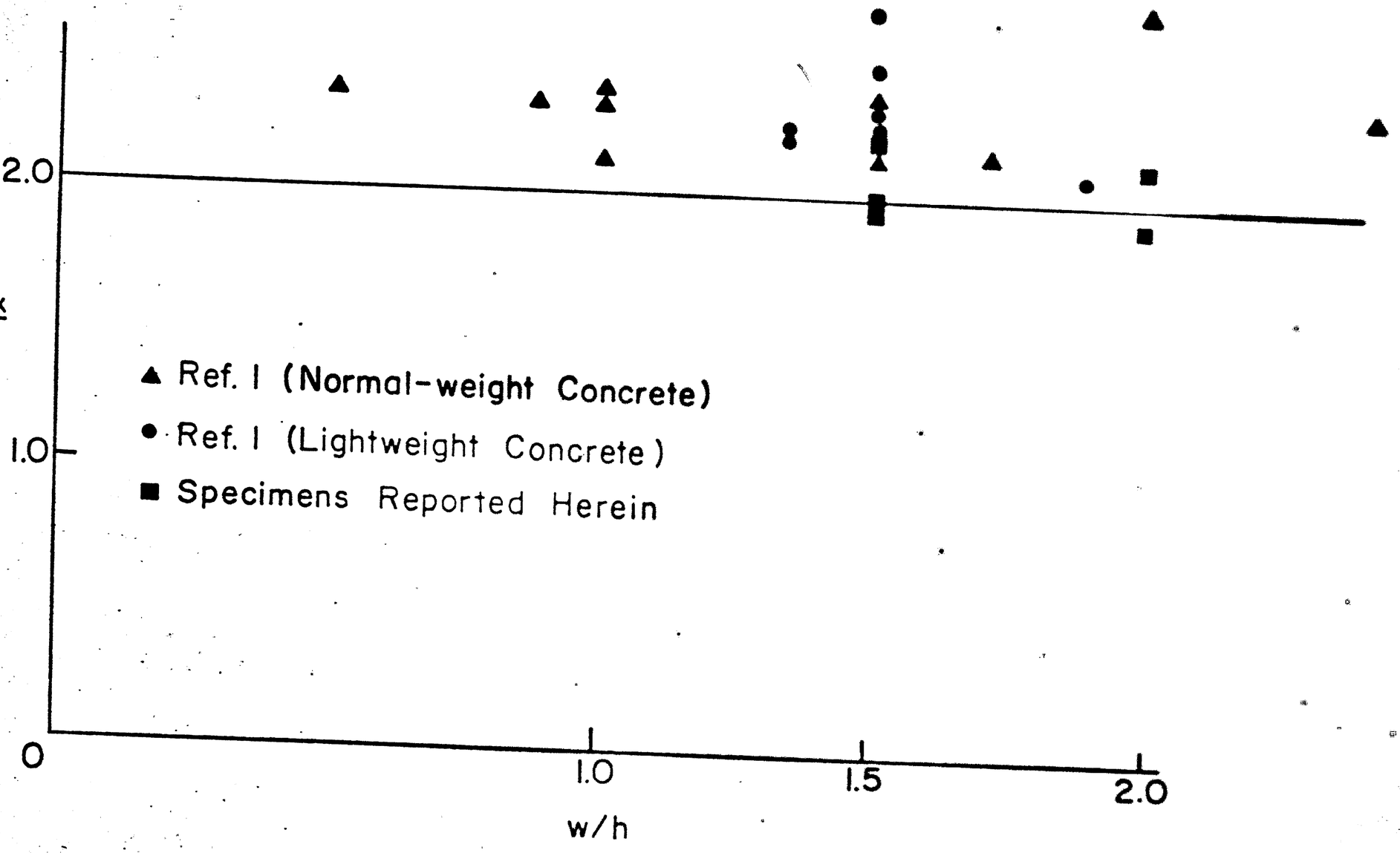

Fig. 21 Safety Factor versus Rib Width Over Height Ratio

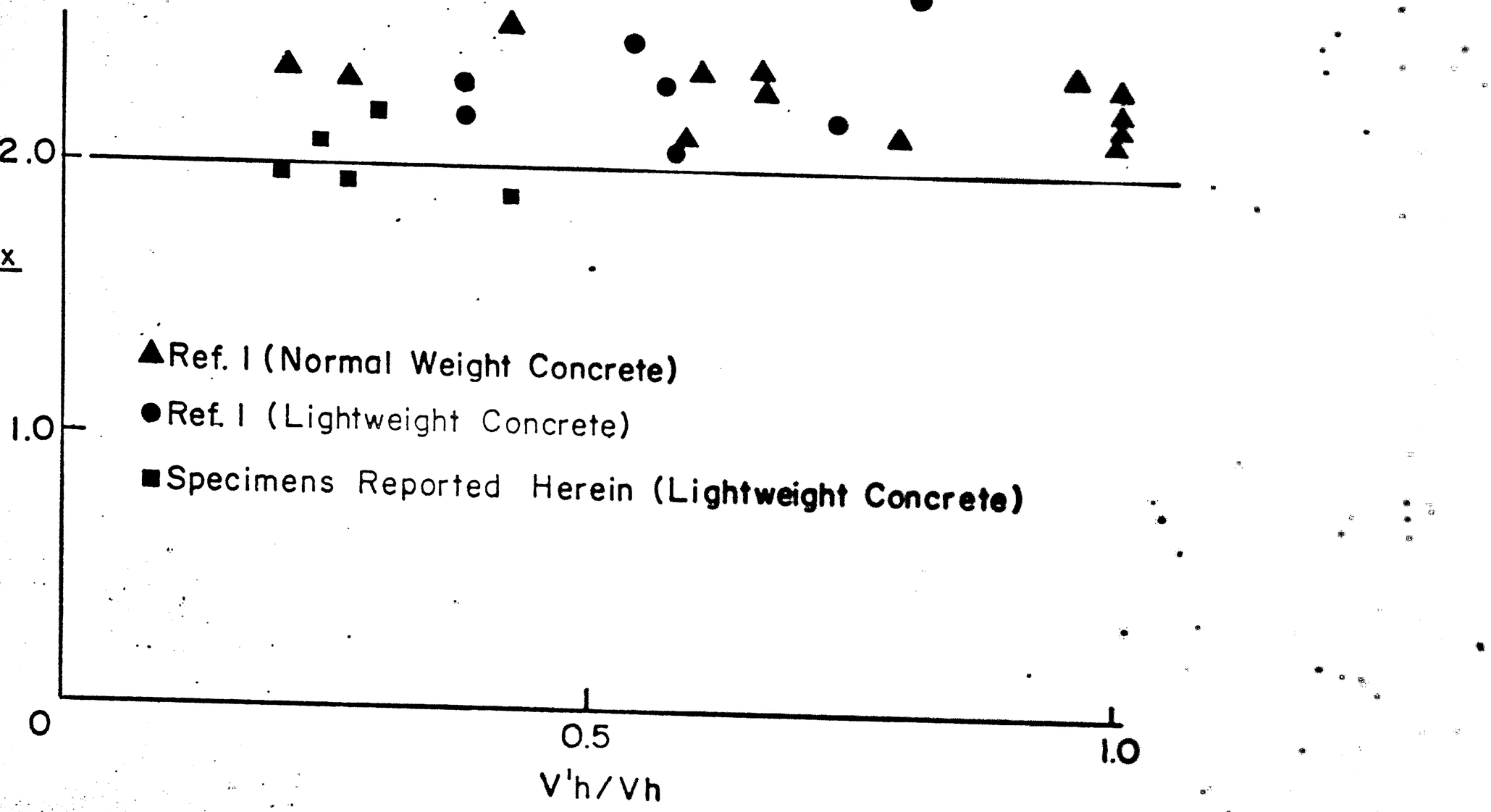

Fig. 22 Safety Factor versus Degree of Shear Connection

(22)

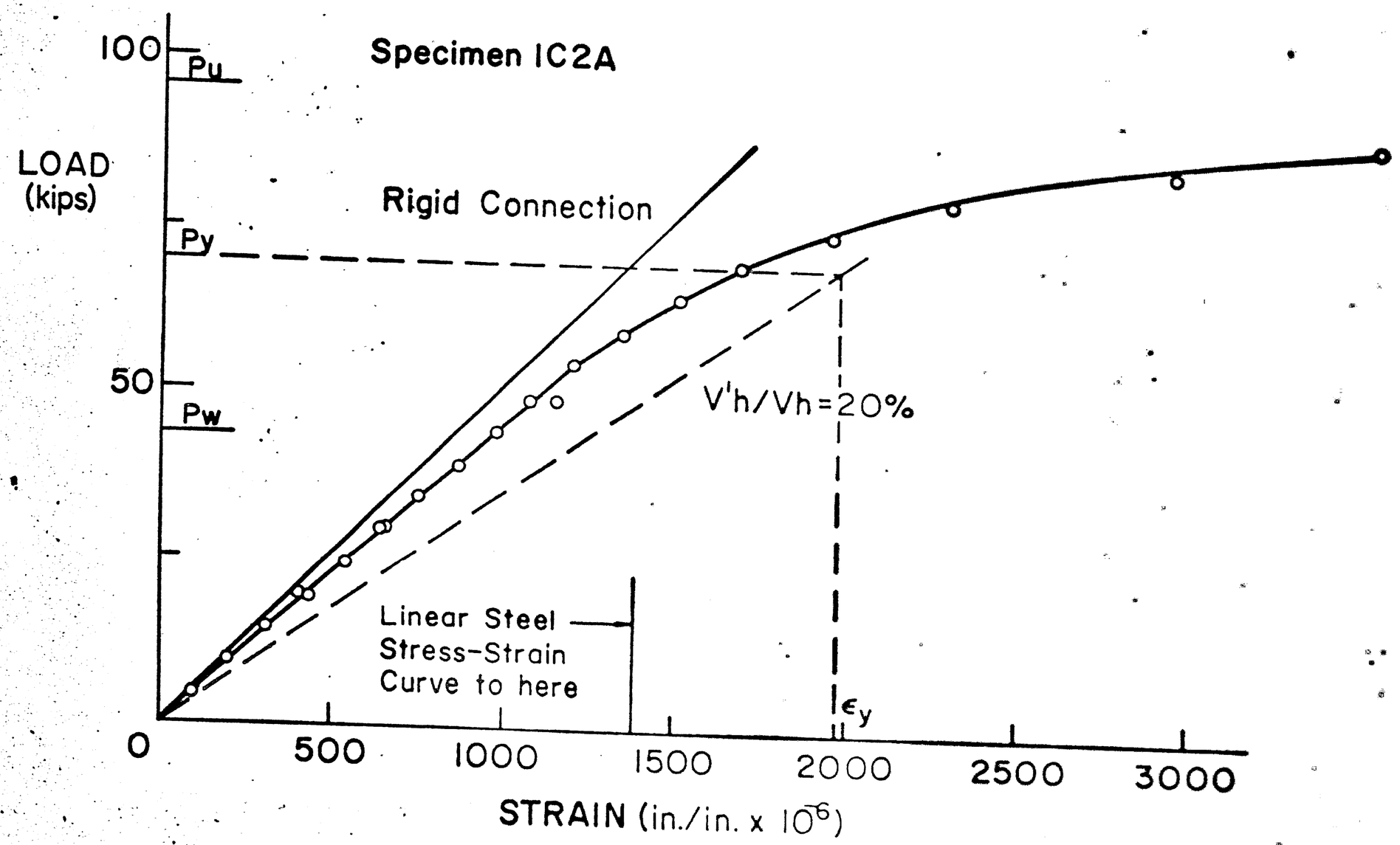

Fig. 23 Load versus Strain in Bottom Fiber - Spec. 1C2a

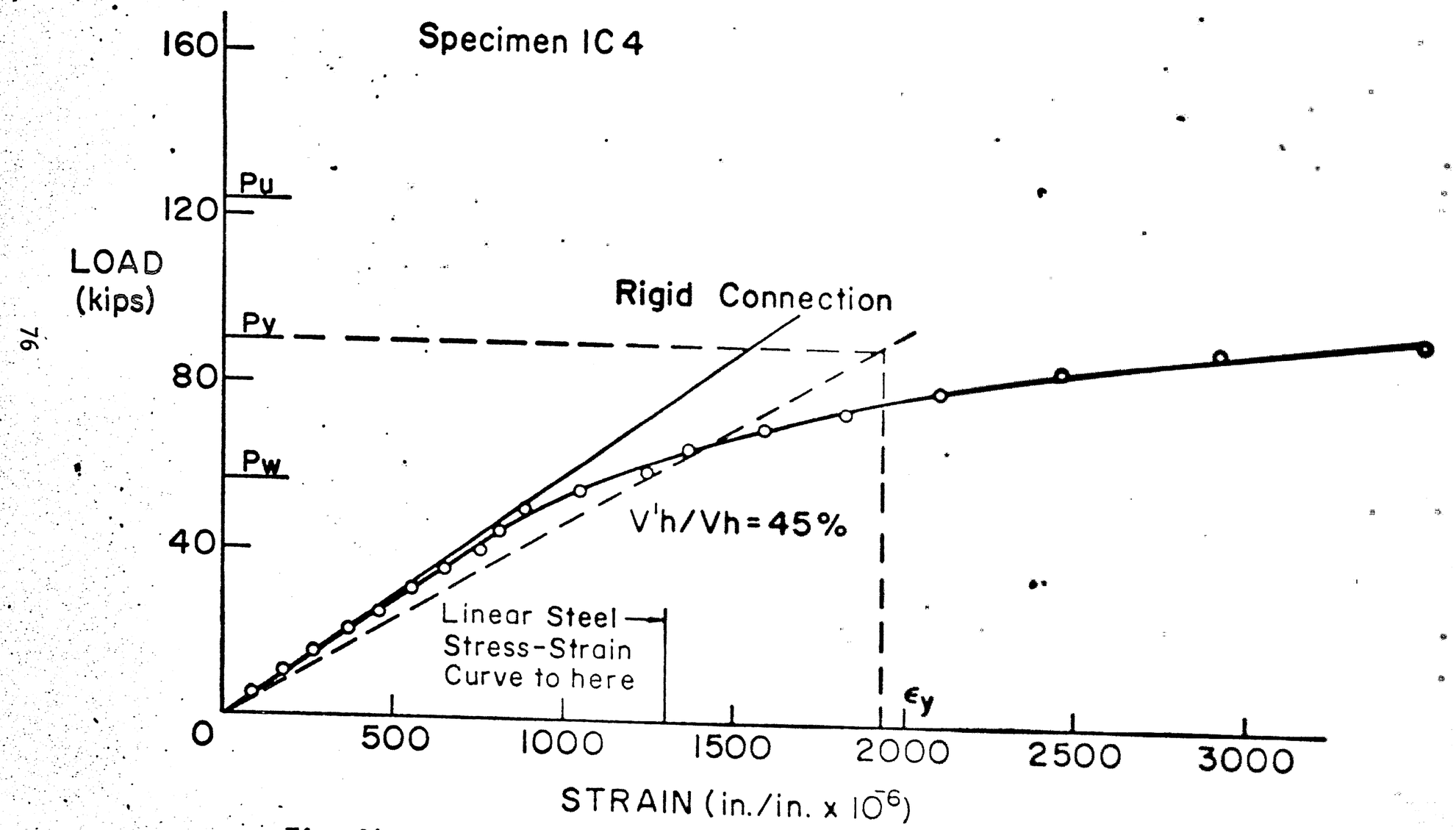

Fig. 24 Load versus Strain in Bottom Fiber - Spec. 1C4

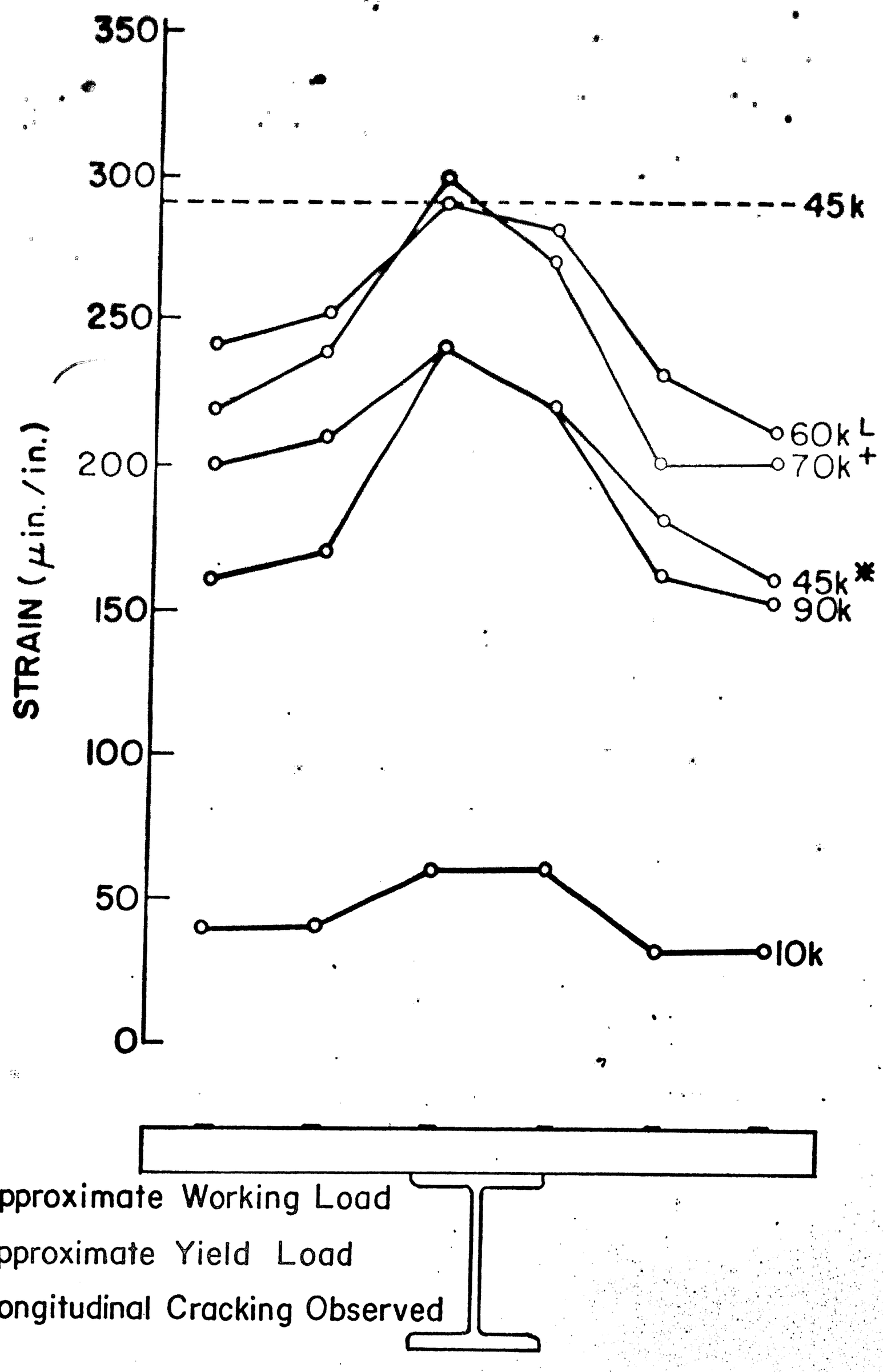

Fig. 25 Stain Distribution Across Slab

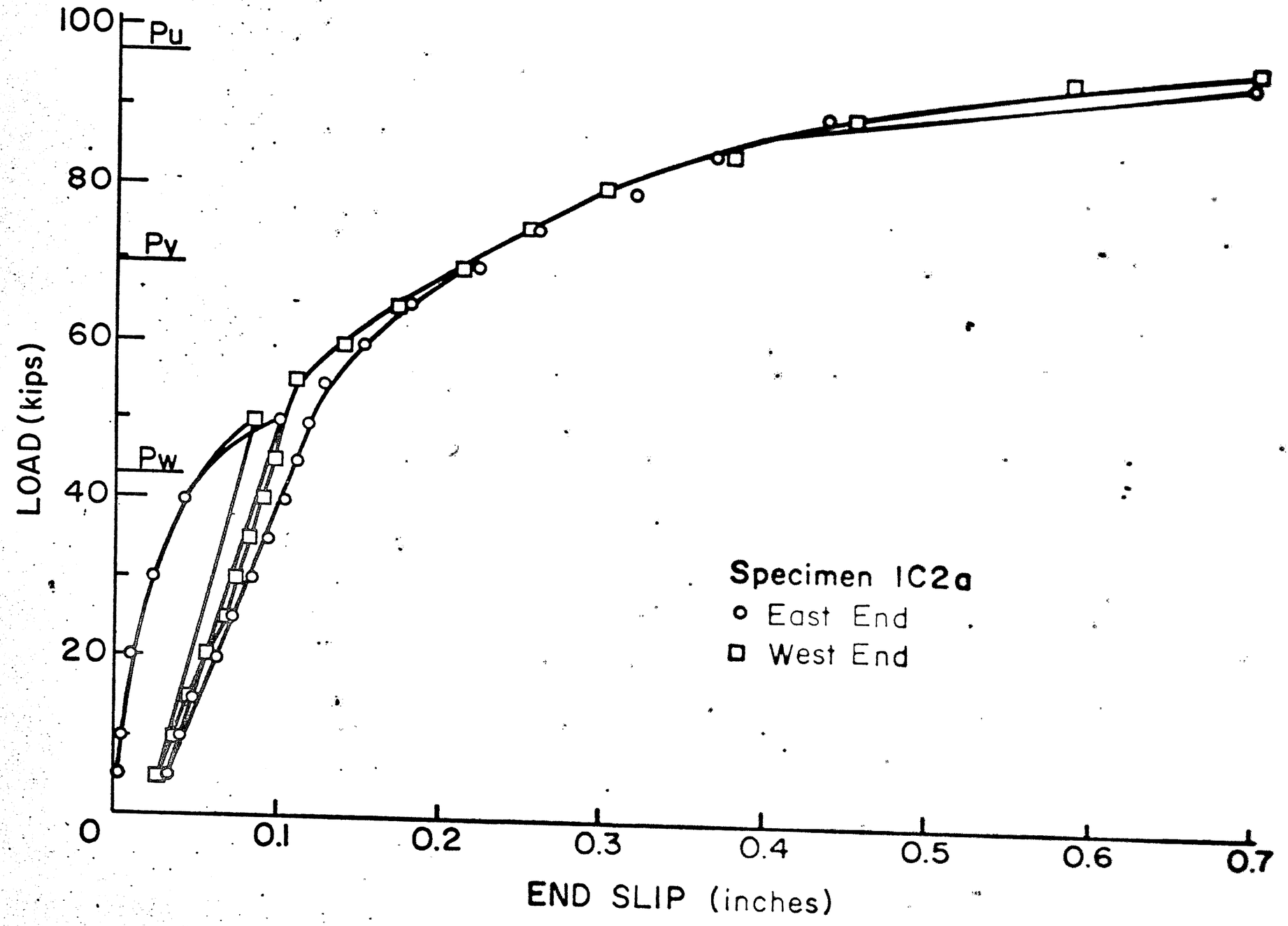

Fig. 26 Load versus Slip - **Spec. 1C2a**

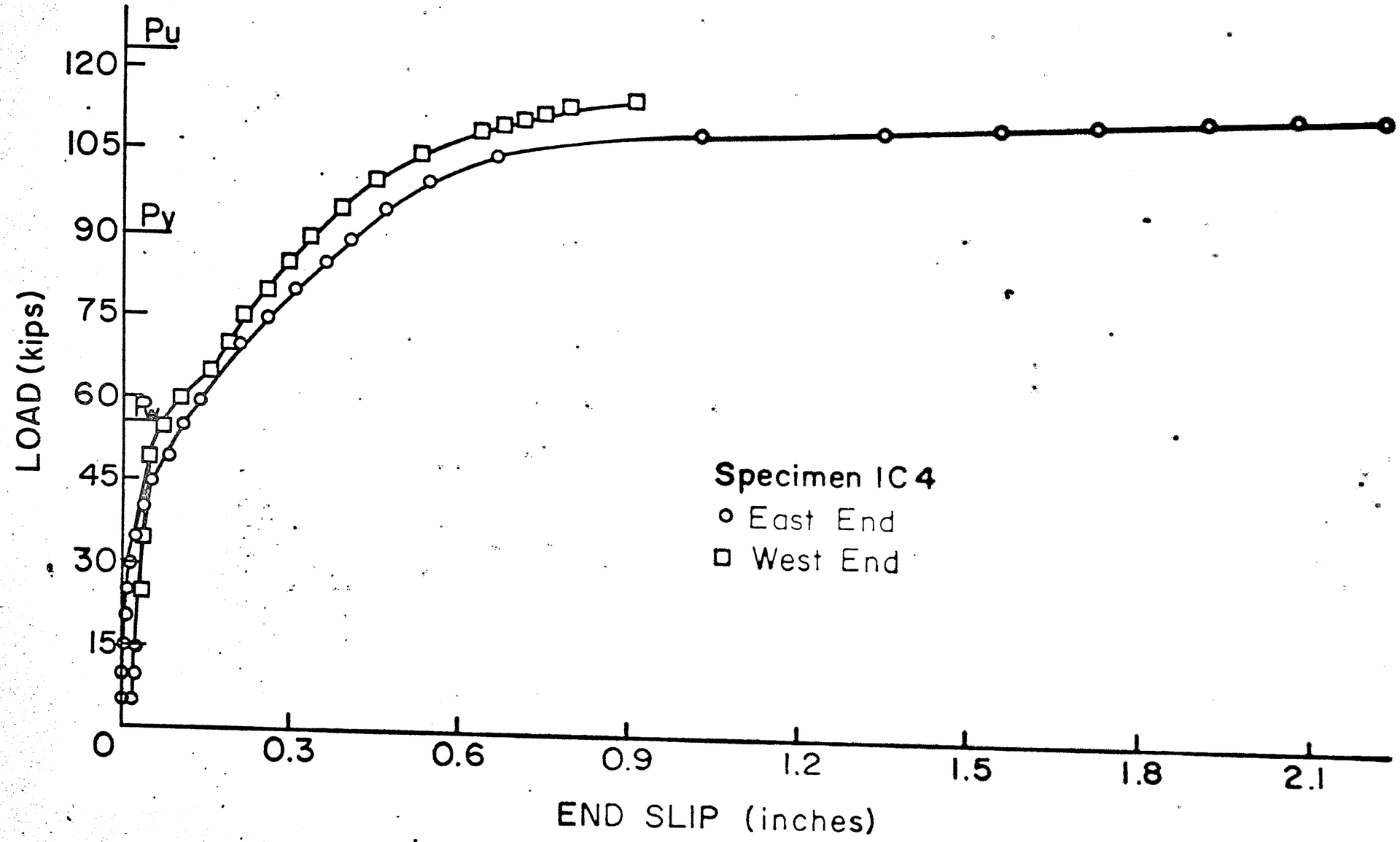

Fig. 27 Load versus Slip - **Spec. 1C4**

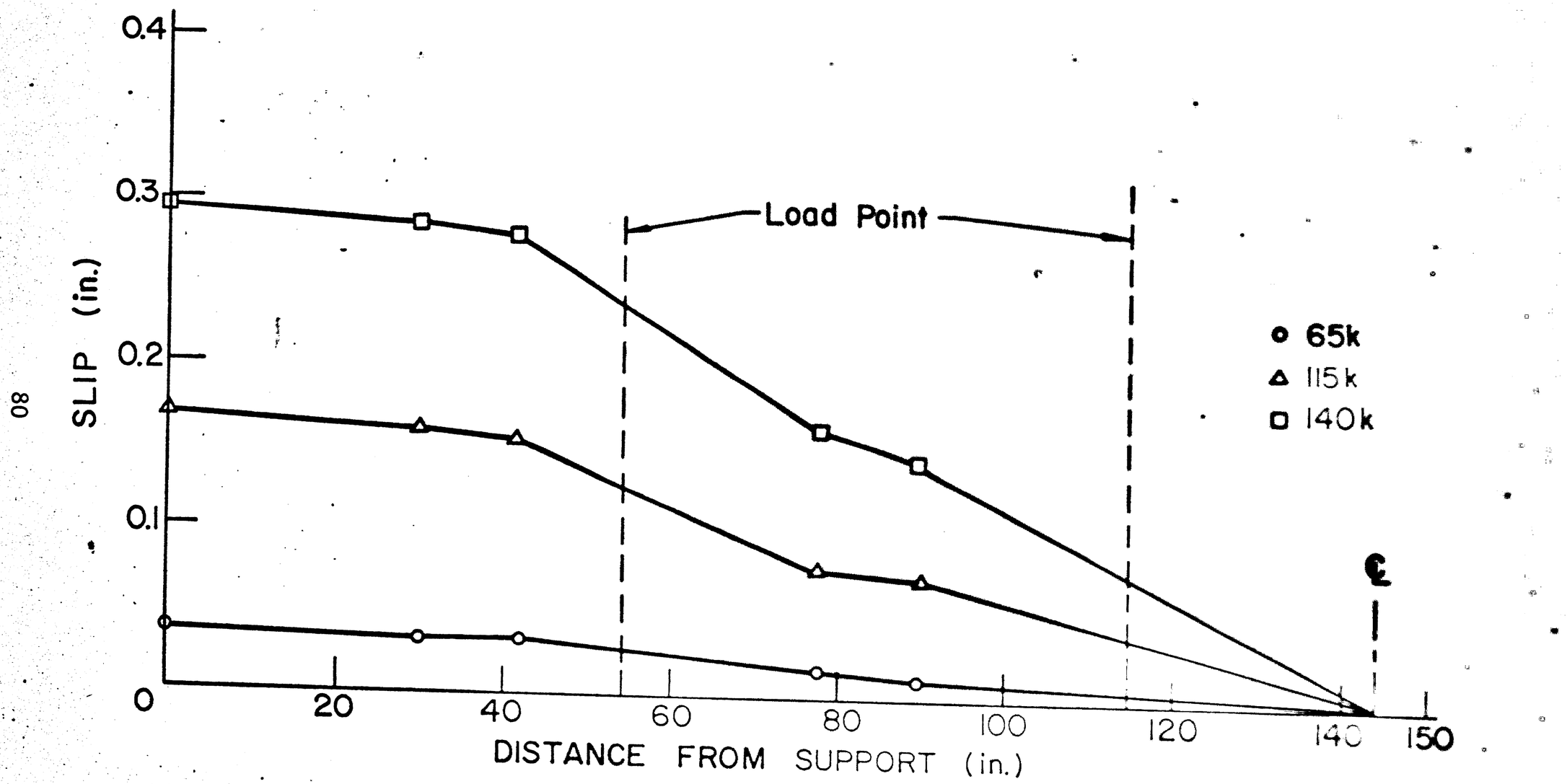

Fig. 28 Slip Distribution - Spec. 1C3

Fig. 29 Typical Rib Failure Mode

Fig. 30 Atypical Rib Failure Mode

Fig. 31 Typical Plastic Hinge

Fig. 32 Typical Local Buckling of Top Flange

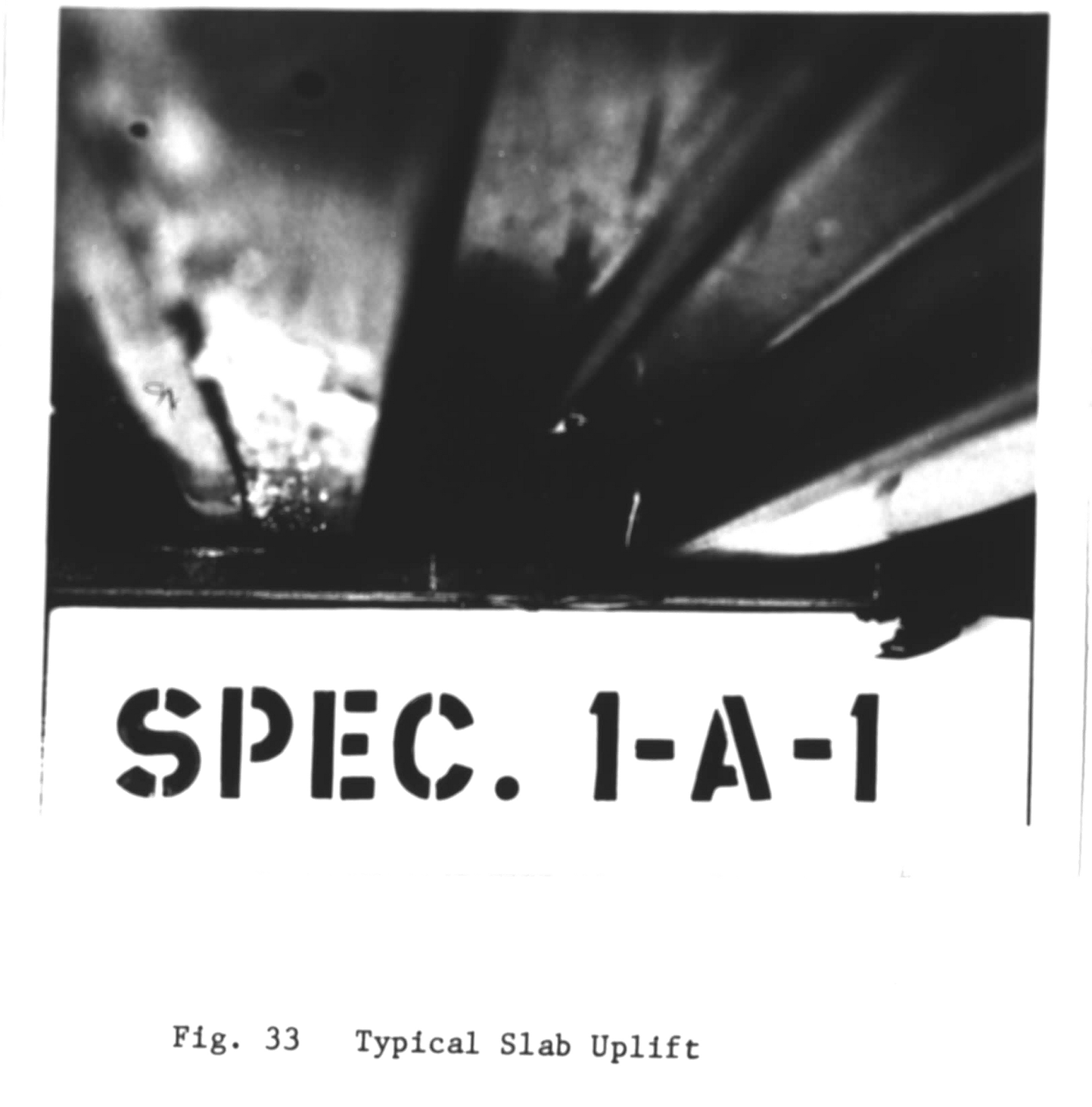

Fig. 33 Typical Slab Uplift

Fig. 34 Typical Flexural Crack

Fig. 35 Typical Longitudinal Cracking

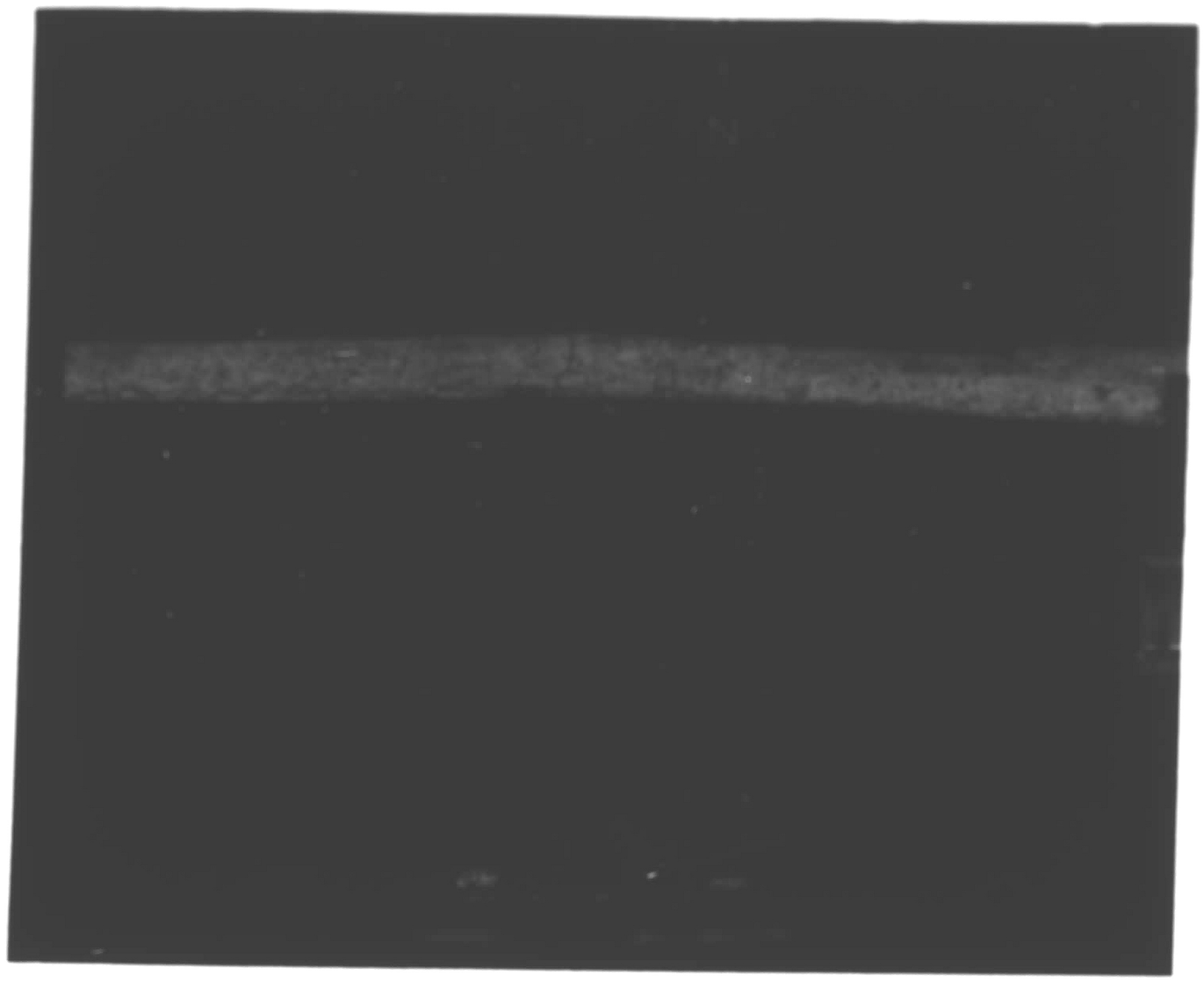

Fig. 36 Typical Transverse Bending

Fig. 36 Typical Transverse Bending

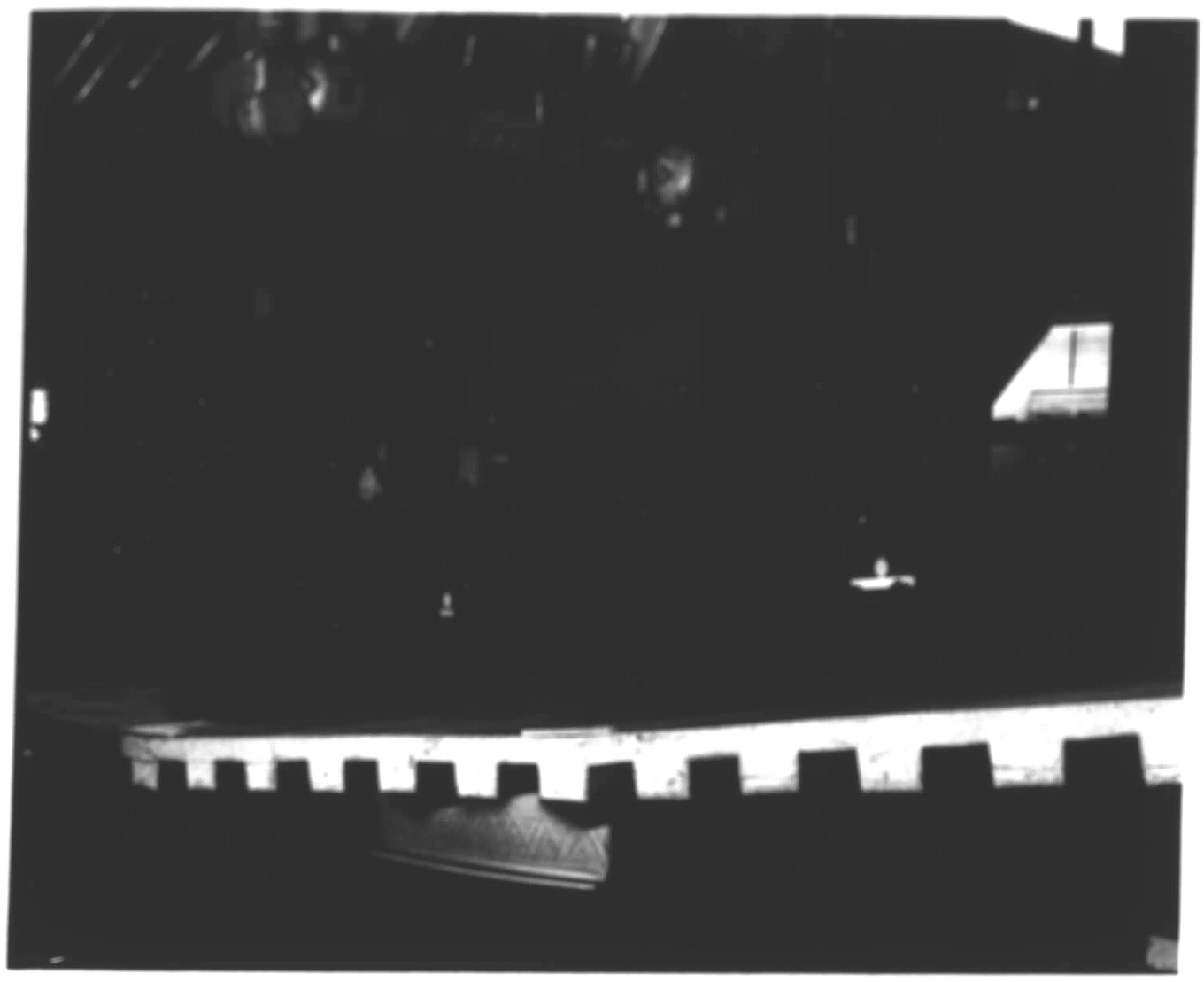

Fig. 37 Typical Bond Failure

Fig. 38 Typical Negative Moment Cracks

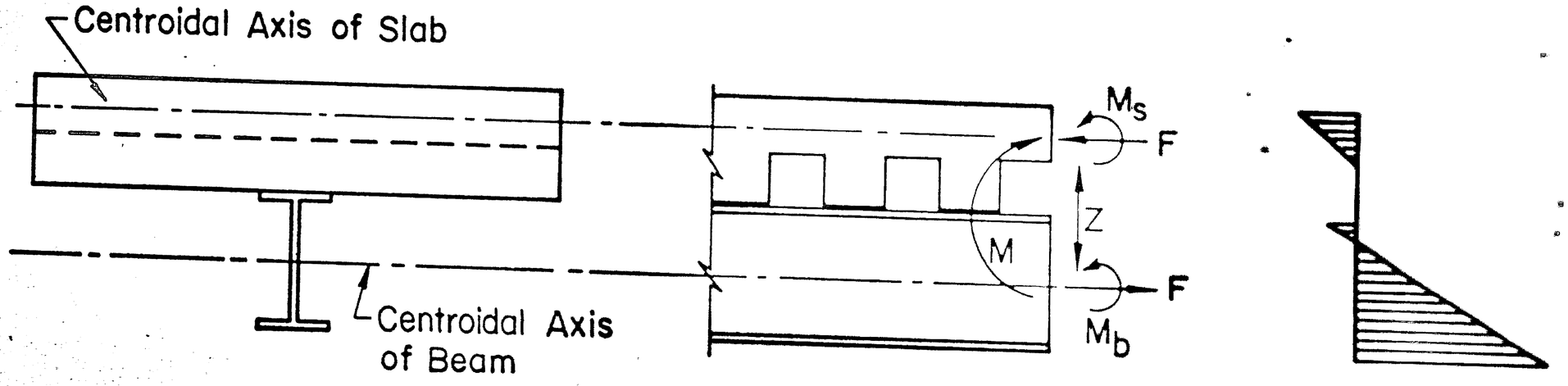

(A) Cross-Section (B) Forces (C) Strain Distribution

$$M = M_b + M_s + F \cdot Z$$

Fig. 39 Model of Force and Strain Distribution

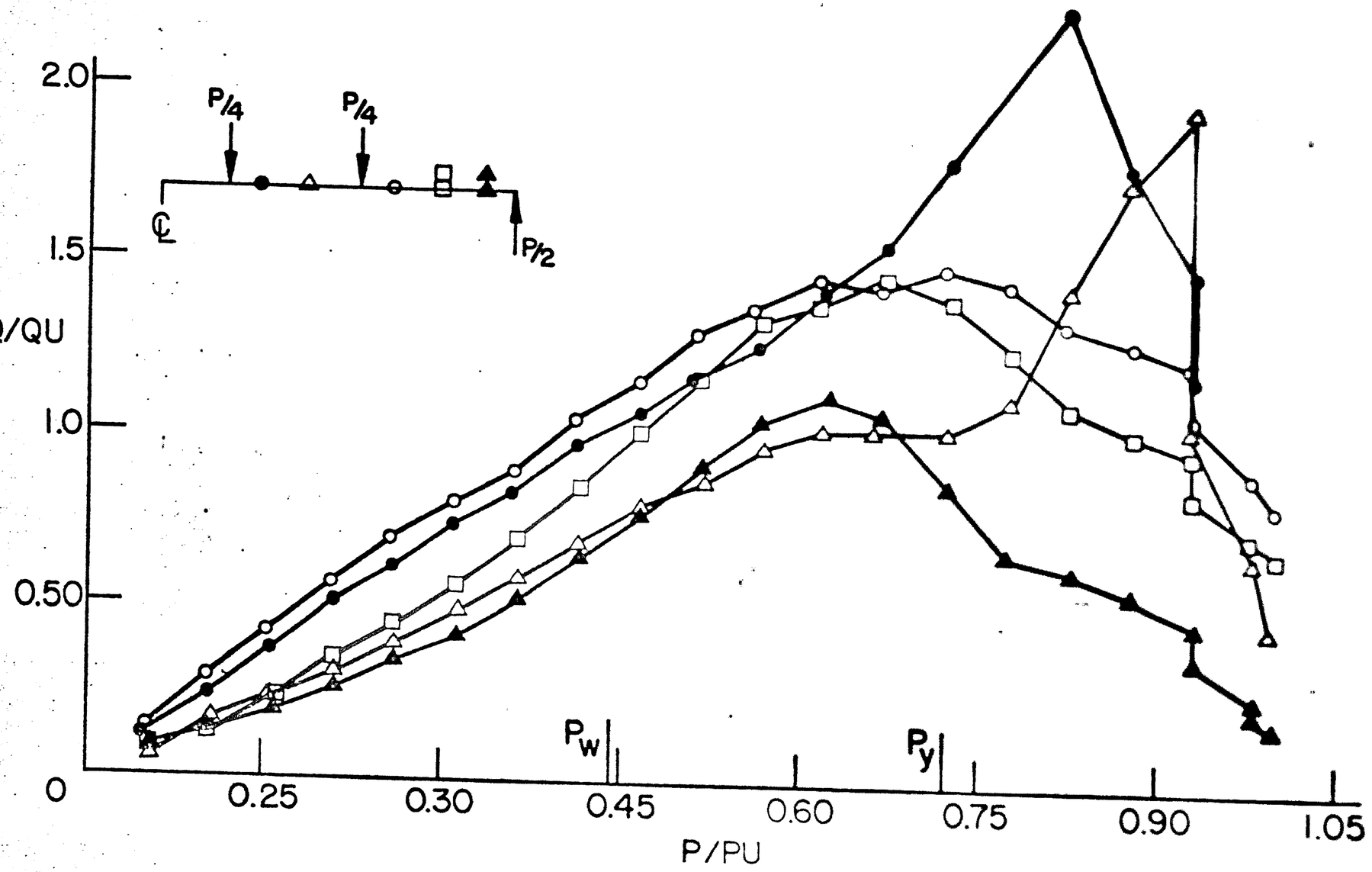

Fig. 40 Connector Force versus Load - Spec 1C2a

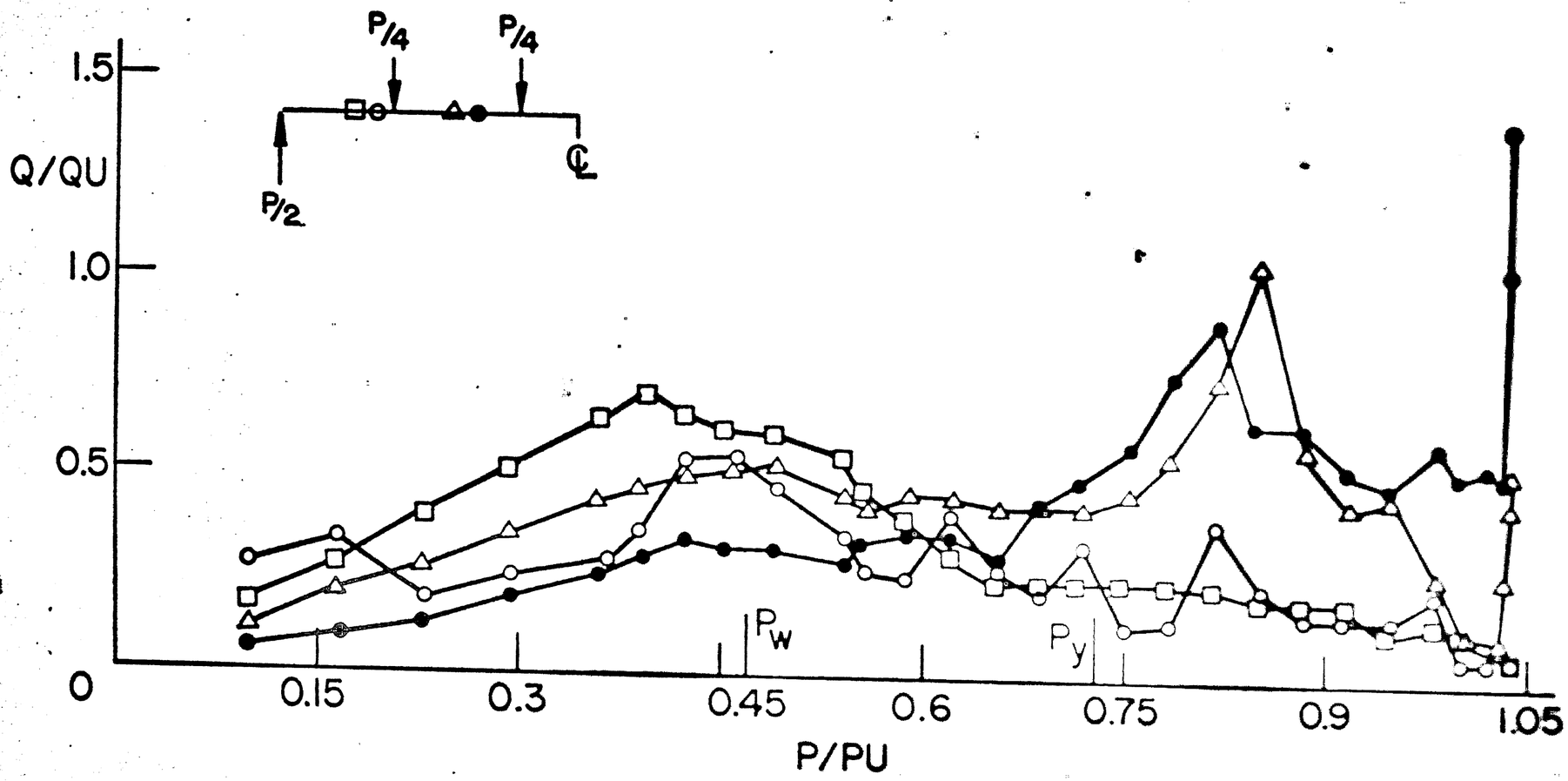

Fig. 41 Connector Force versus Load - Spec. 1C3

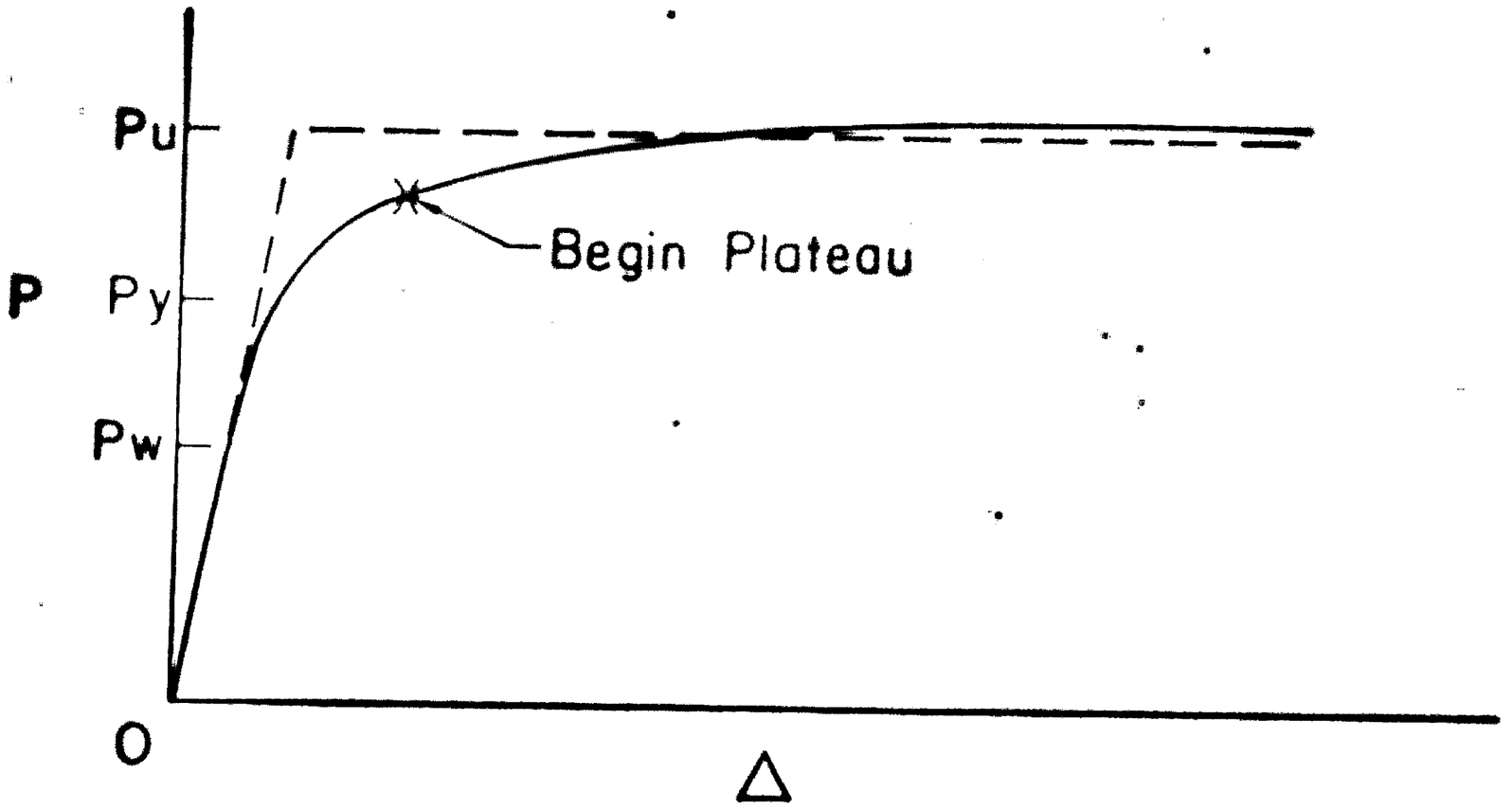

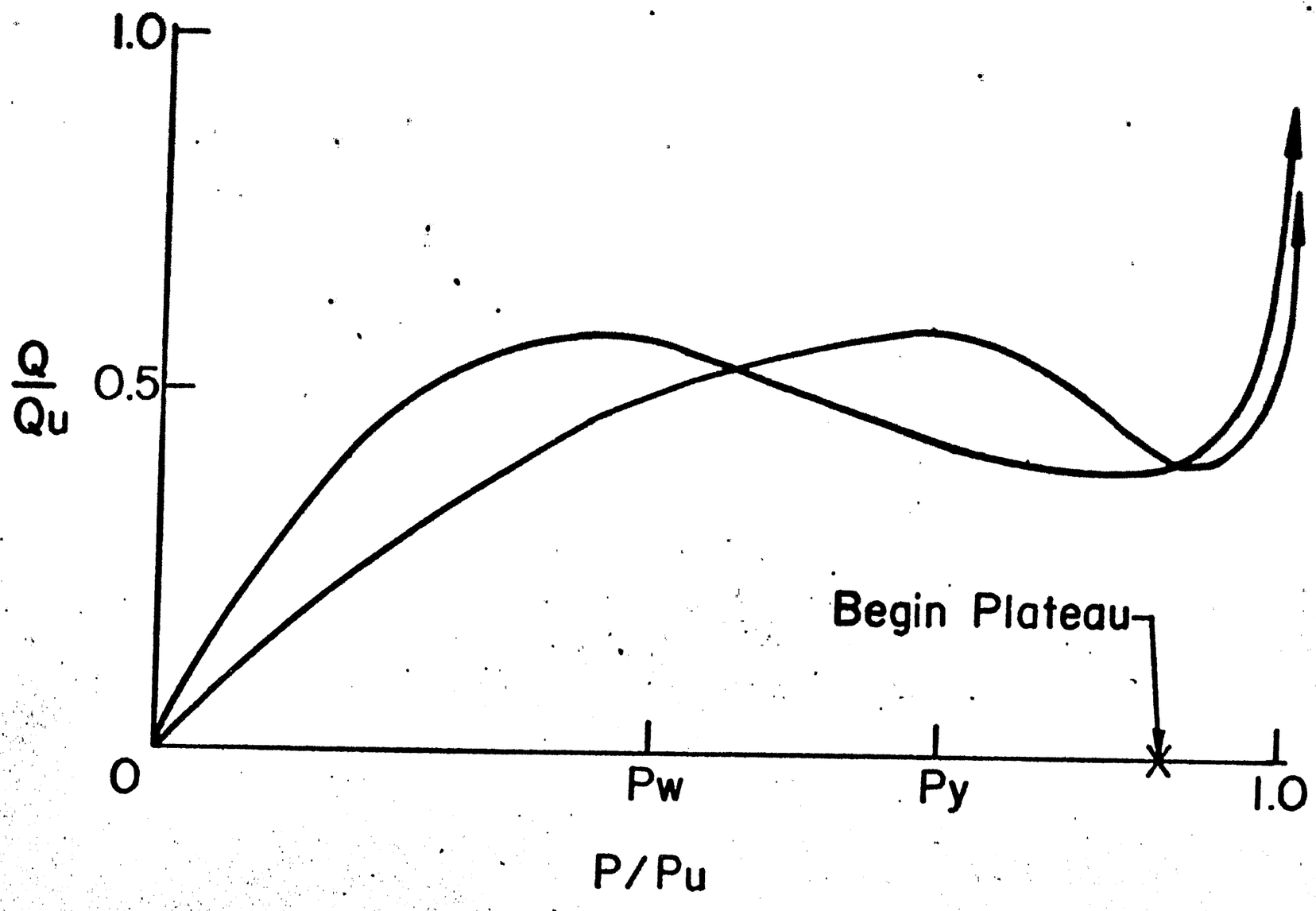

Fig. 42 Idealized Connector Force versus Load Curve

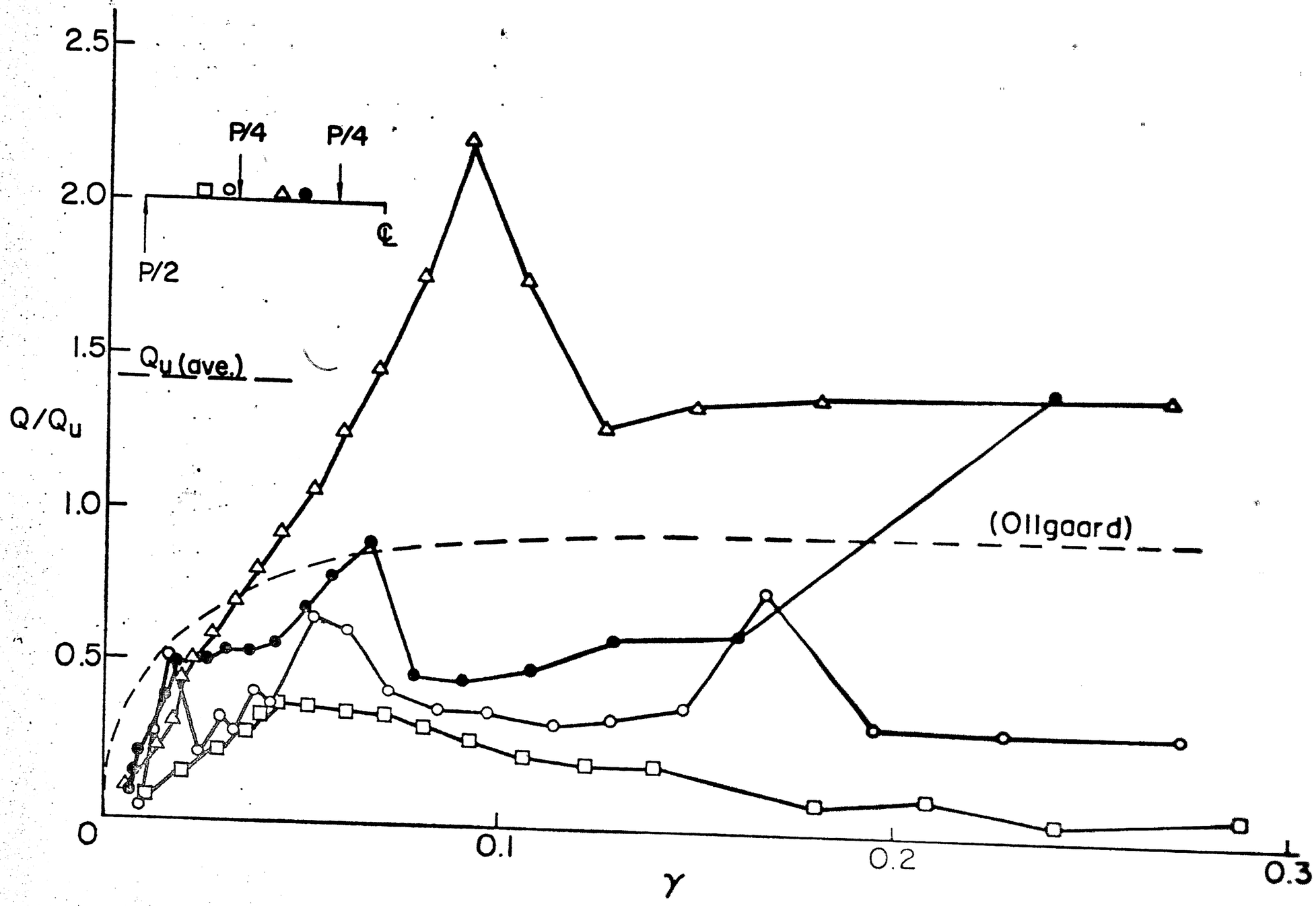

Fig. 43 Connector Force versus Slip - Spec. 1C1

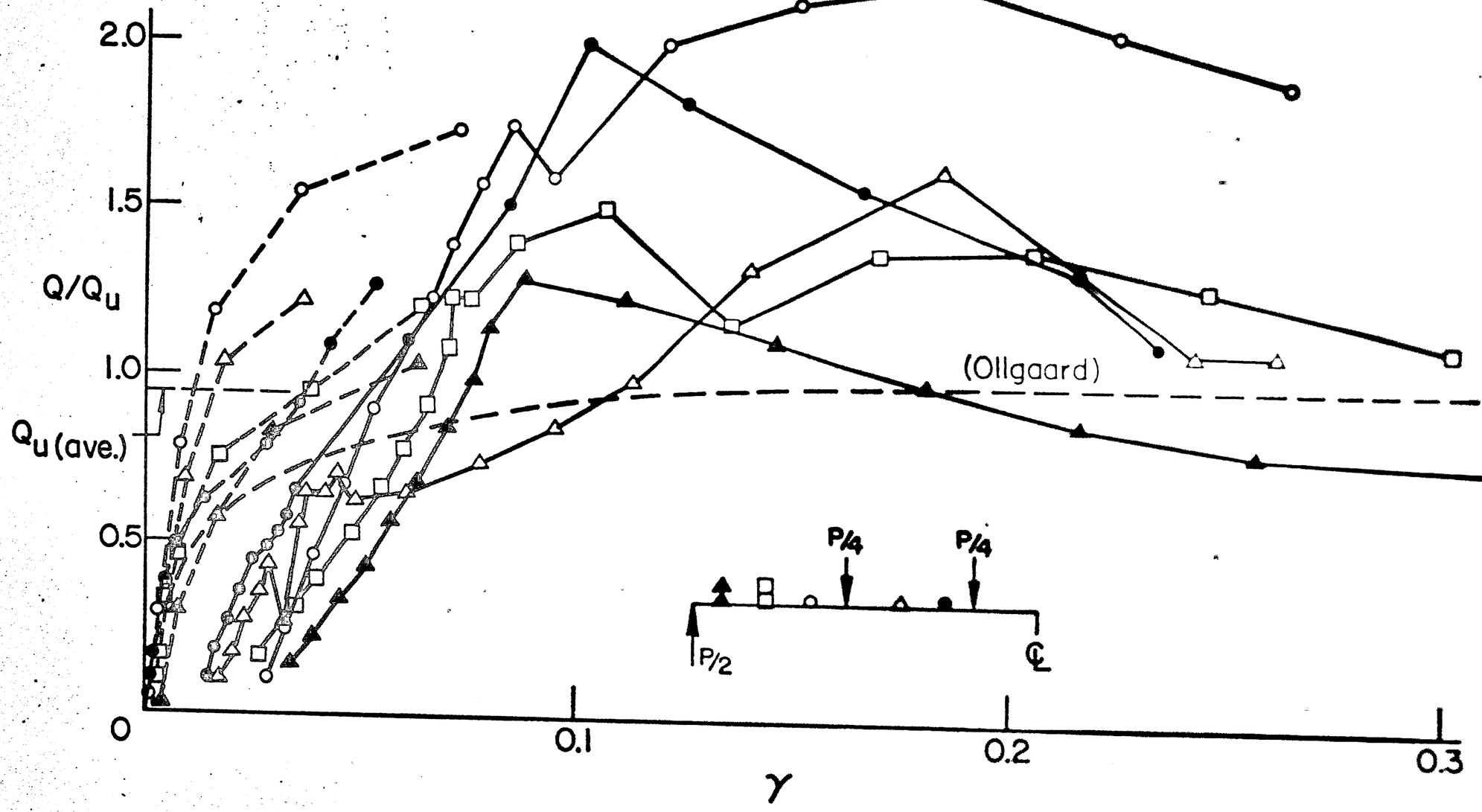

Fig. 44 Connector Force versus Slip - Spec. 1C2a

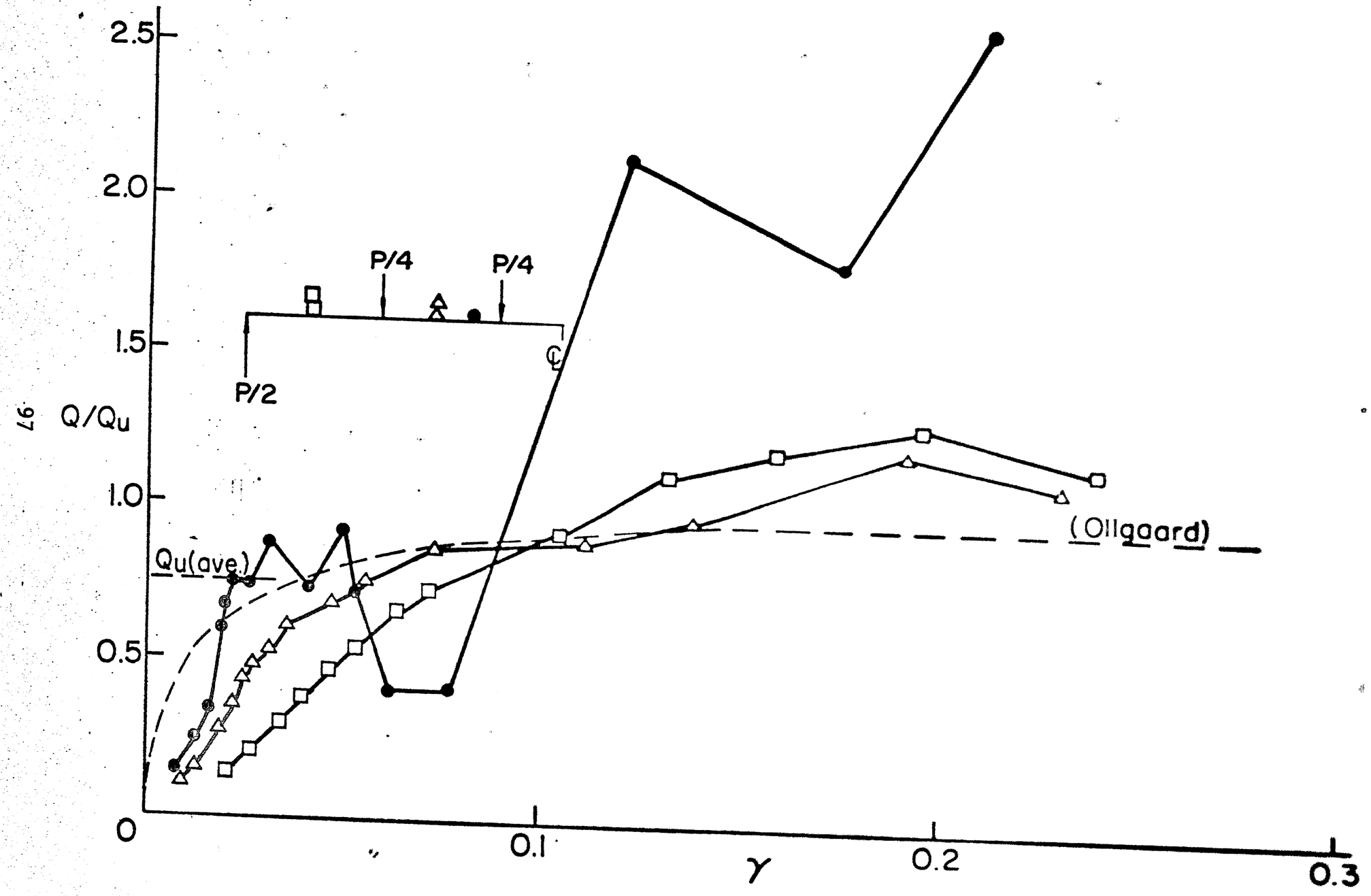

Fig. 45 Connector Force versus Slip - Spec. 1C2b

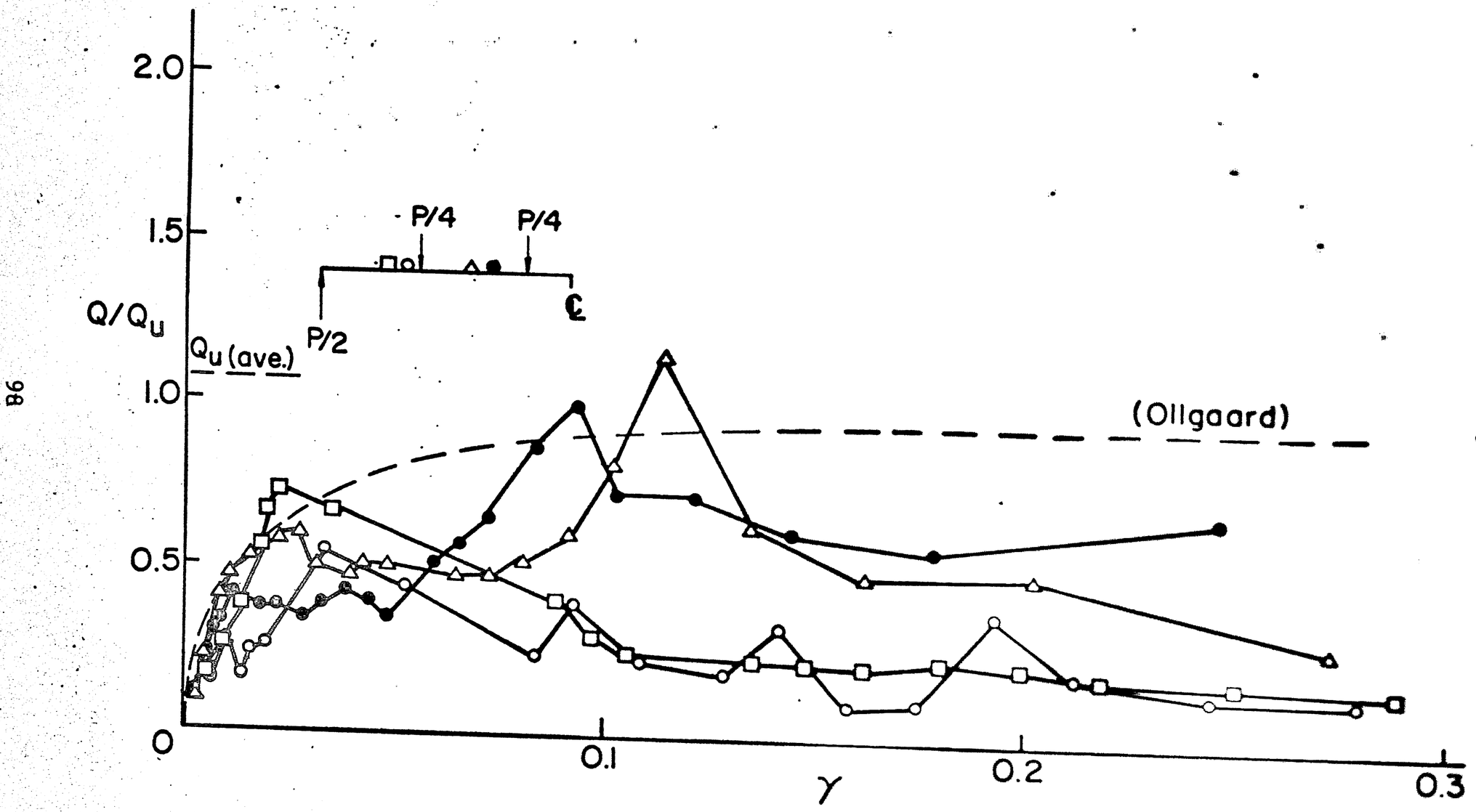

Fig. 46 Connector Force versus Slip - Spec. 1C3

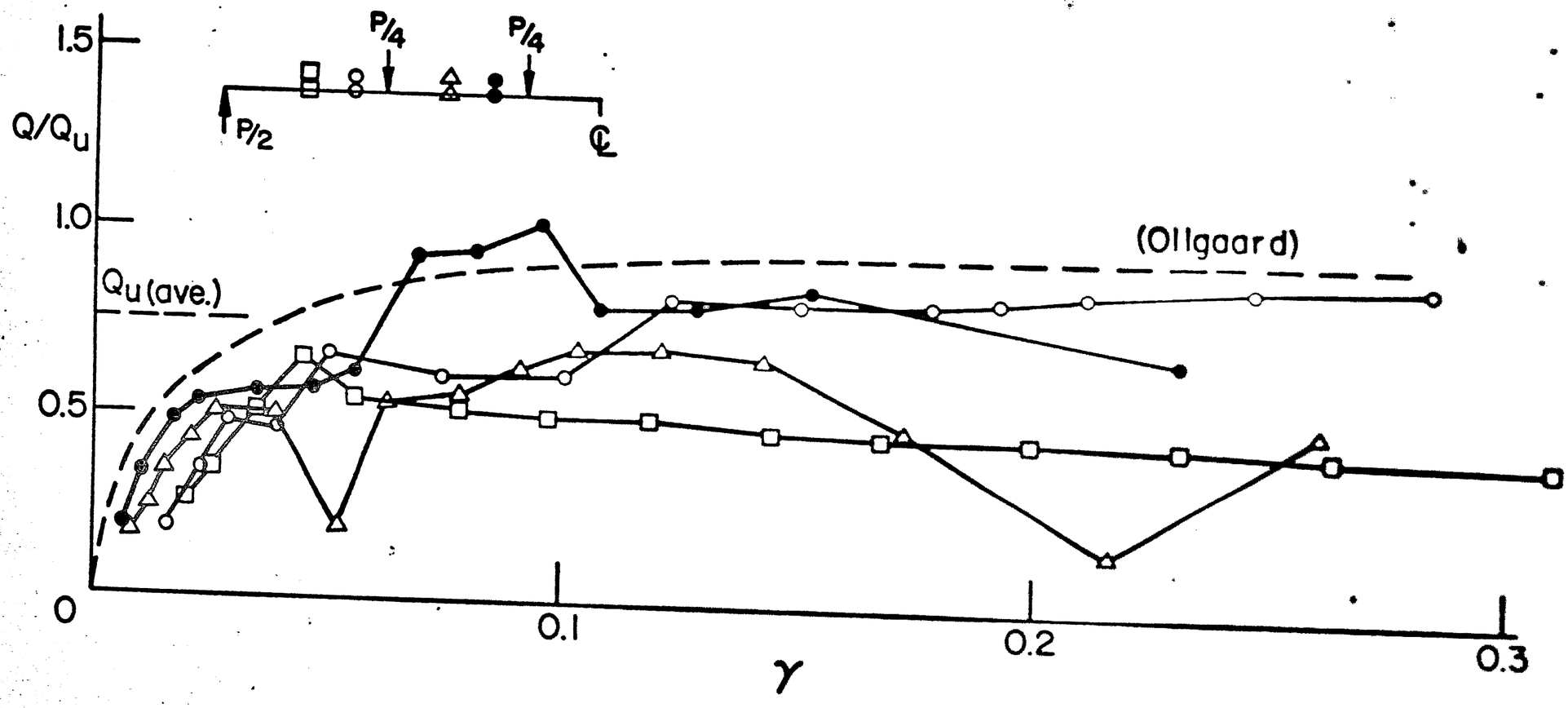

Fig. 47 Connector Force versus Slip - Spec. 1C4

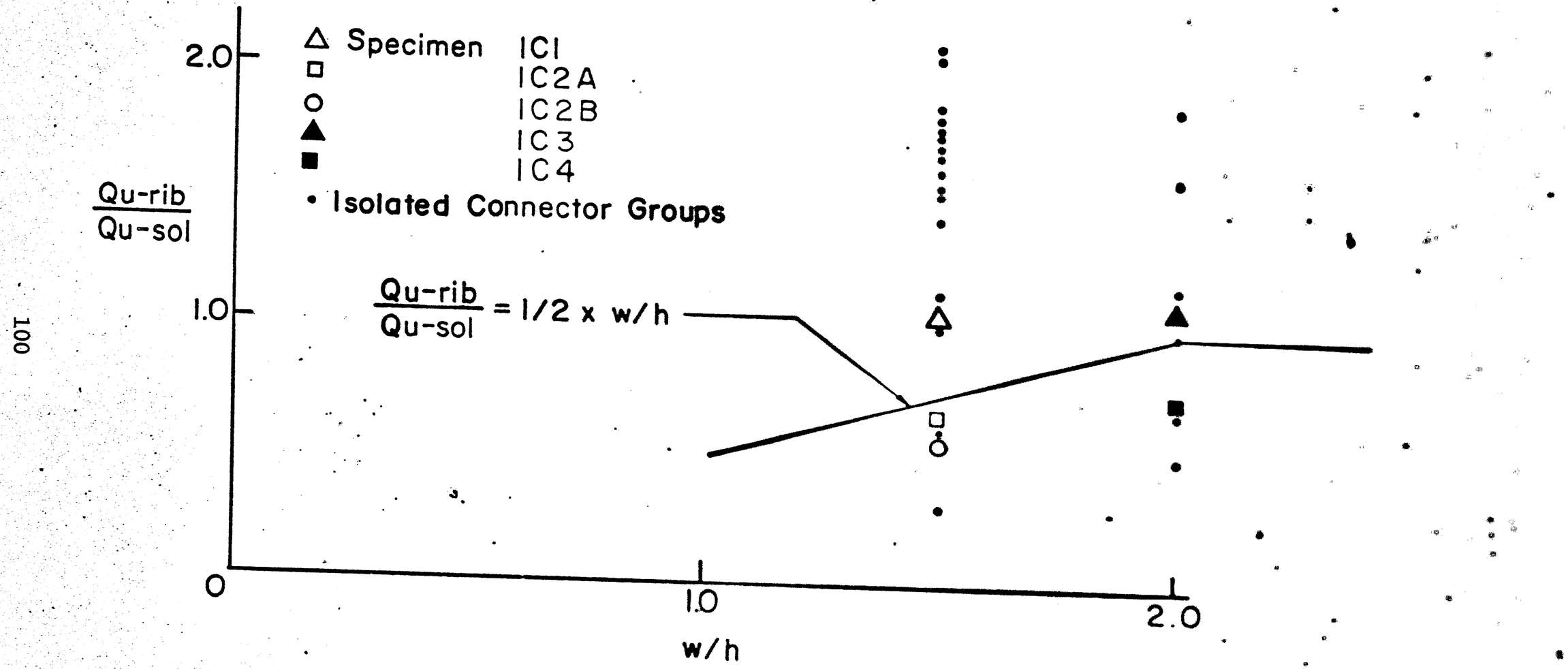

Fig. 48 Connector Strength versus Rib Width Over Height Ratio

8. REFERENCES

1. Fisher, J. W.
DESIGN OF COMPOSITE BEAMS WITH FORMED METAL DECK, AISC Engineering Journal, Vol. 7, No. 3, July 1970.

2. Robinnon, H.
TESTS ON COMPOSITE BEAMS WITH CELLULAR DECK, Journal of the Structural Division, ASCE, Vol. 93, No. ST4, August 1967.

3. Ollgaard, J. G., Slutter, R. G. and Fisher, J. W.
SHEAR STRENGTH OF STUD CONNECTORS IN LIGHTWEIGHT AND NORMAL-WEIGHT CONCRETE, AISC Engineering Journal, Vol. 8, No. 2, April 1971.

4. Slutter, R. G. and Driscoll, G. C.
FLEXURAL STRENGTH OF STEEL-CONCRETE COMPOSITE BEAMS, Journal of the Structural Division, ASCE, Vol. 91, No. ST2, April 1965.

5. McGarraugh, J. B. and Baldwin, J. W.
LIGHTWEIGHT CONCRETE-ON-STEEL COMPOSITE BEAMS", University of Missouri, Columbia, 1970.

6. Siess, C. P.
COMPOSITE CONSTRUCTION FOR I-BEAM BRIDGES, Symposium on Highway Bridge Floors, Transactions, ASCE, Vol. 114, pp. 1023-1045, 1949.

7. Robinson, H.
COMPOSITE BEAMS WITH PARTIAL SHEAR CONNECTION, Presented at ASCE Annual and National Environmental Engineering Meeting at St. Louis, Missouri, October 1971.

8. Winter, G. and Fisher, J. W.
DISCUSSION - "Design of Composite Beams with Formed Metal Deck", ASCE Engineering Journal, Vol. 8, No. 1, 1971.

9. Timoshenko, S. P. and Goodier, J. N.
THEORY OF ELASTICITY, McGraw-Hill, Third Edition, p. 262, 1970.

10. Slutter, R. G. and Adams, R. G.
TESTS OF COMPOSITE BEAMS WITH HOLORIB COMPOSITE SLABS, Fritz Engineering Laboratory Report No. 200.63.408.2, July 1964.

APPENDIX A

COMPUTATION OF SHEAR CONNECTOR STRENGTH FOR SPECIMEN 1C2a

Assumptions

Density of concrete = 113.3 pcf

f'_c = 4.13 ksi

$E_c = 2.48 \times 10^3$ ksi

A_s = 0.4418 in^2

Ultimate Stud Force (Solid Slab)

$$Q_{u\text{ - sol}} = 1.106\, A_s\, f_c'^{0.3}\, E_c^{0.44}$$

$$= 1.106\ (0.4418)\ (4.13)^{0.3}\ (2.48 \times 10^3)^{0.44}$$

$$= 23.3 \text{ kips}$$

Ultimate Stud Force (Ribbed Slab)

$$Q_{u\text{ - rib}} = 0.5\, \frac{w}{h}\, Q_{u\text{ - sol}}$$

$$= 0.5\ (1.5)\ (23.3 \text{ kips})$$

$$= 17.5 \text{ kips}$$

Allowable Stud Force (Ribbed Slab)

$$Q_{\text{all-rib}} = \frac{1}{2}\, Q_{u\text{ - rib}}$$

$$= \frac{1}{2}\ (17.5 \text{ kips})$$

$$= 8.75 \text{ kips}$$

APPENDIX B

COMPUTATION FOR ELASTIC ANALYSIS FOR SPECIMEN 1C2a

Assumptions

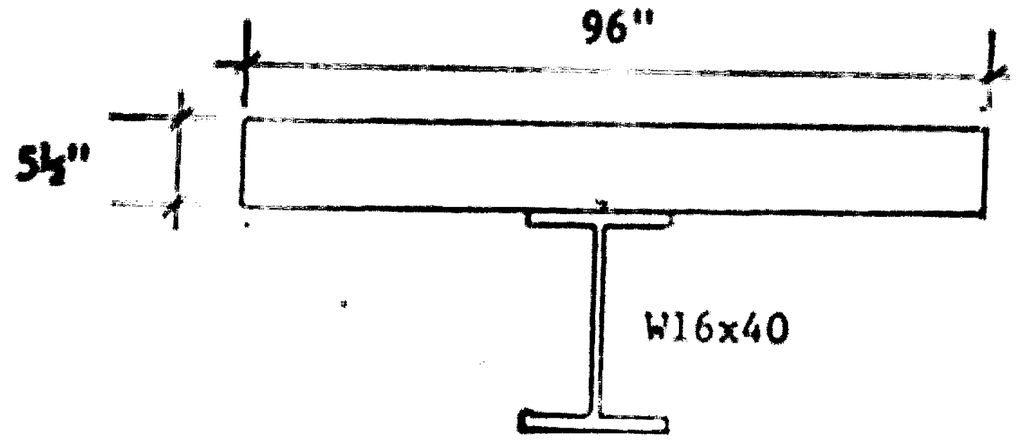

f'_c = 4.13 ksi

f_y = 66.0 ksi

E_c = 2.48 x 10^3 ksi

$$n = \frac{E_s}{E_c} = \frac{29.0 \times 10^3}{2.48 \times 10^3} = 11.7$$

Effective depth of concrete = 2-1/2"

Q rib = 8.75 kips (from Appendix A)

Section Properties

Section	Area	y	M	Y	Y^2	AY^2	I
Slab	20.5	20.25	414.0	4.55	20.7	424.4	10.7
Beam	11.8	8.0	94.4	7.7	59.3	699.7	517.0
Total	32.3		508.4			1124.1	527.7

$$y = \frac{508.4}{32.3} = 15.7" \qquad I = 1651.8 \text{ in.}^4$$

Section Modulus

$$S_{eff} = S_s + \frac{V'h}{Vh}(Sb - S_s)$$

$$S_b = \frac{1651.8}{15.7} = 105.2 \text{ in.}^3$$

$$S_s = 64.4 \text{ in.}^3$$

$$V'_h = 9 \times 8.75 = 78.75 \text{ kips}$$

$$V_h = \frac{11.8 \times 66.0}{2} = 389.4 \text{ kips}$$

$$\frac{V'_h}{V_h} = \frac{78.75}{389.4} = 0.202$$

$$S_{eff} = 64.6 + 0.202\ (105.2 - 64.6) = 72.8 \text{ in.}^3$$

Working Load Moment

$$M_w = f_{all}\ S_{eff}$$

$$= \frac{44 \times 72.8}{12}$$

$$= 266.9 \text{ kip-ft}$$

Yield Moment

$$M_y = f_y\ S_{eff}$$

$$= \frac{66.0 \times 72.8}{12}$$

$$= 400.4 \text{ kip-ft}$$

D. L. Moment

$$M_D = \frac{\omega \ell^2}{8}$$

$$= \frac{0.308\ (32)^2}{8}$$

$$= 39.4 \text{ kip-ft}$$

P working

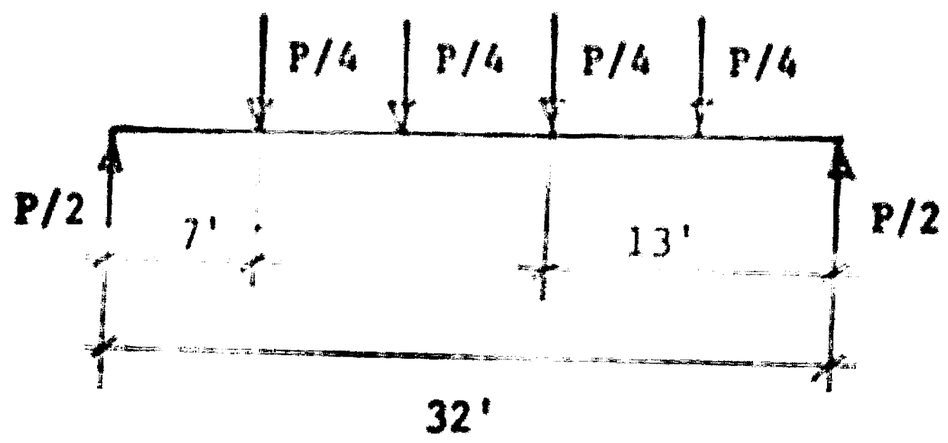

$$P_\omega = \frac{M_\omega - M_D}{5}$$

$$= \frac{266.9 - 39.4}{5}$$

$$= 45.6 \text{ kips}$$

P yield

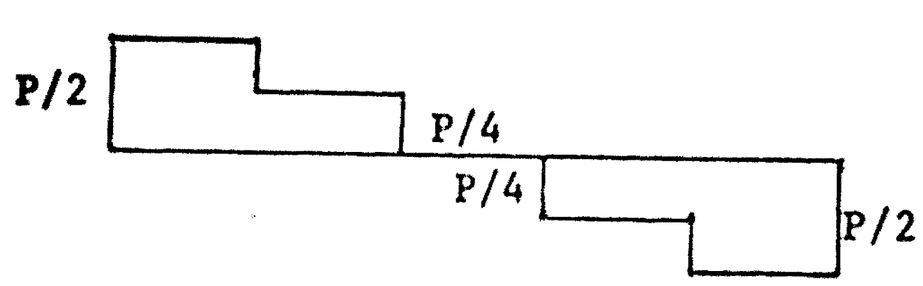

$$P_y = \frac{M_y - M_D}{5}$$

$$= \frac{400.4 - 39.4}{5}$$

$$= 72.4 \text{ kips}$$

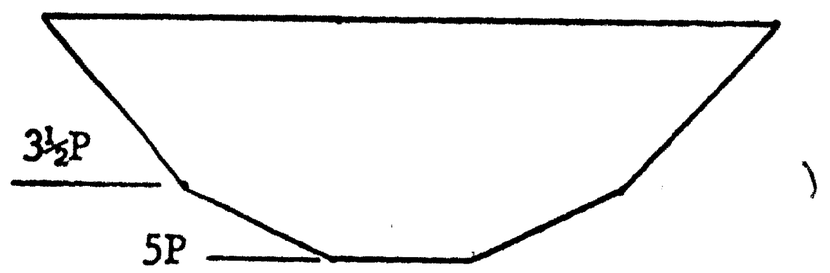

L. L. Deflection

$$\Delta = \Delta_b + \Delta_s$$

$$EI\Delta_b = \frac{1}{2} \times 3.5P \times 7.0 \times 4.67 \quad (= 57.2P)$$

$$+ \quad 5P \times 9.0 \times 11.5 \quad (= 517.5P)$$

$$+ \frac{1}{2} \times 1.5P \times 6.0 \times 9.0 \quad (= 40.5P)$$

$$= 631.9P \quad = 24{,}360$$

$$\Delta_b = \frac{24,630 \times 1728}{29 \times 10^3 \times 1652} = 0.879"$$

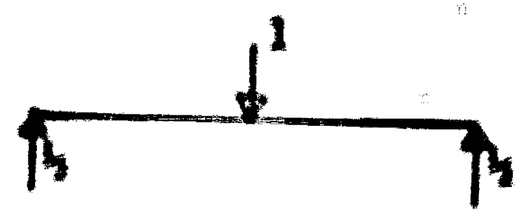

$$\Delta_s = \int_0^L \frac{Vv}{A_\omega G}\, dx = 2 \int_0^{L/2} \frac{Vv}{A_\omega G}\, dx$$

$$= \frac{1}{A_\omega G} \left[\int_0^7 \frac{P}{2}\, dx + \int_7^{13} \frac{P}{4}\, dx \right]$$

$$= \frac{P}{4A_\omega G} (7 + 13) \times 12$$

$$= \frac{45.6 \times 20 \times 12}{4\ (15.0 \times .307) \times 11.5 \times 10^3}$$

$$= 0.052"$$

$$\Delta = 0.879 + 0.052 = 0.931"$$

APPENDIX C

COMPUTATION OF ULTIMATE STRENGTH FOR SPECIMEN 1C2a

Assumptions

f_y = 66.0 ksi

$A_s f_y$ = 11.8 x 66.0 = 778.8 kips

C = 17.5 x 9 = 157.5 kips

$$C' = \frac{778.8 - 157.5}{2} = 310.7 \text{ kips}$$

F = 778.8 - 310.7 = 468.1 kips

Location of Neutral Axis (w.r.t. top of W16 x 40)

c' flange = 66.0 x 7.0 x 0.503 = 232.4

c' web = 66.0 x 0.307 x dw = 310.7 - 232.4

= 78.3 kips

$$dw = 0.503 + \frac{78.3}{66.0\ (0.307)} = 4.37"$$

Location of c' (w.r.t. top of W16 x 40)

Section	A	$\bar{y}$	$A\bar{y}$
Flange	7.0 x 0.503 = 3.52	0.251	0.88
Web	0.307 x(4.37 - 0.50) = 1.19	$0.503 + \frac{(4.37 - 0.50)}{2}$ = 2.44	2.90
Total	4.71		3.78

$$\bar{y}_t = \frac{\Sigma A\bar{y}}{\Sigma A} = \frac{3.78}{4.71} = 0.80"$$

Location of T (w.r.t. top of W16 x 40)

Section	A	$\bar{y}$	$A\bar{y}$
Flange	7.0 x 0.503 = 3.52	15.75	55.4
Web	0.370 x(16.00 - 4.37 - 0.503) = 3.42	$4.37 + \frac{11.13}{2} = 9.93$	34.0
Total	6.94		89.4

$$y_t = \frac{89.4}{6.94} = 12.88"$$

Ultimate Moment (about c')

$$M_u = \frac{1}{12}\left[T\ (y_b - y_t) + C\ (h - \frac{t-h}{2} + y_t\right]$$

$$= \frac{1}{12}\left[468.1 \times (12.8 - 0.8) + 157.5 \times (3.0 + \frac{5.5-3.0}{2} + 0.8)\right]$$

$$= 537.3 \text{ kip-ft}$$

Ultimate Load=

$$P_u = \frac{M_u - M_D}{5}$$

$$= \frac{537.3 - 39.4}{5}$$

$$= 99.6 \text{ kips}$$

10 Vita

John A. Grant, Jr. was born on November 9, 1945 in Washington, D. C. He is the son of John A. and Anni L. Grant.

He attended San Juan High School in Citrus Heights, California at Davis and graduated in December 1967 with a Bachelor of Science Degree in Civil Engineering.

In July 1967 he was employed by the California Department of Water Resources. He worked in the Structural Division of the Dam Design Section and held the position of Jr. Civil Engineer.

In March 1968 he was called to active duty with the U. S. Marine Corps. He served three years as an infantry officer and attained the rank of Captain.

He is an Associate Member of the American Society of Civil Engineers and a member of Sigma Xi.

In January 1971, he entered the Graduate School of Lehigh University as a Special Student. In August 1971 he was granted full status in the Graduate School and accepted the position of Research Assistant on Project 381, Composite Beams with Formed Metal Deck, while working toward the degree of Master of Science in Civil Engineering. He is currently a candidate for the degree of Doctor of Philosophy in Civil Engineering while continuing as a Research Assistant at Lehigh.